รายงานวิจัยฉบับสมบูรณ์

การจดจำแอนไอออนและแคตไอออนที่สำคัญของสารประกอบเอไมด์ขนาดใหญ่

โดย รศ.ดร. วิทยา เรืองพรวิสุทธิ์ และคณะ

กรกฎาคม 2553

สัญญาเลขที่ BRG5180016

รายงานวิจัยฉบับสมบูรณ์

การจดจำแอนไอออนและแคตไอออนที่สำคัญของสารประกอบเอไมด์ขนาดใหญ่

คณะผู้วิจัย	สังกัด
รศ.ดร.วิทยา เรืองพรวิสุทธิ์	จุฬาลงกรณ์มหาวิทยาลัย
ดร.บรรจบ วันโน	มหาวิทยาลัยมหาสารคาม

สนับสนุนโดยสำนักงานกองทุนสนับสนุนการวิจัย
(ความเห็นในรายงานนี้เป็นของผู้วิจัย สกว. ไม่จำเป็นต้องเห็นด้วยเสมอไป)

กิตติกรรมประกาศ

งานวิจัยนี้ได้รับการสนับสนุนจากสำนักงานกองทุนสนับสนุนการวิจัย คณะผู้วิจัยขอขอบคุณสำนักงานกองทุนสนับสนุนการวิจัยเป็นอย่างยิ่ง และขอแสดงความมุ่งมั่นตั้งใจในการแสดงคำขอบคุณสำนักงานกองทุนสนับสนุนการวิจัยสำหรับการตีพิมพ์ผลงานในวารสารนานาชาติครั้งต่อ ๆ ไป ถึงแม้ว่าโครงการนี้สิ้นสุดแล้วก็ตาม เพื่อระลึกความดีของสำนักงานกองทุนสนับสนุนการวิจัยที่มีต่อคณะผู้วิจัย

บทคัดย่อ

พลังงานยึดเกาะแอนไอออนโดยสารประกอบ 1,3-บิส(4-ไนโตรฟีนิล) ยูเรีย หรือ รีเซ็ปเตอร์ **1** กับแอนไอออนเป็นตามลำดับดังนี้ CH_3COO^- > HCO_3^- > $C_6H_5COO^-$ > NO_2^- > $H_2PO_4^-$ > NO_3^- > HSO_4^- และ F^- > Cl^- > Br^- พลังงานยึดเกาะของสารประกอบเชิงซ้อนระหว่างสารประกอบเอไมด์วงแหวนจำนวน 6 รีเซ็ปเตอร์คือ **2**, **3**, **4**, **5**, **6** และ **7** กับไอออน F^-, Cl^-, Br^-, CH_3COO^-, HSO_4^- และ $H_2PO_4^-$ความสามารถการยึดเกาะแอนไอออนโดยรีเซ็ปเตอร์ทั้งหกเป็นลำดับดังนี้ F^- > CH_3COO^- > Br^- > $H_2PO_4^-$ > Cl^- > HSO_4^- สำหรับรีเซ็ปเตอร์ **2**, F^- > Br^- > CH_3COO^- > $H_2PO_4^-$ > Cl^- > HSO_4^- สำหรับรีเซ็ปเตอร์ **3** และ **4**, F^- > $H_2PO_4^-$ > CH_3COO^- ≈ Br^- > Cl^- > HSO_4^- สำหรับรีเซ็ปเตอร์ **5**, F^- > $H_2PO_4^-$ ≈ CH_3COO^- ≈ Br^- > Cl^- > HSO_4^- สำหรับรีเซ็ปเตอร์ **6** และ F^- > $H_2PO_4^-$ > Br^- > CH_3COO^- ≈ > Cl^- ≈ HSO_4^- สำหรับรีเซ็ปเตอร์ **7** พลังงานยึดเกาะแอนไอออนโดยสารประกอบเชิงซ้อน Li^+, Na^+ and K^+/คาลิก[4]เอรีน (**L** หรือ **8**) กับเฮไลด์ไอออน F^-, Cl^-, Br^-, ไอออนที่มีออกซิเจนเป็นองค์ประกอบ HCO_3^-, HSO_4^- และ CH_3COO^- และค่าอุณหพลศาสตร์ของสารประกอบเชิงซ้อน Li**L**$^+$, Na**L**$^+$ และ K**L**$^+$ กับแอนไอออนเหล่านี้ได้รับการคำนวณ พลังงานยึดเกาะแอนไอออนโดย Li**L**$^+$, Na**L**$^+$ และ K**L**$^+$ เป็นลำดับดังนี้ F^- >> CH_3COO^- > HCO_3^- > Br^- > HSO_4^- > Cl^-, F^- >> CH_3COO^- > HCO_3^- > Br^- > Cl^- > HSO_4^- และ F^- >> CH_3COO^- > HCO_3^- > Br^- > Cl^- > HSO_4^- ตามลำดับ รีเซปเตอร์ Li**L**$^+$, Na**L**$^+$ และ K**L**$^+$ พบว่ามีความสามารถในการเลือกจับฟลูออไรด์ โครงสร้างของสารประกอบ 8,8'-บิส(3-ฟีนิลไธโอยูไรโดเมทิล)-2,2'-ไบแนบทัลลีน (**9**) 8,8'-บิส(3-บิวทิลไธโอยูไรโดเมทิล)-2,2'-ไบแนบทัลลีน (**10**) และสารประกอบเชิงซ้อนกับเกสต์ที่เป็นคาร์บอกซิเลต (อะซิเตต, ออกซาเลต, มัลโลเนต, ซัคซิเนต, กลูตาเรต, อะดิเพต, พิมีเลต, ซับเบอเลต และ อะซีเลต) และไอออนสารอินทรีย์ที่มีออกซิเจนเป็นองค์ประกอบ (NO_3^-, SO_4^{2-}, HCO_3^-, HPO_4^{2-}, และ $H_2PO_4^-$) และเฮไลด์ไอออนได้รับการคำนวณ สารประกอบไดพิโคลิลยูเรียถูกพบว่ามีสี่โครงรูป และพบว่าโครงสร้างพันธะไฮโดรเจนแบบภายในโมเลกุลเป็นโครงรูปที่เสถียรที่สุด ค่าพลังงาน ค่าอุณหพลศาสตร์ ค่าคงที่อัตราเร็ว ค่าคงที่การเกิดสมดุลเคมี ของการเปลี่ยนแปลงโครงรูปได้รับการคำนวณ สารประกอบเชิงซ้อนกับกรดฟอร์มิก กรดน้ำส้ม กรดเบ็นโซอิก กรดออกซาลิก และแอนไอออนของกรดเหล่านี้ได้รับการสืบสวน ค่าพลังงาน ค่าอุณหพลศาสตร์ ค่าคงที่อัตราเร็ว ค่าคงที่การเกิดสมดุลเคมี ของการรวมตัวกันได้รับการคำนวณ

คำสำคัญ: สารประกอบเอไมด์ พลังงานยึดเกาะ การจดจำแอนไอออน แคตไอออน

Abstract

Binding energies of 1,3-bis(4-nitrophenyl)urea receptor **1** are in decreasing orders: CH_3COO^- > HCO_3^- > $C_6H_5COO^-$ > NO_2^- > $H_2PO_4^-$ > NO_3^- > HSO_4^- for oxygen-containing anions and F^- > Cl^- > Br^- for halide ions. Binding energies of complexes between six cyclic amide receptors **2**, **3**, **4**, **5**, **6** and **7** and anions F^-, Cl^-, Br^-, CH_3COO^-, HSO_4^- and $H_2PO_4^-$ and thermodynamic properties of these complexations were obtained. The binding abilities of these six receptors are in decreasing orders: F^- > CH_3COO^- > Br^- > $H_2PO_4^-$ > Cl^- > HSO_4^- for receptor **2**, F^- > Br^- > CH_3COO^- > $H_2PO_4^-$ > Cl^- > HSO_4^- for receptors **3** and **4**, F^- > $H_2PO_4^-$ > CH_3COO^- ≈ Br^- > Cl^- > HSO_4^- for receptor **5**, F^- > $H_2PO_4^-$ ≈ CH_3COO^- ≈ Br^- > Cl^- > HSO_4^- for receptor **6** and F^- > $H_2PO_4^-$ > Br^- > CH_3COO^- ≈ > Cl^- ≈ HSO_4^- for receptor **7**. Binding energies of Li^+, Na^+ and K^+/calix[4]arene (**L**, **8**) complexes and halide ions F^-, Cl^-, Br^-, oxygen–containing anions HCO_3^-, HSO_4^- and CH_3COO^- ions were obtained. Binding energies and thermodynamic properties of complex receptors Li$\mathbf{L}^+$, Na$\mathbf{L}^+$ and K$\mathbf{L}^+$ with these anions were determined. Binding energies of receptors Li$\mathbf{L}^+$, Na$\mathbf{L}^+$ and K$\mathbf{L}^+$ are in decreasing orders: F^- >> CH_3COO^- > HCO_3^- > Br^- > HSO_4^- > Cl^-, F^- >> CH_3COO^- > HCO_3^- > Br^- > Cl^- > HSO_4^- and F^- >> CH_3COO^- > HCO_3^- > Br^- > Cl^- > HSO_4^-. All the alkaline–metal receptors Li$\mathbf{L}^+$, Na$\mathbf{L}^+$ and K$\mathbf{L}^+$exhibit their abilities to selectively fluoride ion. The structures of 8,8'-bis(3-phenylthioureidomethyl)-2,2'-binaphthalene (**9**), 8,8'-bis(3-butylthioureidomethyl)-2,2'-binaphthalene (**10**) and their complexes with anionic guests such as carboxylate ions (acetate, oxalate, malonate, succinate, glutarate, adipate, pimelate, suberate, and azelate), inorganic oxygen-containing anions (NO_3^-, SO_4^{2-}, HCO_3^-, HPO_4^{2-} and $H_2PO_4^-$), and halide ions were obtained. Four isomers of dipicolyl urea were obtained and the intramolecular hydrogen-bonded structure was found to be the most stable isomer. Energetics, thermodynamic properties, rate constants, and association constants of their isomerizations were obtained. Complexes of all isomers of dipicolyl urea with formic acid, acetic acid, benzoic acid, oxalic acid, and their deprotonated species were investigated. Energetics, thermodynamic properties, and rate constants of their associations were obtained. Stabilities of all complexes in terms of association constants of the most stable species were determined.

Keywords: Amide compound, binding energy, anion recognition, cation

สารบัญ

หน้า

หน้าสรุปโครงการ (Executive Summary)

การพัฒนาเคโมเซ็นเซอร์ (chemosensors) สำหรับการจดจำอย่างจำเพาะต่อแอนไอออนที่สำคัญ ๆ นับเป็นประเด็นวิจัยที่ได้รับความสนใจอย่างกว้างขวางในวิชาเคมีที่ว่าด้วยโฮสต์-เกสต์ (Host-guest Chemistry) เนื่องจากระบบการจดจำของเลกุล และระบบโฮสต์-เกสต์ มีบทบาทสำคัญต่อระบบสิ่งมีชีวิตและสิ่งแวดล้อม การยึดเกาะระหว่างแอนไอออน (เกสต์) กับโมเลกุลโฮสต์ (หรือเรียกว่ารีเซ็ปเตอร์) นั้นเป็นการเกิดพันธะไฮโดรเจนและแสดงผลให้สังเกตได้ โมเลกุลโฮสต์เหล่านี้ได้แก่ สารประกอบยูเรีย (urea) สารประกอบไธโอยูเรีย (thiourea) สารประกอบอิมิดาโซเลียม (imidazolium) และ สารประกอบกัวนิดิเนียม (guanidinium) ซึ่งหากโมเลกุลเหล่านี้ต่อเข้ากับหมู่ฟลูออโรฟอร์จะมีสมบัติเป็นเซนเซอร์สำหรับแอนไอออนนั้น ๆ ได้ โมเลกุลโฮสต์ หรือรีเซ็ป)เตอร์ชนิดใหม่ ๆ จึงถูกออกแบบและสังเคราะห์เพื่อให้มีสมบัติในการจดจำแออนไอออน ผ่านอันตรปฏิกิริยาพันธะไฮโดรเจน (hydrogen bonding interaction) และอิเล็กโทรสแตติค (electrostatic interaction) ความสามารถในการจดจำของรีเซปเตอร์สามารถศึกษาโดยวิธีสเปกโตรเมทตรี ได้แก่ วิธีการวัดฟลูออเรสเซนซ์ (fluorescence) ยูวีวิสิเบิล (UV–VIS) และ เอ็นเอ็มอาร์ (NMR) ผลลัพธ์ที่แสดงให้เห็นความสามารถในการจดจำของรีเซปเตอร์ต่อแอนไอออน ได้แก่ความแรงของการยึดเกาะ (binding) งานวิจัยก่อนหน้านี้ได้ทำการศึกษาโครงสร้างของสารประกอบเอโซฟีนอล-ไธโอยูเรีย (azophenol–thiourea) และการเกิดสารประกอบเชิงซ้อนกับ acetate, oxalate, malonate, succinate, glutarate, adipate, pimelate, suberate และ azelate พลังงานในการยึดเกาะและการเกิดสารประกอบเชิงซ้อนของเอโซฟีนอล-ไธโอยูเรีย และ ลำดับความเสถียรของรีเซปเตอร์เหล่านี้ต่อแอนไอออนดังกล่าวได้รับการศึกษาโดยคำนวณด้วยวิธีทางเคมีควอนตัม

สารประกอบวงแหวนขนาดใหญ่ชนิดอะไมด์ (macrocyclic amide compound) ที่สังเคราะห์ขึ้นจำนวนหนึ่งได้รับการศึกษาทางโครงสร้าง และการเกิดสารประกอบเชิงซ้อนกับแอนไอออน สำหรับสารประกอบคาลิกซารีนนับเป็นโมเลกุลที่มีบทบาทในระบบโฮสต์เป็นอย่างมาก สารประกอบคาลิกซารีนที่มีการสังเคราะห์และพัฒนาให้เป็นรีเซปเตอร์เพื่อการจดจำแอนไอออน ได้แก่ สารประกอบคาลิก[4]เอรีนที่เชื่อมต่อกับอะโรมาติกอะไมด์ (calix[4]arenes bearing aromatic amide moieties) ซึ่งพบว่าปลายด้านบนของมันสามารถยึดเกาะ และจดจำแอนไอออนได้อย่างดี งานวิจัยก่อนหน้านี้ได้ทำการศึกษาการจดจำเกสต์ที่เป็นแอนไอออนของสารประกอบคาลิก[4]เอรีนอะมิโดยูเรีย (calix[4]arene amidourea) โดยเกสต์เหล่านี้ได้แก่ acetate, fluoride, hydrogen phosphate และ hydrogenpyrophosphate ในสารละลาย DMSO สมบัติทางเทอร์โมไดนามิก ค่าพลังงานพรีออร์กาไนเซชัน (preorganization energy) และ ค่าพลังงานการเกิดสารประกอบเชิงซ้อนของสารประกอบ tetraamino-tert-butylthiacalix[4]arene (tatbtc4a) และ tetraamino-tert-butylcalix[4]arene (tatbc4a) กับ

โมเลกุลเกสต์ ได้แก่ acetate, oxalate, malonate, succinate, glutarate, adipate และ pimelate ได้รับการศึกษาโดยวิธี ONIOM(B3LYP/6-31G(d):AM1)

ในงานวิจัยครั้งนี้สารประกอบซุปราชนิดเอไมด์ที่มีการสังเคราะห์ขึ้นแล้วและเป็นโมเลกุลที่มีแนวโน้มที่มีการจดจำต่อแอนไอออน จะได้รับการสืบค้น และทำการศึกษาวิจัยโดยวิธีการคำนวณทางเคมีควอนตัม เพื่อนำไปสู่การพัฒนาให้เป็นเซนเซอร์โดยการวิจัยทางเคมีวิเคราะห์ต่อไป

วัตถุประสงค์

- เพื่อค้นหาโมเลกุลชนิดซุปราโมเลกุลาร์ที่สามารรถจดจำต่อแอนไอออนของสารประกอบอินทรีย์
- เพื่อหาค่าความเสถียรของสารประกอบเชิงซ้อนระหว่างซุปราโมเลกุลาร์รีเซปเตอร์ กับแอนไอออนของสารประกอบอินทรีย์
- เพื่อหาค่าทางเทอร์โมไดนามิกของการแกิดสารประกอบเชิงซ้อนระหว่างซุปราโมเลกุลาร์ รีเซปเตอร์ กับแอนไอออนของสารประกอบอินทรีย์
- เพื่อเป็นพื้นฐานในการค้นหาสารประกอบที่เป็นเคโมเซนเซอร์สำหรับการตรวจหาแอนไอออนโดยโมเลกุลชนิดซุปราโมเลกุลาร์

ระเบียบวิธี

- ค้นคว้าและรวบรวมข้อมูลที่เกี่ยวข้องกับงานการวิจัย และสร้างฐานข้อมูลสำหรับตรวจสอบ และเปรียบเทียบข้อมูลเพื่อเป็นแนวทางในการทำวิจัย
- หาโครงสร้างของสารประกอบซุปราโมเลกุลาร์รีเซปเตอร์ที่คาดว่าสามารถจดจำแอนไอออนของสารประกอบอินทรีย์ที่ต้องการตรวจวัด โดยการคำนวณทางเคมีควอนตัม และโดยการค้นหาจากฐานข้อมูล CCDC (ConQuest Version 1.2, 2002)
- ศึกษาการเกิดสารประกอบเชิงซ้อนระหว่างซุปราโมเลกุลาร์รีเซปเตอร์ กับแอนไอออนของสารประกอบอินทรีย์ โดยการคำนวณทางเคมีควอนตัม
- วิเคราะห์สมบัติทางสเปกโทรเมทรี
- ศึกษาการเกิดสารประกอบเชิงซ้อนระหว่างซุปราโมเลกุลาร์รีเซปเตอร์ กับแอนไอออนของสารประกอบอินทรีย์ โดยแบบจำลองโมเลกุล
- วิเคราะห์สมบัติทางเทอร์โมไดนามิกส์
- สรุปผลการวิจัย และเขียนต้นฉบับเพื่อการตีพิมพ์

ตารางแสดงแผนงานและผลงาน (ในแต่ละช่วงเวลา) นับตั้งแต่เริ่มโครงการจนถึงสิ้นสุดโครงการ

ตารางที่ 1 : แสดงแผนงาน

กิจกรรม	ปีที่ 1		ปีที่ 2	
	เดือน 1-6	เดือน 7-12	เดือน 13-18	เดือน 19-24
1. ค้นคว้าข้อมูล การสังเคราะห์ และโครงสร้าง X-ray ของสารประกอบอะไมด์ทั้งหมด	√			
2. จัดกลุ่มสารประกอบอะไมด์ทั้งหมด และ คำนวณหาโครงสร้าง พลังงาน และ การเกิดสารประกอบเชิงซ้อนกับแอนไอออนที่สำคัญ ๆ โดยการคำนวณด้วยทฤษฎีต่ำ เพื่อสำรวจแนวโน้ม และ ความสำคัญของรีเซปเตอร์เพื่อนำไปศึกษาอย่างละเอียดต่อไป	√			
3. หาโครงสร้างของสารประกอบอะไมด์กลุ่มที่มีความสำคัญมาก และการเกิดสารประกอบเชิงซ้อนกับแอนไอออนที่สำคัญ ๆ โดยทฤษฎีสูง	√	√		
4. หาพลังงานปฏิกิริยาของสารประกอบอะไมด์กลุ่มที่มีความสำคัญมาก และการเกิดสารประกอบเชิงซ้อนกับแอนไอออนที่สำคัญ ๆ โดยทฤษฎีสูง	√	√		
5. หาค่าเทอร์โมไดนามิกโดยการคำนวณความถี่ของสะปีชีส์ที่เกี่ยวข้องทั้งหมด		√		
6. เขียนรายงานและเขียนต้นฉบับเพื่อการตีพิมพ์ และเผยแพร่		√		
7. หาโครงสร้าง พลังงานปฏิกิริยาของสารประกอบอะไมด์ และการเกิดสารประกอบเชิงซ้อนกับแอนไอออนที่สำคัญ ๆ ในสารละลายน้ำ			√	
8. การคำนวณสเปกตรัม UV-VIS และ nmr ของสะปีชีส์ที่เกี่ยวข้องทั้งหมดของสารประกอบอะไมด์			√	
9. การคำนวณพลังงานออร์บิทัล และ Chemical indices ของสะปีชีส์ที่เกี่ยวข้องทั้งหมดของสารประกอบอะไมด์				√
10. เขียนรายงานและเขียนต้นฉบับเพื่อการตีพิมพ์ และเผยแพร่				√
11. เขียนรายงานฉบับสมบูรณ์				√

ผลงานที่คาดว่าจะได้รับการตีพิมพ์

ปีที่ 1: ชื่อเรื่อง “Carboxylate recognition of macrocyclic amide receptors”
คาดว่าจะตีพิมพ์ในวารสาร Supramol. Chem. (Impact factor = 1.640)

ปีที่ 2: ชื่อเรื่อง “Anion recognition of amide receptors”
คาดว่าจะตีพิมพ์ในวารสาร J. Mol. Model. (Impact factor = 1.669)

การทดลองและผลการทดลอง

1. ระบบสารประกอบ dipicolyl urea derivative

การคำนวณหาโครงสร้างของสารประกอบเอไมด์จำนวน 6 ชนิดและสารประกอบเชิงซ้อนที่เกิดระหว่างสารประกอบ dipicolyl urea derivative กับแอนไอออน และพลังงานการรวมตัวของสารประกอบเชิงซ้อนโดยการคำนวณด้วยวิธี DFT/B3LYP ได้ผลลัพธ์ดังนี้
โครงสร้างของสารประกอบ dipicolyl urea derivative พบว่ามี 4 โครงรูปดังแสดงในรูปที่ 1.1 (Isomers a, b, c และ c') โดยวิธี B3LYP/6–311+G(d,p)

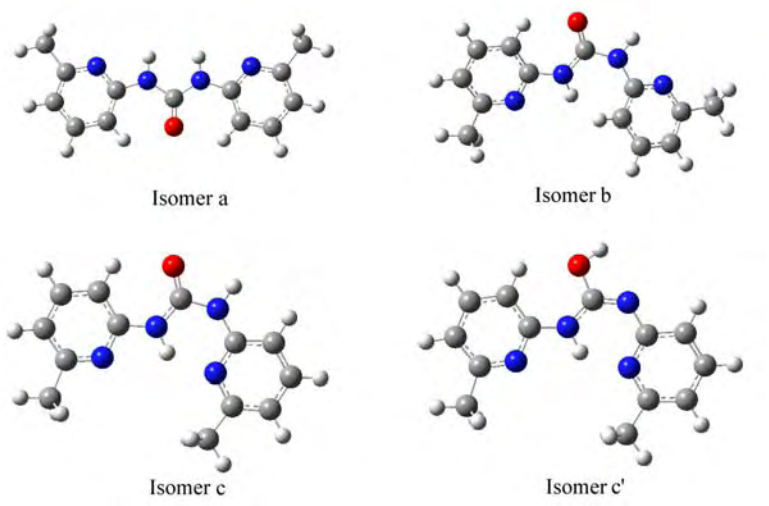

รูปที่ 1.1 สารประกอบ dipicolyl urea derivative และโครงรูปต่าง ๆ

1.1 พลังงานการเปลี่ยนแปลงของโครงรูปของสารประกอบ Dipicolyl urea derivative

โครงรูปของสารประกอบ dipicolyl urea derivative สามารถเปลี่ยนแปลงโครงรูประหว่างกันโดยผ่าน transition states ts_1a_1b, ts_1b_1c และ ts_1c_1c' ดังแสดงในรูปที่ 1.2 พลังงานสัมพัทธ์ (หน่วย kcal/mol) ของโครงรูปต่างๆ และ transition states ที่สอดคล้องกันได้กำกับไว้ใต้ภาพโมเลกุลที่แสดงในรูปที่ 1.2 การเปลี่ยนแปลงพลังงานสัมพัทธ์ของโครงรูปผ่าน transition states ดังกล่าวได้แสดงในรูปที่ 1.3

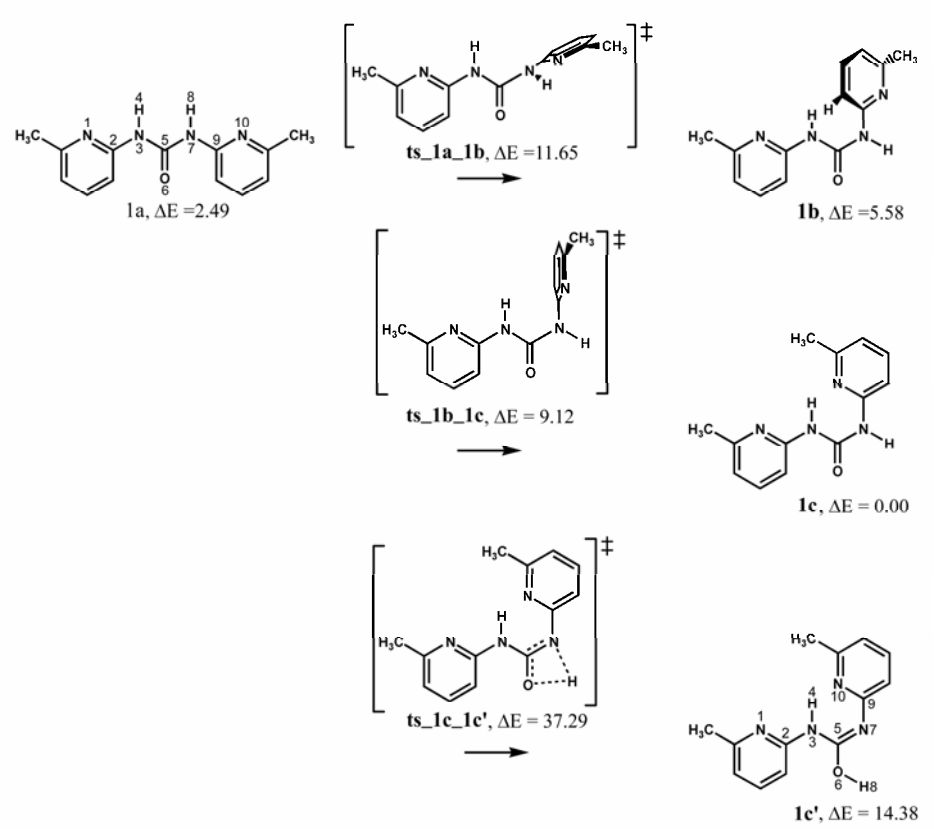

รูปที่ 1.2 การเปลี่ยนแปลงระหว่างกันของโครงรูปของสารประกอบ dipicolyl urea derivative

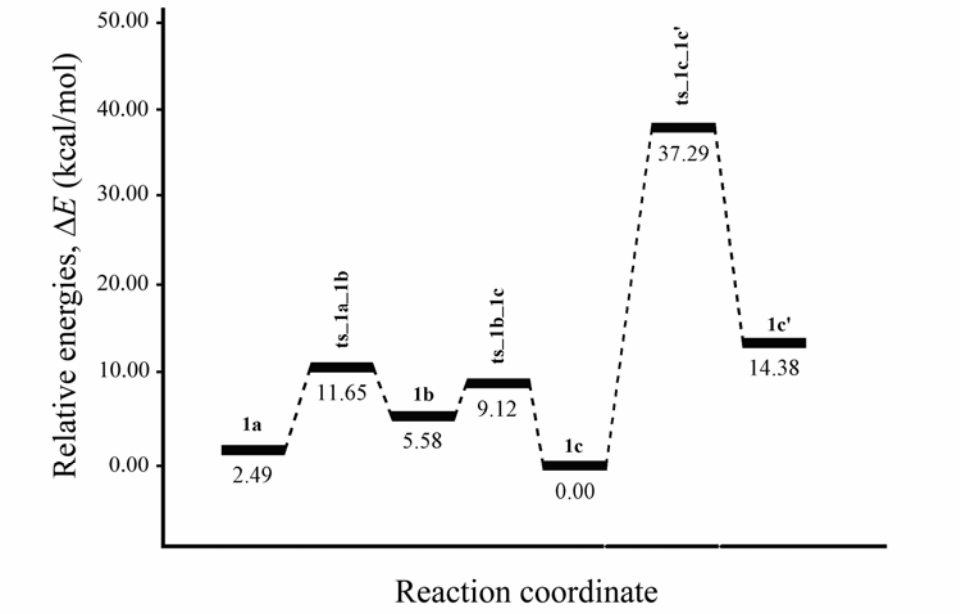

รูปที่ 1.3 แสดงระดับพลังงานสัมพัทธ์ของปฏิกิริยาการเปลี่ยนแปลงโครงรูป

1.2 พลังงานการรวมตัวของสารประกอบเชิงซ้อนของ Dipicolyl urea derivative กับ แอนไอออนชนิดต่าง ๆ

ค่าพลังงานการรวมตัวของสารประกอบเชิงซ้อนที่เกิดระหว่างโครงรูปต่าง ๆ ของ dipicolyl urea derivative กับ formic acid, formate ion, acetic acid, acetate ion, benzoic acid, benzoate ion, oxalic acid และ oxalate ion ได้แสดงในตารางที่ 1.1 และการนำเสนอเป็นกราฟเปรียบเทียบดังแสดงในรูปที่ 1.4 ตัวอย่างปฏิกิริยาการเกิดสารประกอบเชิงซ้อนระหว่างโครงรูปต่าง ๆ ของ dipicolyl urea derivative กับ formic acid ได้แสดงในรูปที่ 1.5

ตารางที่ 1.1 ค่าพลังงานการรวมตัวของสารประกอบเชิงซ้อนที่เกิดระหว่างโครงรูปต่าง ๆ ของ dipicolyl urea derivative กับ carboxylic acids และ carboxylate ions โดยวิธี B3LYP/6–31+G(d,p)

Reaction	ΔE , kcal/mol
Formic acid/formate ion	
a + fma → a/fma	–6.08
b + fma → b/fma″	–4.12
b + fma → b/fma	–12.22
b + fma → b/fma′	–1.39
c + fma → c/fma	–15.30
c′ + fma → c′/fma	–19.98
a + fm^- → $[a/fm]^-$	–26.67
Acetic acid/acetate ion	
a + aca → a/aca	–3.79
b + aca → b/aca″	–1.56
b + aca → b/aca	–11.89
b + aca → b/aca′	–1.29
c + aca → c/aca	–15.03
c′ + aca → c′/aca	–17.97
a + ac^- → $[a/ac]^-$	–28.15
Benzoic acid/benzoate ion	
a + bza → a/bza	–2.22
b + bza → b/bza	–12.25
b′ + bza → b/bza′	–1.87
b″ + bza → b/bza″	–0.31
c + bza → c/bza	–15.34
c′ + bza → c′/bza	–18.59
a + bz^- → $[a/bz]^-$	–25.10
Oxalic acid/oxalate ion	
a + oxa → a/oxa	–9.63
b + oxa → b/oxa	–14.39
b′ + oxa → b/oxa′	–2.48
b″ + oxa → b/oxa″	–8.45
c + oxa → c/oxa [b]	–17.54
a + ox^{2-} → $[a/ox]^{2-}$	–16.47
2 a + ox^{2-} → $[a/ox/a]^{2-}$	–51.48

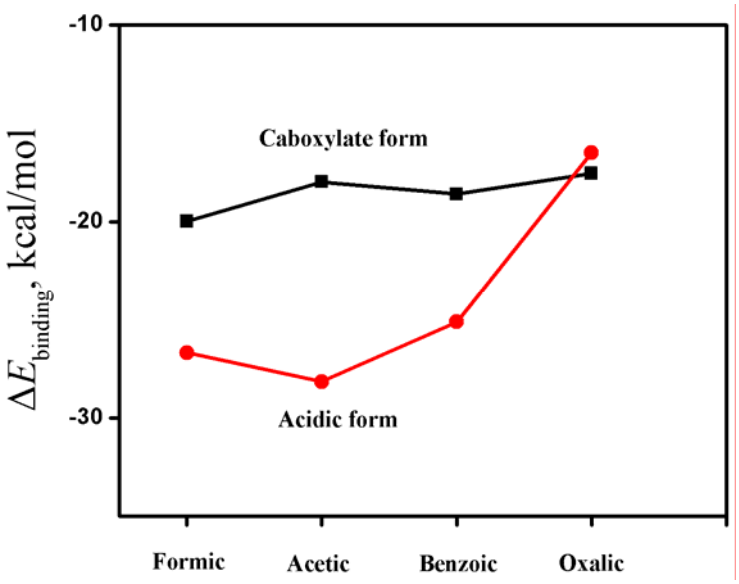

รูปที่ 1.4 พลังงานการรวมตัวของสารประกอบเชิงซ้อนที่เกิดระหว่างสารประกอบ dipicolyl urea derivative กับ carboxylic acids และ carboxylate ions

ค่าเทอร์โมไดนามิกการรวมตัวของสารประกอบเชิงซ้อนของ dipicolyl urea derivative กับ แอนไอออนชนิดต่าง ๆ ได้แสดงในตารางที่ 1.2

ตารางที่ 1.2 ค่าเทอร์โมไดนามิก (หน่วย kcal/mol) การรวมตัวของสารประกอบเชิงซ้อนที่เกิดระหว่างโครงรูปต่าง ๆ ของ Dipicolyl urea derivative กับ carboxylic acids และ carboxylate ions และค่าคงที่สมดุล ณ อุณหภูมิ 298 K ซึ่งคำนวณด้วยวิธี B3LYP/6–31+G(d,p)

Reaction	ΔH_{298}	ΔG_{298}	K_{298}
Formic acid/formate ion			
a + fma → a/fma	–5.81	4.11	9.68×10^{-4}
b + fma → b/fma″	–3.72	5.57	8.27×10^{-5}
b + fma → b/fma	–12.16	–1.37	1.01×10^{1}
b + fma → b/fma′	–1.50	9.46	1.16×10^{-7}
c + fma → c/fma	–15.36	–3.97	8.13×10^{2}
c′ + fma → c′/fma	–20.52	–8.17	9.70×10^{5}
a + fm^- → $[a/fm]^-$	–26.61	–16.40	1.05×10^{12}
Acetic acid/acetate ion			
a + aca → a/aca	–3.50	7.21	5.15×10^{-6}
b + aca → b/aca″	–1.12	8.39	7.05×10^{-7}
b + aca → b/aca	–11.61	–1.08	6.15×10^{0}
b + aca → b/aca′	–1.20	9.83	6.21×10^{-8}
c + aca → c/aca	–14.88	–3.66	4.83×10^{2}
c′ + aca → c′/aca	–18.47	–5.54	1.15×10^{4}
a + ac^- → $[a/ac]^-$	–27.93	–17.88	1.27×10^{13}
Benzoic acid/benzoate ion			
a + bza → a/bza	–1.72	8.77	3.71×10^{-7}
b + bza → b/bza	–11.88	–1.12	6.60×10^{0}
b′ + bza → b/bza′	–1.65	9.60	9.12×10^{-8}
b″ + bza → b/bza″	0.25	10.44	2.24×10^{-8}
c + bza → c/bza	–15.06	–3.73	5.42×10^{2}
c′ + bza → c′/bza	–18.44	–6.63	7.20×10^{4}
a + bz^- → $[a/bz]^-$	–24.76	–14.42	3.71×10^{10}
Oxalic acid/oxalate ion			
a + oxa → a/oxa	–8.85	2.45	1.61×10^{-2}
b + oxa → b/oxa	–13.17	–2.73	9.96×10^{1}
b′ + oxa → b/oxa′	–2.96	7.88	1.67×10^{-6}
b″ + oxa → b/oxa″	–7.53	3.62	2.22×10^{-3}
c + oxa → c/oxa [b]	–16.24	–5.01	4.73×10^{3}
a + ox^{2-} → $[a/ox]^{2-}$	–64.24	–56.50	2.65×10^{41}
2 a + ox^- → $[a/ox]^-$	–23.34	–14.93	8.86×10^{10}

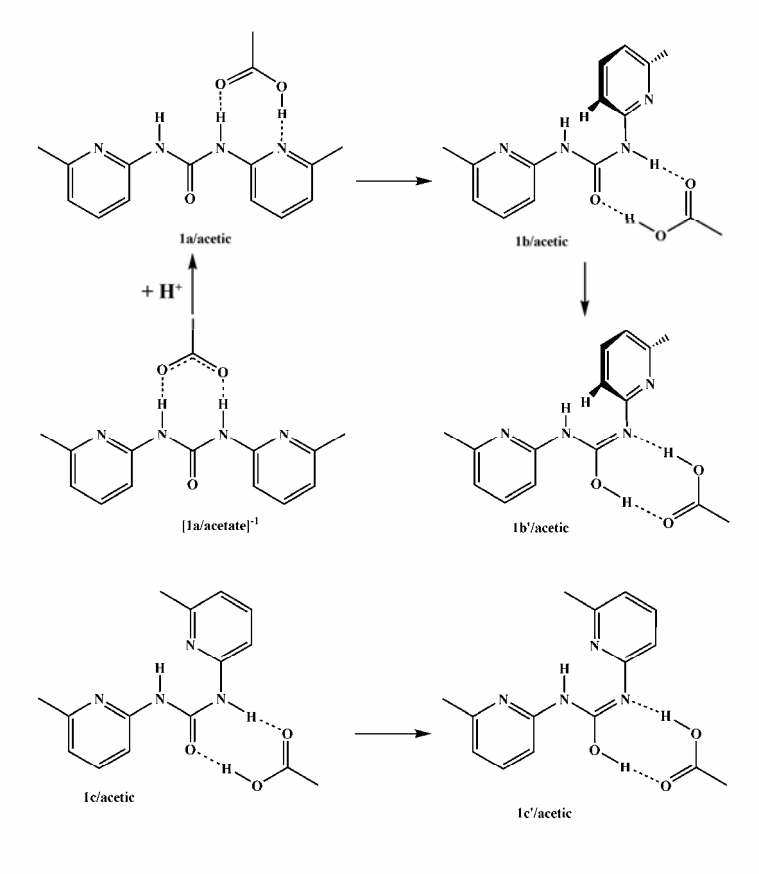

รูปที่ 1.5 ปฏิกิริยาการเกิดสารประกอบเชิงซ้อนระหว่างโครงรูปต่าง ๆ ของ dipicolyl urea derivative กับ acetic acid และ acetate ion

2. ระบบสารประกอบ tetraamide receptors

โครงสร้างสารประกอบ tetraamide receptors 1 (n=0), 2 (n=1), 3 (n=2), 4, 5 และ 6 คำนวนโดยวิธี B3LYP/6–31G(d) ได้แสดงในรูปที่ 2.1

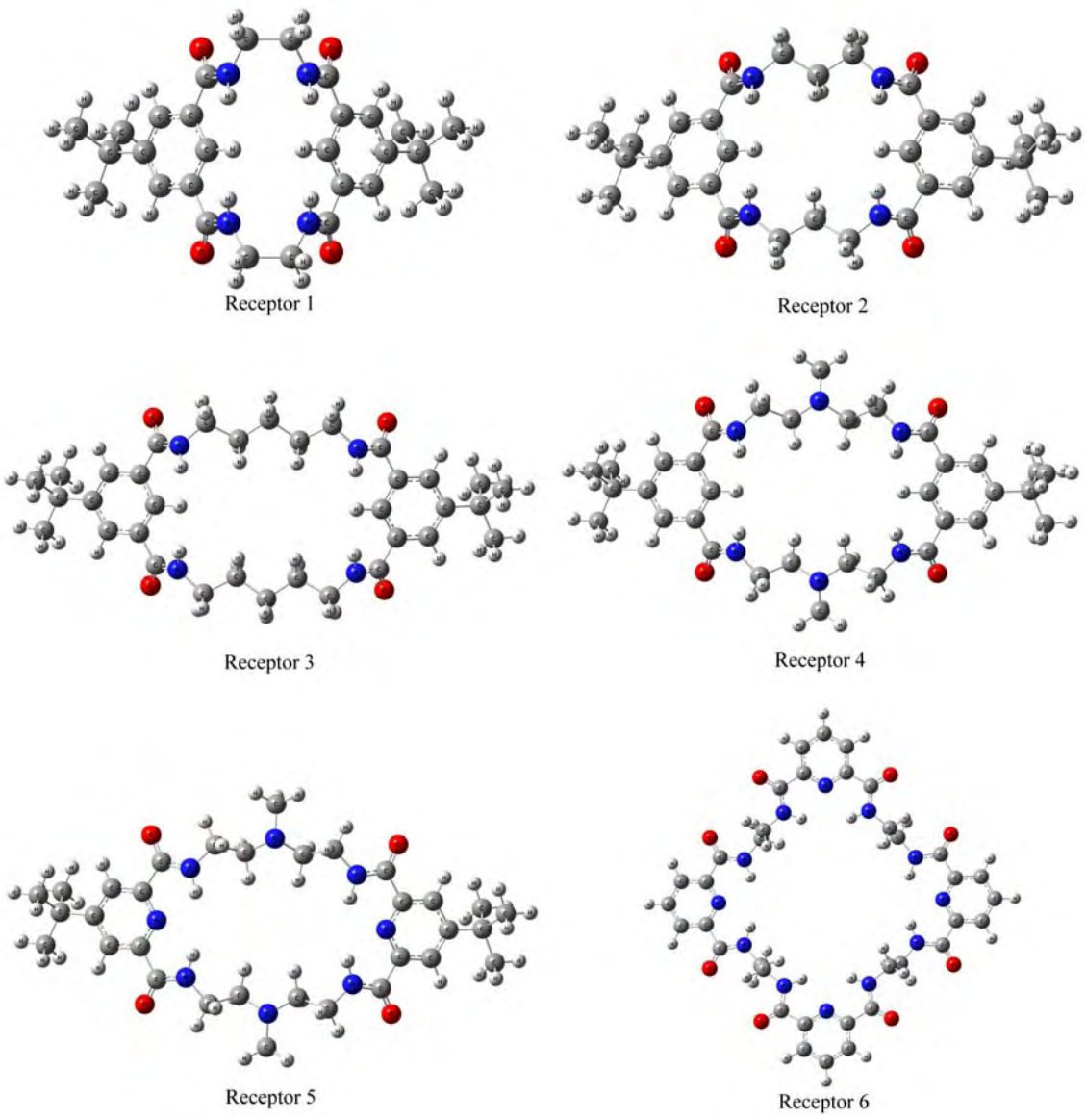

รูปที่ 2.1 โครงสร้างที่เสถียรที่สุดของสารประกอบ tetraamide receptors 1 (n=0), 2 (n=1), 3 (n=2), 4, 5 และ 6

2.1 พลังงานการรวมตัวของสารประกอบเชิงซ้อนระหว่างสารประกอบ tetraamide receptors กับแอนไอออนชนิดต่าง ๆ

ค่าพลังงานการรวมตัวของสารประกอบเชิงซ้อนที่เกิดระหว่างสารประกอบ tetraamide receptors 1, 2, 3, 4, 5, และ 6 กับ แอนไอออน F^-, Cl^-, Br^-, AcO^-, HSO_4^-, $H_2PO_4^-$ ได้แสดงในตารางที่ 2.1 และการนำเสนอเป็นกราฟเปรียบเทียบดังแสดงในรูปที่ 2.2

ตารางที่ 2.1 ค่าพลังงานการรวมตัวของสารประกอบเชิงซ้อนที่เกิดระหว่างสารประกอบ tetraamide receptors 1, 2, 3, 4, 5, และ 6 กับแอนไอออน F^-, Cl^-, Br^-, AcO^-, HSO_4^-, $H_2PO_4^-$ โดยวิธี B3LYP/6–31G(d)

Complexes with anions	ΔE, kcal/mol					
	Receptor 1	Receptor 2	Receptor 3	Receptor 4	Receptor 5	Receptor 6
F^-	-131.34	-135.33	-139.36		-127.57	
Cl^-	–58.10	–66.73	–66.71	–64.98	–48.32	–55.87
Br^-	–64.63	–74.79	–73.97	–71.10	–54.84	–61.84
AcO^-	–67.65	–67.89	–73.02	–71.12	–53.88	–57.36
HSO_4^-	–46.77	–56.98	–59.42	–57.06	–40.01	–56.39
$H_2PO_4^-$	–60.63	–66.88	–71.35	–73.79	–56.26	–64.00

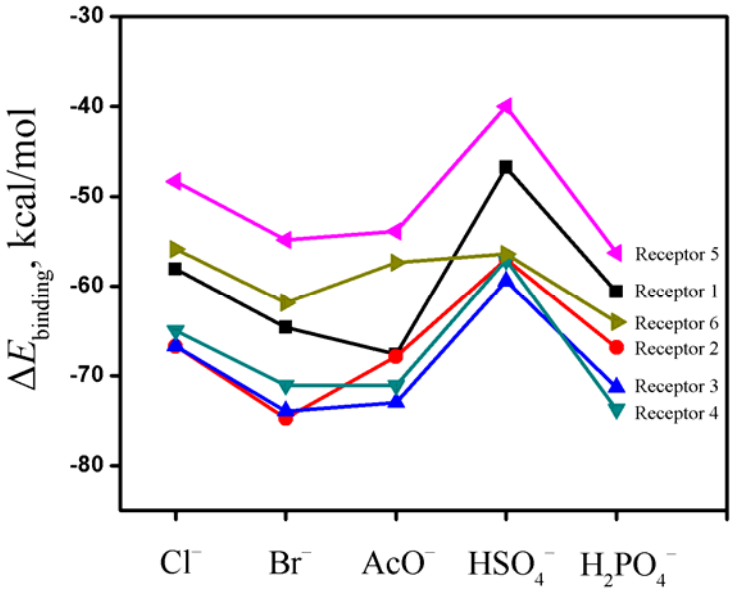

รูปที่ 2.2 พลังงานการรวมตัวของสารประกอบเชิงซ้อนที่เกิดระหว่างสารประกอบ tetraamide receptors 1, 2, 3, 4, 5, และ 6 กับแอนไอออน

ค่าเทอร์โมไดนามิกการรวมตัวของสารประกอบเชิงซ้อนที่เกิดระหว่างโครงรูปต่าง ๆ ของ tetraamide receptors 1, 2, 3, 4, 5, และ 6 กับ F^-, Cl^-, Br^-, AcO^-, HSO_4^-, $H_2PO_4^-$ ได้แสดงในตารางที่ 2.2

ตารางที่ 2.2 ค่าเทอร์โมไดนามิก (หน่วย kcal/mol) การรวมตัวของสารประกอบเชิงซ้อนที่เกิดระหว่างสารประกอบ tetraamide receptors 1, 2, 3, 4, 5, และ 6 กับ F^-, Cl^-, Br^-, AcO^-, HSO_4^-, $H_2PO_4^-$ โดยวิธี B3LYP/6–31G(d)

Complexes with anions	Receptor 1		Receptor 2		Receptor 3		Receptor 4		Receptor 5		Receptor 6	
	ΔH_{298}	ΔG_{298}	ΔH_{298}	ΔG_{298}	ΔH_{298}	ΔG_{298}	ΔH_{298}	ΔG_{298}	ΔH_{298}	ΔG_{298}	ΔH_{298}	ΔG_{298}
F^-	-132.49	-122.56	-136.39	-127.02	-140.98	-128.80			-129.27	-116.19		
Cl^-	–58.62	–49.88	–67.14	–59.79	–67.65	–57.52	–66.21	–54.50	–49.58	–37.50	–57.10	–43.68
Br^-	–65.19	–55.71	–76.24	–64.62	–74.78	–64.61	–72.29	–60.28	–55.92	–43.87	–62.42	–51.13
AcO^-	–67.21	–56.75	–68.02	–55.72	–73.42	–60.60	–71.23	–58.12	–54.06	–39.68	–56.98	–43.29
HSO_4^-	–46.08	–35.30	–56.36	–45.57	–59.14	–47.23	–57.56	–41.47	–40.11	–24.44	–55.90	–41.19
$H_2PO_4^-$	–59.94	–48.90	–66.52	–54.14	–71.17	–57.54	–74.45	–57.17	–56.87	–39.27	–63.79	–46.76

3. ระบบสารประกอบเอไมด์–คาลิกซ์[4]เอรีน

การคำนวณหาโครงสร้างของสารประกอบเอไมด์ลิแกนด์ LiL^+, NaL^+ และ KL^+ เมื่อ **L** เป็นสารประกอบเอไมด์–คาลิกซ์[4]เอรีน และสารประกอบเชิงซ้อนที่เกิดระหว่างเอไมด์ลิแกนด์เหล่านี้ กับแอนไอออน และ การคำนวณหาพลังงานการรวมตัวของสารประกอบเชิงซ้อนโดยการคำนวณด้วยวิธี ONIOM(B3LYP/6–31G(d):AM1) ได้ผลลัพธ์ดังนี้

3.1 โครงสร้างของสารประกอบเอไมด์ลิแกนด์ LiL^+, NaL^+ และ KL^+

โครงสร้างของสารประกอบเอไมด์ลิแกนด์ LiL^+, NaL^+ และ KL^+ ดังแสดงในรูปที่ 3.1 โดยวิธี ONIOM(B3LYP/6–31G(d):AM1)

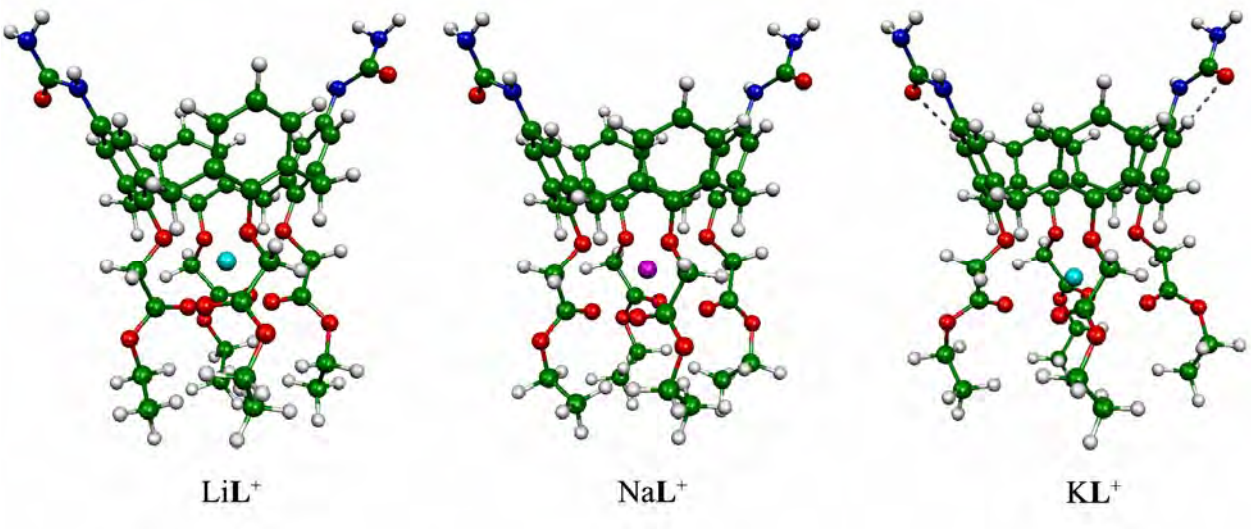

รูปที่ 3.1 โครงสร้างของสารประกอบเอไมด์ชนิด (a) LiL^+, (b) NaL^+ และ (c) KL^+

โครงสร้างสารประกอบเชิงซ้อนที่เกิดระหว่างเอไมด์ลิแกนด์ LiL^+, NaL^+ และ KL^+ กับไอออนชนิดเฮไลด์ (F^-, Cl^- และ Br^-) และแอนไอออน HCO_3^-, HSO_4^- และ CH_3COO^- ดังแสดงในรูปที่ 3.2, 3.3 และ 3.4

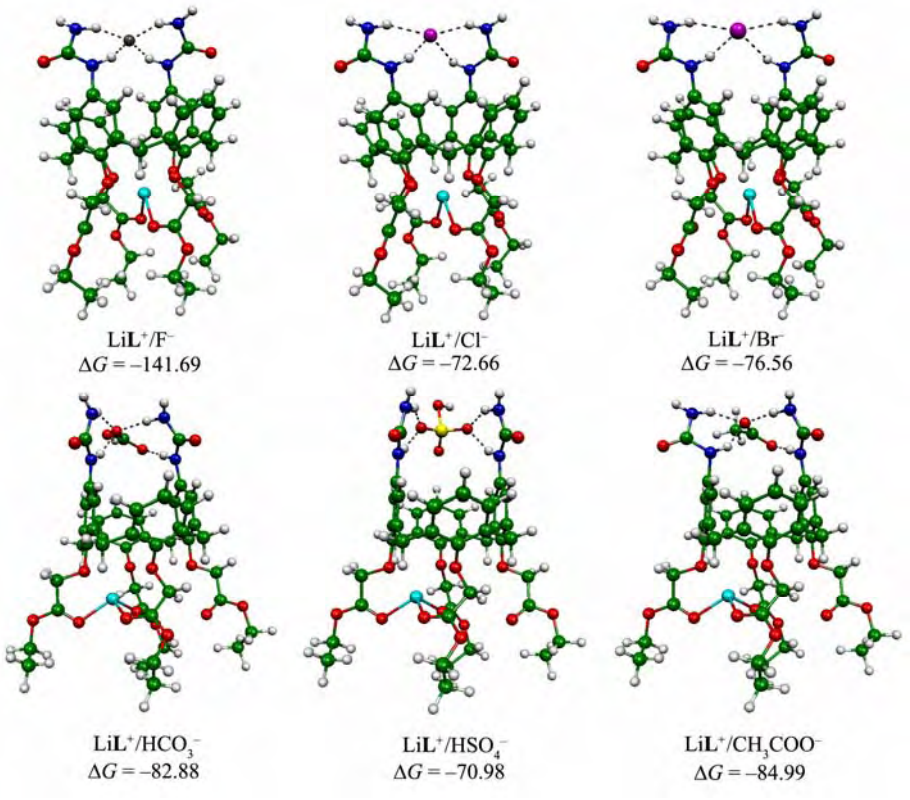

รูปที่ 3.2 โครงสร้างที่เสถียรที่สุดของสารประกอบเชิงซ้อนที่เกิดระหว่างเอไมด์ลิแกนด์ Li**L**$^{+}$ กับไอออนชนิดเฮไลด์ (F^{-}, Cl^{-} และ Br^{-}) และแอนไอออน HCO_3^{-}, HSO_4^{-} และ CH_3COO^{-}

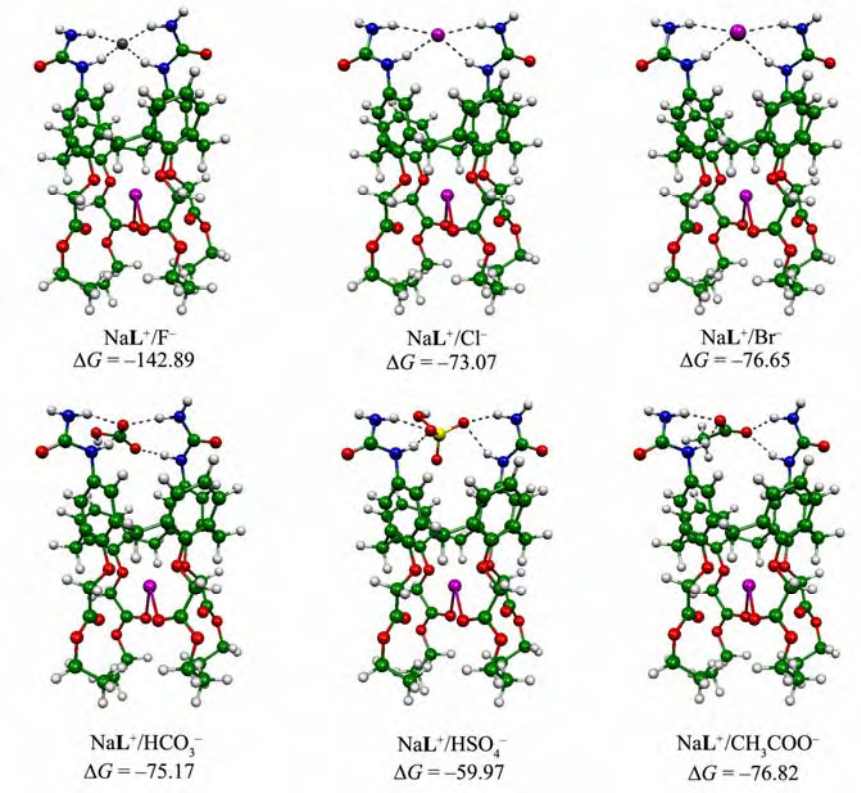

รูปที่ 3.3 โครงสร้างที่เสถียรที่สุดของสารประกอบเชิงซ้อนที่เกิดระหว่างเอไมด์ลิแกนด์ NaL^+ กับไอออนชนิดเฮไลด์ (F^-, Cl^- และ Br^-) และแอนไอออน HCO_3^-, HSO_4^- และ CH_3COO^-

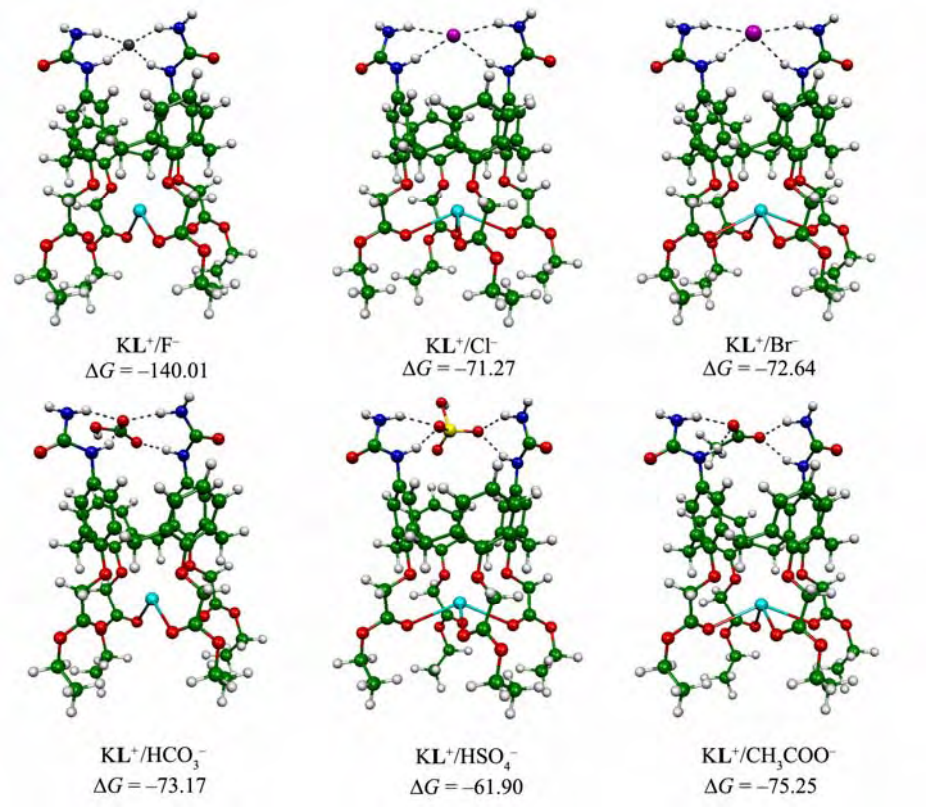

รูปที่ 3.4 โครงสร้างที่เสถียรที่สุดของสารประกอบเชิงซ้อนที่เกิดระหว่างเอไมด์ลิแกนด์ $\mathbf{KL}^+$ กับไอออนชนิดเฮไลด์ F^-, Cl^- และ Br^- และแอนไอออน HCO_3^-, HSO_4^- และ CH_3COO^-

3.2 พลังงานยึดเกาะของแอนไอออนกับสารประกอบเอไมด์ลิแกนด์ $\mathbf{LiL}^+$, $\mathbf{NaL}^+$ และ $\mathbf{KL}^+$

พลังงานยึดเกาะของแอนไอออนกับสารประกอบเอไมด์ลิแกนด์ $\mathbf{LiL}^+$, $\mathbf{NaL}^+$ และ $\mathbf{KL}^+$ ค่าทางเทอร์โมไดนามิกของการยึดเกาะ ค่าคงที่สมดุล และ ที่สัมประสิทธิ์การเลือกเฉพาะ (selectivity coefficient, K_B^A) ได้แสดงในตารางที่ 3.1

ตารางที่ 3.1 พลังงานยึดเกาะของแอนไอออนกับสารประกอบเอไมด์ลิแกนด์ Li**L**$^+$, Na**L**$^+$ และ K**L**$^+$ ค่าทางเทอร์โมไดนามิกของการยึดเกาะ ค่าคงที่สมดุล และ ที่สัมประสิทธิ์การเลือกเฉพาะ

Host/guest complexes	ΔE [a]	ΔH^{o}_{298} [a]	ΔG^{o}_{298} [a]	K	Log K	K^{A}_{B} [b]
Receptor Li**L**$^+$:						
Li**L**$^+$/F^-	–152.81	–154.52	–141.69	2.44×10^{10}	10.39	1.53×10^{5}
Li**L**$^+$/Cl^-	–82.95	–84.07	–72.66	2.12×10^{5}	5.33	1.33×10^{0}
Li**L**$^+$/Br^-	–86.40	–87.43	–76.56	4.10×10^{5}	5.61	2.57×10^{0}
Li**L**$^+$/HCO_3^-	–96.75	–97.30	–82.84	1.18×10^{6}	6.07	7.41×10^{0}
Li**L**$^+$/HSO_4^-	–84.68	–84.50	–70.98	1.60×10^{5}	5.20	1.00×10^{0}
Li**L**$^+$/CH_3COO^-	–99.15	–99.96	–84.99	1.70×10^{6}	6.23	1.07×10^{1}
Receptor Na**L**$^+$:						
Na**L**$^+$/F^-	–153.03	–154.40	–142.89	2.98×10^{10}	10.47	1.20×10^{6}
Na**L**$^+$/Cl^-	–82.86	–83.65	–73.07	2.27×10^{5}	5.36	9.13×10^{0}
Na**L**$^+$/Br^-	–86.29	–87.03	–76.65	4.16×10^{5}	5.62	1.67×10^{1}
Na**L**$^+$/HCO_3^-	–89.63	–90.13	–75.17	3.24×10^{5}	5.51	1.30×10^{1}
Na**L**$^+$/HSO_4^-	–74.38	–74.51	–59.97	2.49×10^{4}	4.40	1.00×10^{0}
Na**L**$^+$/CH_3COO^-	–91.00	–91.44	–76.82	4.28×10^{5}	5.63	1.72×10^{1}
Receptor K**L**$^+$:						
K**L**$^+$/F^-	–153.02	–154.71	–140.01	1.84×10^{10}	10.26	5.33×10^{5}
K**L**$^+$/Cl^-	–82.78	–83.78	–71.27	1.68×10^{5}	5.22	4.86×10^{0}
K**L**$^+$/Br^-	–86.22	–87.73	–72.64	2.12×10^{5}	5.33	6.14×10^{0}
K**L**$^+$/HCO_3^-	–89.74	–90.49	–73.17	2.31×10^{5}	5.36	6.71×10^{0}
K**L**$^+$/HSO_4^-	–76.00	–75.76	–61.90	3.45×10^{4}	4.54	1.00×10^{0}
K**L**$^+$/CH_3COO^-	–91.03	–91.65	–75.25	3.28×10^{5}	5.52	9.52×10^{0}

[a] In kcal/mol.

[b] Selectivity coefficient of guests with respect to HSO_4^- complex.

3.3 พลังงานยึดเกาะของแอนไอออนกับสารประกอบเอไมด์ลิแกนด์

การคำนวณหาโครงสร้างของสารประกอบเอไมด์ลิแกนด์ Mg**L**$^{2+}$ และสารประกอบเชิงซ้อนที่เกิดระหว่างเอไมด์ลิแกนด์เหล่านี้ กับไดคาร์บอกซาเลต แอนไอออน และการคำนวณหาพลังงานการรวมตัวของสารประกอบเชิงซ้อนโดยการคำนวณด้วยวิธี ONIOM(B3LYP/6–31G(d):AM1) ได้ผลลัพธ์ดังนี้

โครงสร้างของสารประกอบเชิงซ้อนที่เกิดระหว่างเอไมด์ลิแกนด์ $Mg\mathbf{L}^{2+}$ กับไดคาร์บอกซาเลต แอนไอออน ดังแสดงในรูปที่ 5 โดยวิธี ONIOM(B3LYP/6–31G(d):AM1)

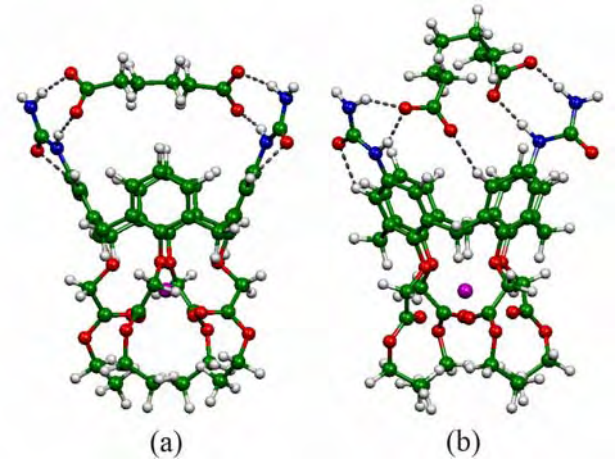

รูปที่ 3.5 โครงสร้างที่เสถียรที่สุดของสารประกอบเชิงซ้อนที่เกิดระหว่างเอไมด์ลิแกนด์ $Mg\mathbf{L}^{2+}$ กับ (a) adipate and (b) succinate ions.

4. ระบบสารประกอบ 1,3–bis(4–nitrophenyl)urea

โครงสร้างของสารประกอบเชิงซ้อนระหว่าง receptor 1 กับ แอนไอออน และพลังงานอิสระการเกิดสารประกอบเชิงซ้อนโดยวิธี B3LYP/6-311+G(d,p) ได้แสดงในรูปที่ 4.1 พลังงาน และค่าอุณหพลศาสตร์ของการเกิดสารประกอบเชิงซ้อนระหว่างรีเซปเตอร์ 1 กับแอออนไอออน ได้แสดงในตารางที่ 4.1 ส่วนค่าพลังงานออร์บิทัล LUMO, HOMO และพลังงานแถบ ของการเกิดสารประกอบเชิงซ้อนระหว่างรีเซปเตอร์ 1 กับแอออนไอออน ได้แสดงในตารางที่ 4.2

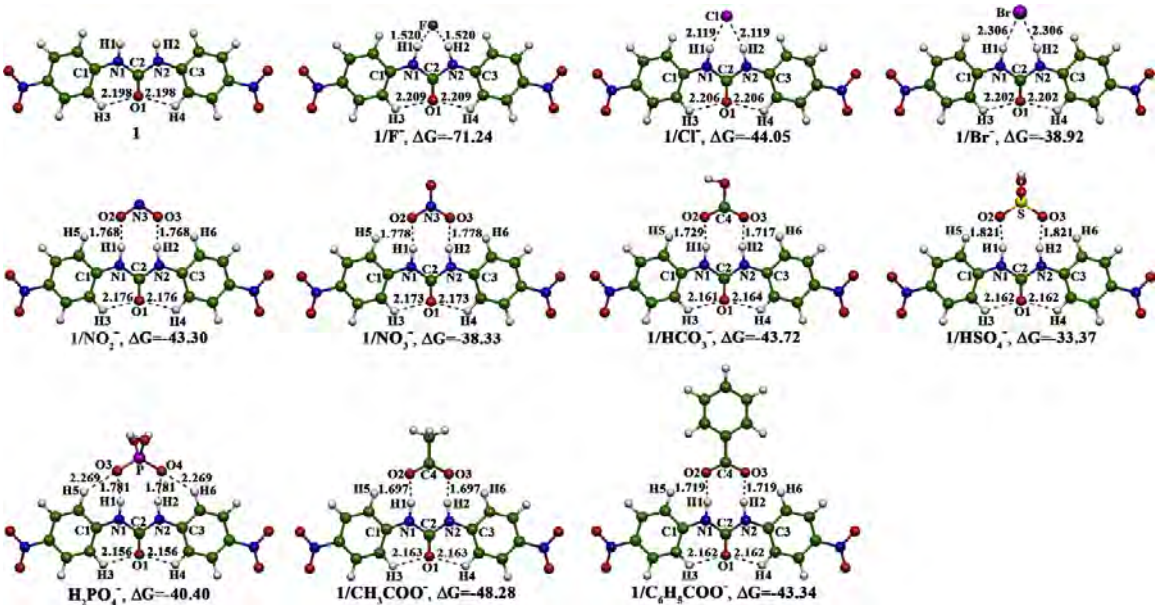

รูปที่ 4.1 แสดงโครงสร้างของสารประกอบเชิงซ้อนระหว่าง receptor **1** กับ แอนไอออน และพลังงานอิสระการเกิดสารประกอบเชิงซ้อน

ตารางที่ 4.1 พลังงาน และค่าอุณหพลศาสตร์ของการเกิดสารประกอบเชิงซ้อนระหว่างรีเซปเตอร์ **1** กับแอออนไอออน โดยการคำนวณโดยวิธี B3LYP/6-311+G(d,p)

Host/guest complexes	ΔE [a]	ΔH^{o}_{298} [a]	ΔG^{o}_{298} [a]	log K
1/F^-	-79.62	-80.42	-71.24	52.41
1/Cl^-	-52.21	-52.78	-44.05	32.41
1/Br^-	-47.02	-47.45	-38.92	28.63
1/NO_2^-	-54.76	-55.02	-43.30	31.86
1/NO_3^-	-48.67	-48.65	-38.33	28.20
1/HCO_3^-	-55.80	-55.92	-43.72	32.17
1/HSO_4^-	-45.24	-45.16	-33.37	24.55
1/$H_2PO_4^-$	-52.28	-52.24	-40.40	29.72
1/CH_3COO^-	-60.47	-60.60	-48.24	35.49
1/$C_6H_5COO^-$	-55.68	-55.68	-43.34	31.89

[a] In kcal/mol

ตารางที่ 4.2 แสดงค่าพลังงานออร์บิทัล LUMO, HOMO และพลังงานแถบ ของการเกิดสารประกอบเชิงซ้อนระหว่างรีเซปเตอร์ **1** กับแอออนไอออน

Host/guest	E_{LUMO} [a]	E_{HOMO} [a]	ΔE_{gap} [a]
1	–3.020	–7.129	4.109
1/F^-	–0.463	–3.701	3.238
1/Cl^-	–0.626	–3.701	3.075
1/Br^-	–0.680	–3.347	2.667
1/NO_2^-	–0.599	–3.320	2.721
1/NO_3^-	–0.653	–4.136	3.483
1/HCO_3^-	–0.544	–3.918	3.374
1/HSO_4^-	–0.680	–4.163	3.483
1/$H_2PO_4^-$	–0.544	–3.973	3.429
1/CH_3COO^-	–0.463	–3.810	3.347
1/$C_6H_5COO^-$	–0.544	–3.918	3.374

[a] In eV.

5. ระบบสารประกอบ 8,8'–dithioureido–2,2'–binaphthalene

โครงสร้างของสารประกอบเชิงซ้อนที่เกิดขึ้นระหว่างสารประกอบ 8,8'–dithioureido–2,2'–binaphthalene (**1**) กับคาร์บอกซิเลตและไดคาร์บอกซิเลต ได้แสดงในรูปที่ 5.1 ส่วนการเกิดสารประกอบเชิงซ้อนกับแอนไอออนชนิดเฮไลด์ และไอออนชนิดที่มีออกซิเจนเป็นองค์ประกอบได้แสดงในรูปที่ 5.2 ค่าพลังงานจัดตัวของรีเซปเตอร์ **1** (host) แอนไอออน (guest) และพลังงานการเกิดสารประกอบเชิงซ้อน โดยวิธี ONIOM (B3LYP/6-31G(d):AM1) ได้แสดงไว้ในตารางที่ 5.1

โครงสร้างของสารประกอบเชิงซ้อนที่เกิดขึ้นระหว่างสารประกอบ 8,8'-bis(3-butylthioureido methyl)-2,2'-binaphthalene (**2**) กับคาร์บอกซิเลตและไดคาร์บอกซิเลต ได้แสดงในรูปที่ 5.3 ส่วนการเกิดสารประกอบเชิงซ้อนกับแอนไอออนชนิดเฮไลด์และไอออนชนิดที่มีออกซิเจนเป็นองค์ประกอบได้แสดงในรูปที่ 5.4 ค่าพลังงานจัดตัวของรีเซปเตอร์ **2** (host) แอนไอออน (guest) และพลังงานการเกิดสารประกอบเชิงซ้อน โดยวิธี ONIOM (B3LYP/6-31G(d):AM1) ได้แสดงไว้ในตารางที่ 5.12

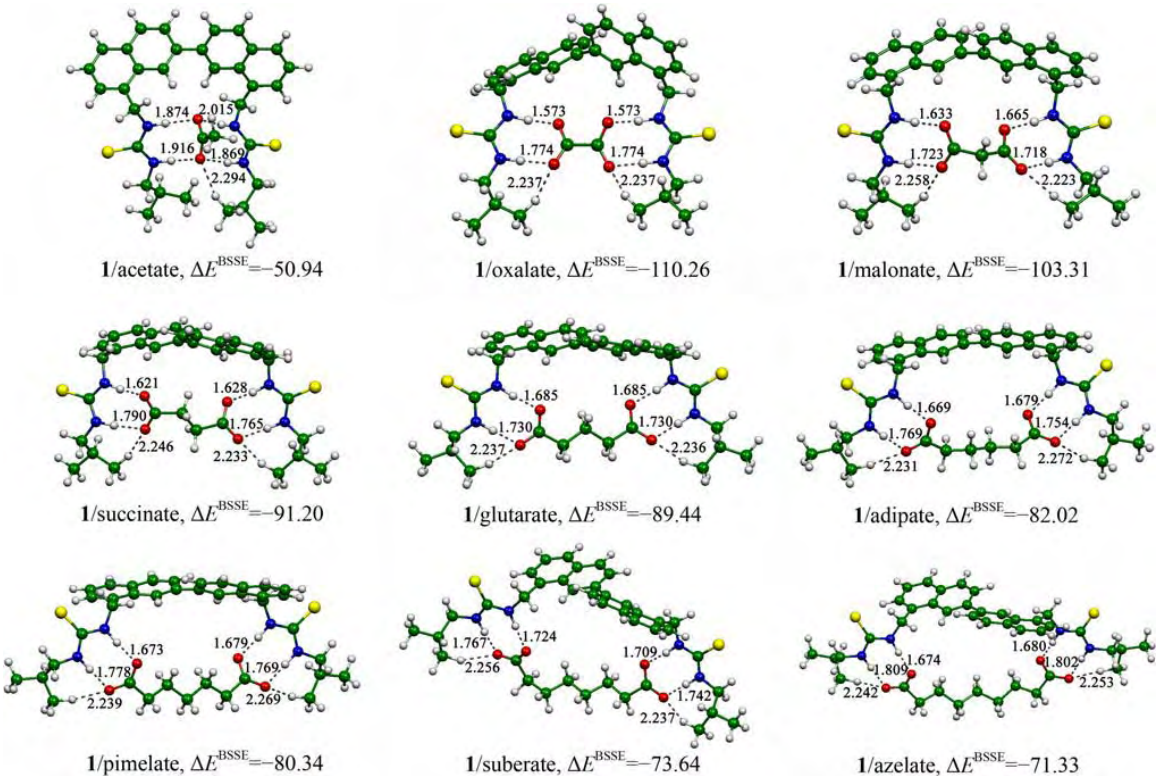

รูปที่ 5.1 แสดงโครงสร้างของสารประกอบเชิงซ้อนระหว่างสารประกอบ 8,8'–dithioureido–2,2'–binaphthalene (**1**) กับคาร์บอกซิเลตและไดคาร์บอกซิเลต

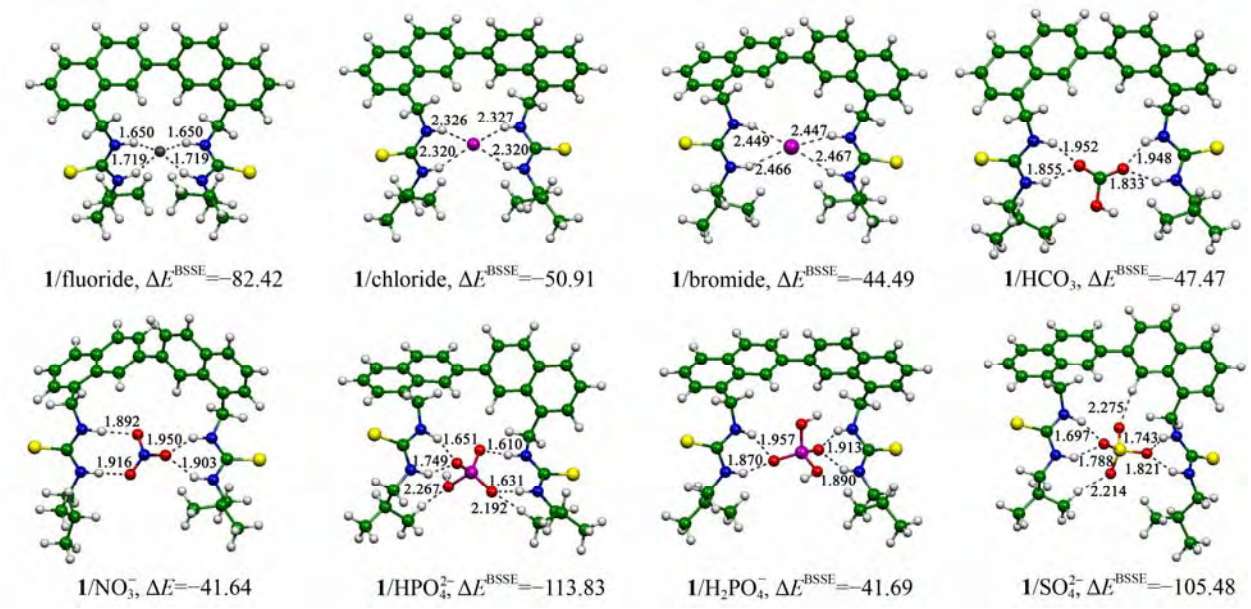

รูปที่ 5.2 แสดงโครงสร้างของสารประกอบเชิงซ้อนระหว่างสารประกอบ 8,8'–dithioureido–2,2'–binaphthalene (**1**) กับแอนไอออนชนิดเฮไลด์ และไอออนชนิดที่มีออกซิเจนเป็นองค์ประกอบ

ตารางที่ 5.1 แสดงค่าพลังงานจัดตัวของรีเซปเตอร์ **1** (host) แอนไอออน (guest) และพลังงานการเกิดสารประกอบเชิงซ้อน โดยวิธี ONIOM (B3LYP/6-31G(d):AM1)

Host:guest	Host			Guest			$\Delta E_{\text{preorg.}}^{\text{total}}$ [a]	$\Delta E_{\text{complex}}$ [a]
	$\Delta E_{\text{preorg}}^{\text{host}}$ [a]	ΔH^{298} [a]	ΔG^{298} [a]	$\Delta E_{\text{preorg.}}^{\text{guest}}$ [b]	ΔH^{298} [b]	ΔG^{298} [b]		
1/acetate	11.66	10.43	13.71	1.85	1.30	2.89	13.51	-80.65
1/oxalate	14.80	12.66	19.26	0.39	0.40	-0.02	15.19	-156.05
1/malonate	14.66	13.04	17.47	1.75	1.22	2.37	16.41	-144.93
1/succinate	12.43	10.76	15.87	4.56	3.52	6.14	16.99	-132.95
1/glutarate	12.34	10.68	15.63	1.79	0.74	3.79	14.13	-125.45
1/adipate	13.05	11.96	14.91	4.72	5.21	3.00	17.77	-118.29
1/pimelate	13.46	12.37	15.55	3.04	3.01	2.54	16.50	-114.62
1/suberate	13.30	12.30	14.92	7.12	7.06	6.57	20.42	-111.12
1/azelate	13.60	12.64	15.02	7.32	6.67	8.50	20.92	-109.13
$1/NO_3^-$	5.72	4.56	7.98	0.37	0.37	-0.27	6.09	-61.34
$1/SO_4^{2-}$	15.66	13.67	19.73	2.53	2.52	1.06	18.19	-146.99
$1/HCO_3^-$	7.21	6.03	8.86	1.53	1.50	1.55	8.74	-70.27
$1/HPO_4^{2-}$	18.13	16.09	22.32	4.22	4.35	3.99	22.35	-162.34
$1/H_2PO_4^-$	6.73	5.47	8.43	3.14	2.98	3.31	9.87	-65.68
$1/F^-$	13.96	12.17	17.49	0.00	0.00	0.00	13.96	-147.01
$1/Cl^-$	8.08	6.99	9.56	0.00	0.00	0.00	8.08	-66.82
$1/Br^-$	9.02	7.92	11.04	0.00	0.00	0.00	9.02	-69.97

[a] In kcal/mol, derived at the ONIOM (B3LYP/6-31G(d):AM1) level with ZPVE correction.

[b] In kcal/mol, derived at the B3LYP/6-31G(d) level with ZPVE correction.

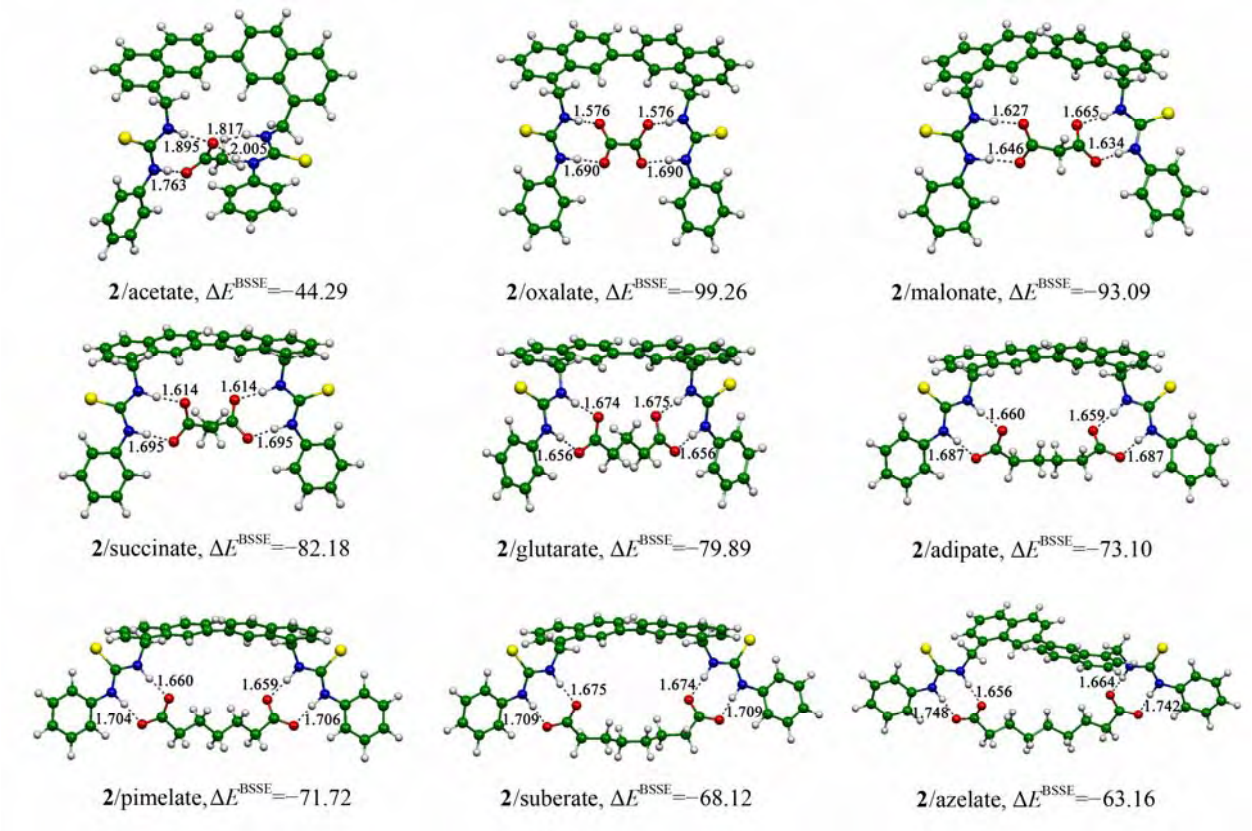

รูปที่ 5.3 แสดงโครงสร้างของสารประกอบเชิงซ้อนระหว่างสารประกอบ 8,8'-bis(3-butylthioureido methyl)-2,2'-binaphthalene (**2**) กับคาร์บอกซิเลตและไดคาร์บอกซิเลต

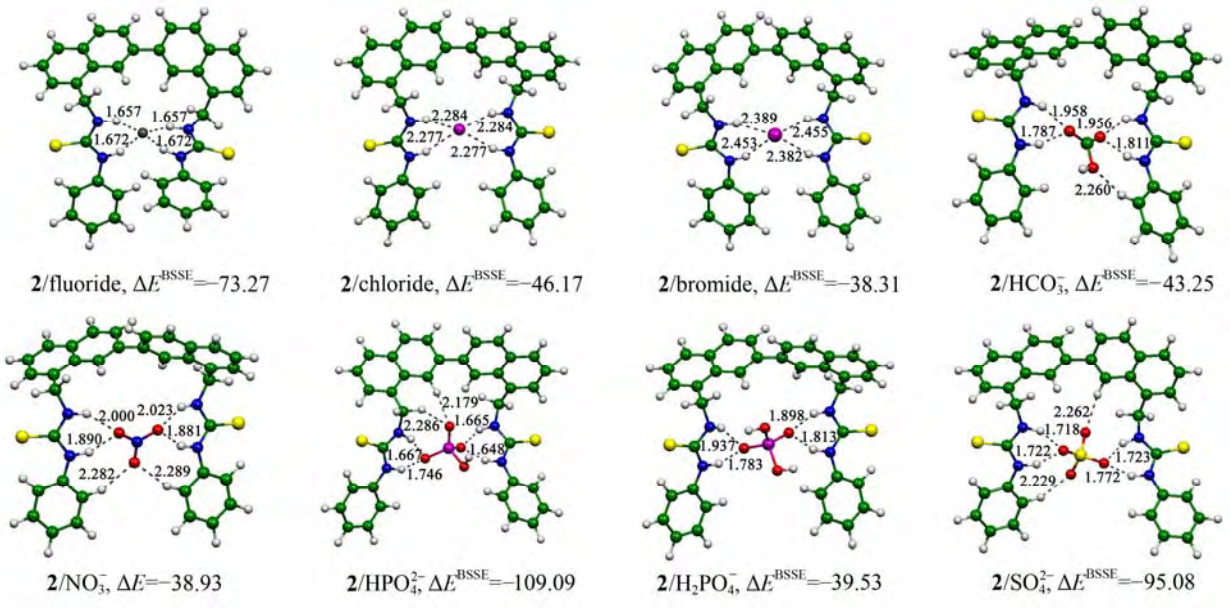

รูปที่ 5.4 แสดงโครงสร้างของสารประกอบเชิงซ้อนระหว่างสารประกอบ 8,8'-bis(3-butylthioureido methyl)-2,2'-binaphthalene (**2**) กับแอนไอออนชนิดเฮไลด์ และไอออนชนิดที่มีออกซิเจนเป็นองค์ประกอบ

ตารางที่ 5.2 แสดงค่าพลังงานจัดตัวของ 8,8'-bis(3-butylthioureido methyl)-2,2'-binaphthalene รีเซปเตอร์ **2** (host) แอนไอออน (guest) และพลังงานการเกิดสารประกอบเชิงซ้อน โดยวิธี ONIOM (B3LYP/6-31G(d):AM1)

Host:guest	Host			Guest			$\Delta E_{\text{preorg.}}^{\text{total}}$ [a]	$\Delta E_{\text{complex}}$ [a]
	$\Delta E_{\text{preorg}}^{\text{host}}$ [a]	ΔH^{298} [a]	ΔG^{298} [a]	$\Delta E_{\text{preorg.}}^{\text{guest}}$ [b]	ΔH^{298} [b]	ΔG^{298} [b]		
2/acetate	10.44	10.13	11.80	1.52	0.97	2.56	11.96	-73.10
2/oxalate	13.39	12.34	14.05	1.09	1.08	0.71	14.48	-145.69
2/malonate	13.07	11.95	14.05	1.57	1.04	2.17	14.64	-133.75
2/succinate	11.21	10.01	13.03	2.62	1.57	4.38	13.83	-121.44
2/glutarate	2.57	3.75	-2.78	0.00	0.00	0.00	2.57	-105.17
2/adipate	11.92	11.35	11.52	4.30	4.80	2.48	16.22	-108.38
2/pimelate	12.34	11.77	12.31	2.70	2.10	3.95	15.04	-105.11
2/suberate	3.23	4.31	-2.07	2.48	3.50	0.09	5.71	-92.20
2/azelate	12.57	12.09	12.20	6.85	6.21	8.04	19.42	-99.94
$2/NO_3^-$	7.54	7.44	5.18	0.31	0.30	-0.34	7.85	-61.15
$2/SO_4^{2-}$	16.02	14.93	17.55	2.22	2.21	0.75	18.24	-138.70
$2/HCO_3^-$	0.00	0.58	-2.17	0.00	0.00	0.00	0.00	-57.97
$2/HPO_4^{2-}$	17.29	16.13	18.80	3.07	3.16	2.91	20.36	-155.32
$2/H_2PO_4^-$	2.57	3.75	-2.77	0.00	0.00	0.00	2.57	-55.35
$2/F^-$	13.15	11.85	14.76	0.00	0.00	0.00	13.15	-139.46
$2/Cl^-$	7.79	7.08	8.36	0.00	0.00	0.00	7.79	-62.54
$2/Br^-$	7.09	6.39	7.68	0.00	0.00	0.00	7.09	-64.35

[a] In kcal/mol, derived at the ONIOM (B3LYP/6-31G(d):AM1) level with ZPVE correction.

[b] In kcal/mol, derived at the B3LYP/6-31G(d) level with ZPVE correction.

ผลที่ได้รับจากโครงการ

1. ผลการวิจัยที่ตีพิมพ์ในวารสารวิชาการ

   บทความได้รับการตีพิมพ์ในวารสารนานาชาติดังต่อไปนี้

   - B. Wanno, W. Rakrai, S. Keawwangchai, N. Morakot, N. Morakot, N. Nunthaboot, V. Ruangpornvisuti, “A density functional investigation of 1,3–bis(4–nitrophenyl)urea as anion receptor” J. Mol. Struct. THEOCHEM 902 (2009) 33–40. (impact factor ปี 2009 = 1. 1.167)
   - S. Piyaauksornsak, T. Tangthongkul, R. Wanbayor, B. Wanno, V. Ruangpornvisuti, “Molecular structures of 8,8'–dithioureido–2,2'–binaphthalene derivatives and their anions recognition: an ONIOM investigation” Struct. Chem. 20 (2009) 767–780. (impact factor ปี 2009 = 1.433)
   - Boosayarat Tomapatanageta and Vithaya Ruangpornvisuti, “A DFT study of structures of dipicolyl urea isomers and their recognition with carboxylic acids and their carboxylate anions” J. Phys. Org. Chem. (2010), in press. (impact factor ปี 2009 = 1.415)

   บทความที่ได้ส่งตีพิมพ์ในวารสารนานาชาติ และคาดว่าจะได้รับการตีพิมพ์ในปี 2010 ดังต่อไปนี้

   - P. Chanapiwat, K. Navakhun, V. Ruangpornvisuti, “A DFT investigation of cyclic amide receptors and their recognition with monovalent anions”.
   - P. Chanapiwat, V. Vchirawongkwin, V. Ruangpornvisuti, “Anion recognition of alkaline–metal complexes of calix[4]arene receptors: An ONIOM investigation”.

2. พื้นความรู้ในงานวิจัยทางเคมีวิเคราะห์

   ค่าคงที่การรวมตัวระหว่างรีเซปเตอร์ชนิดสารประกอบเอไมด์ และยูเรีย กับแอนไอออนชนิดต่าง ๆ ที่พบได้ในสารละลายต่าง ๆ โดยเป็นค่าบ่งชี้การจดจำต่อแอนไอออน ซึ่งแสดงในรูปของค่า selectivity coefficients ข้อมูลดังกล่าวทำให้ทราบว่ารีเซปเตอร์ชนิดสารประกอบเอไมด์และยูเรีย ชนิดใดนำไปใช้เป็นเซนเซอร์ในการตรวจวัด หรือตรวจหาแอนไอออน โดยวิธีต่าง ๆ เช่น การใช้เป็นสารประกอบในคอลัมน์ในเครื่อง HPLC (High Performance Liquid Chromatography)

3. กิจกรรมอื่น ๆ ที่เกี่ยวข้อง

   การนำเสนอผลงานในการประชุมทางวิชาการและการเป็นกรรมการ

- การนำเสนอผลงานใน การประชุมวิชาการวิทยาศาสตร์และเทคโนโลยีแห่งประเทศไทย ครั้งที่ 34 ระหว่างวันที่ 31 ตุลาคม – 2 พฤศจิกายน 2551 ณ ศูนย์การประชุมแห่งชาติสิริกิติ์
- เป็นกรรมการสาขาเคมีฟิสิกัล ของการประชุมวิชาการวิทยาศาสตร์และเทคโนโลยีแห่งประเทศไทย ครั้งที่ 34 ระหว่างวันที่ 31 ตุลาคม – 2 พฤศจิกายน 2551 ณ ศูนย์การประชุมแห่งชาติสิริกิติ์
- การนำเสนอผลงานใน การประชุมวิชาการวิทยาศาสตร์และเทคโนโลยีแห่งประเทศไทย ครั้งที่ 35 ระหว่างวันที่ 15–17 ตุลาคม 2552 จัดโดยมหาวิทยาลัยบูรพา
- เป็นประธานกรรมการสาขาเคมีฟิสิกัล ของการประชุมวิชาการวิทยาศาสตร์และเทคโนโลยีแห่งประเทศไทย ครั้งที่ 35 ระหว่างวันที่ 15–17 ตุลาคม 2552 จัดโดยมหาวิทยาลัยบูรพา

ผลงานวิจัยอื่น ๆ ที่ตีพิมพ์ในวารสารวิชาการระดับนานาชาติ

- V. Ruangpornvisuti “A DFT Study of transformation of nitrosothiol isomers and their decomposition to nitric oxide in gas phase” Int. J. Quant. Chem. 109 (2009), 275–284.
- V. Ruangpornvisuti “A DFT Investigation of Dissociation of Nitrous Acid, Transformation of Its Monomeric Isomers, Their Dimeric Isomers, and Dimerization” Int. J. Quant. Chem. 110 (2010) 1019–1029.

การเชื่อมโยงทางวิชาการและร่วมทำงานวิจัยภายในสถาบันเดียวกัน ดังปรากฏเป็นผลงานวิจัยที่ตีพิมพ์ในวารสารวิชา การระดับนานาชาติดังนี้

- M. Jamkratoke, V. Ruangpornvisuti, G. Tumcharern, T. Tuntulani, B. Tomapatanaget, “A–D–A Sensors Based on Naphthoimidazoledione and Boronic Acid as Turn–On Cyanide Probes in Water” J. Org. Chem. 74 (2009) 3919–3922.

การเชื่อมโยงทางวิชาการและร่วมทำงานวิจัยกับภาควิชาเคมี คณะวิทยาศาสตร์ มหาวิทยาลัยบูรพา ดังปรากฏเป็นผลงานวิจัยที่ตีพิมพ์ในวารสารวิชาการระดับนานาชาติดังนี้

- A. Suwattanamala, V. Ruangpornvisuti “Isomeric structures of benzimidazole, benzoxazole, and benzothiazole derivatives, their electronic properties and transformations”, Struct. Chem. 20 (2009) 619–631.
- K.Thipyapong, V. Ruangpornvisuti, “Isomers of various species of 1–hydroxy–2–pyridinone–6–carboxylic acid, their proton dissociation and complexes with Cr(III) and Zn(II)” Journal of Molecular Structure 891 (2008) 1–10.

การเชื่อมโยงทางวิชาการและร่วมทำงานวิจัยกับภาควิชาเคมี คณะวิทยาศาสตร์ มหาวิทยาลัยรามคำแหง ดังปรากฏเป็นผลงานวิจัยที่ตีพิมพ์ในวารสารวิชาการระดับนานาชาติดังนี้

- K. Navakhun, V. Ruangpornvisuti, “Non–rigid bis–(2,5–diamidopyrrole) receptor, its deprotonated species and their complexes with fluoride, chloride and hydroxide ions” Journal of Molecular Structure: THEOCHEM 907 (2009) 131–134.
- K. Navakhun, V. Ruangpornvisuti, “Anion binding of 3,4–dichloro–2,5–diamidopyrrole and anionic self–assembly dimerization of its deprotonated species” Journal of Molecular Structure: THEOCHEM 864 (2008) 26–30.

การเชื่อมโยงทางวิชาการและร่วมทำงานวิจัยกับภาควิชาเคมี คณะวิทยาศาสตร์ มหาวิทยาลัยมหาสารคาม ดังปรากฏเป็นผลงานวิจัยที่ตีพิมพ์ในวารสารวิชาการระดับนานาชาติดังนี้

- B. Wanno, W. Rakrai, S. Keawwangchai, N. Morakot, N. Morakot, N. Nunthaboot, V. Ruangpornvisuti, “A density functional investigation of 1,3–bis(4–nitrophenyl)urea as anion receptor” J. Mol. Struct. THEOCHEM 902 (2009) 33–40.

การเชื่อมโยงทางวิชาการและร่วมทำงานวิจัยกับภาควิชาเคมี คณะวิทยาศาสตร์ มหาวิทยาลัยพระจอมเกล้าธนบุรี วิทยาเขตราชบุรี ดังปรากฏเป็นผลงานวิจัยที่ตีพิมพ์ในวารสารวิชาการระดับนานาชาติดังนี้

- A. Pinisakul, C. Kritayakornupong, V. Ruangpornvisuti, “Molecular modeling of nitrosamines adsorbed on H–ZSM–5 zeolite: An ONIOM study”, Journal Molecular Modeling 14 (2008) 1035–1041.

ปัญหาและอุปสรรค

ในงานวิจัยพบอุปสรรคและปัญหาที่อาจไม่ใช่ปัญหา กล่าวคือในการคำนวณสเปกตรัม UV-VIS ของโมเลกุลที่เป็นรีเซปเตอร์และสารประกอบเชิงซ้อน เนื่องจากเป็นการคำนวณที่ขึ้นกับตัวทำละลาย ทำให้การคำนวณเป็นที่ใช้เวลาค่อนข้างนาน ดังนั้นการวิเคราะห์ผลจึงล่าช้ามาก ดังนั้นการส่งผลงานวิจัยเพื่อการตีพิมพ์จึงไม่ได้รวมการคำนวณสเปกตรัม UV-VIS ไว้ และผลการวิจัยสามารถนำไปตีพิมพ์ในโอกาสต่อ ๆ ไปได้ อย่างไรก็ตามผลงานวิจัยที่เป็นผลต่อเนื่องจากการได้รับทุนของโครงการ และหรือไม่ต่อเนื่อง ข้าพเจ้าได้ทำกิตติกรรมประกาศต่อสำนักงานกองทุนสนับสนุนการวิจัยทุก ๆ ครั้ง

ภาคผนวก

ภาคผนวก A

Reprint บทความเรื่อง “A density functional investigation of 1,3–bis(4–nitrophenyl) urea as anion receptor”

ภาคผนวก B

Reprint บทความเรื่อง “Molecular structures of 8,8'–dithioureido–2,2'–binaphthalene derivatives and their anions recognition: an ONIOM investigation”

ภาคผนวก C

Reprint บทความเรื่อง “A DFT study of structures of dipicolyl urea isomers and their recognition with carboxylic acids and their carboxylate anions”

ภาคผนวก D

Manuscript บทความเรื่อง “A DFT investigation of cyclic amide receptors and their recognition with monovalent anions”

ภาคผนวก E

Manuscript บทความเรื่อง “Anion recognition of alkaline–metal complexes of calix[4] arene receptors: An ONIOM investigation”

Journal of Molecular Structure: THEOCHEM 902 (2009) 33–40

Contents lists available at ScienceDirect

Journal of Molecular Structure: THEOCHEM

journal homepage: www.elsevier.com/locate/theochem

A density functional investigation of 1,3-bis(4-nitrophenyl)urea as anion receptor

Banchob Wanno [a], Wandee Rakrai [a], Somchai Keawwangchai [a], Neramit Morakot [a], Nongnit Morakot [a], Nadtanet Nunthaboot [a], Vithaya Ruangpornvisuti [b,*]

[a] Department of Chemistry, Faculty of Science, Mahasarakham University, Mahasarakham 44150, Thailand
[b] Supramolecular Chemistry Research Unit, Department of Chemistry, Faculty of Science, Chulalongkorn University, Bangkok 10330, Thailand

ARTICLE INFO

Article history:
Received 13 November 2008
Received in revised form 28 January 2009
Accepted 7 February 2009
Available online 20 February 2009

Keywords:
Halide
Oxygen-containing anion
Nitrophenyl urea
Binding energy
DFT

ABSTRACT

The B3LYP/6-311+G(d,p) optimized structures of 1,3-bis(4-nitrophenyl)urea receptor (**1**) and its complexes with halide ions F^-, Cl^-, Br^-, oxygen-containing anions NO_2^-, NO_3^-, HCO_3^-, HSO_4^-, $H_2PO_4^-$, CH_3COO^- and $C_6H_5COO^-$ ions were obtained. Binding energies and thermodynamic properties of binding between the receptor **1** and these anions were determined. Binding energies of receptor **1** are in decreasing orders: $CH_3COO^- > HCO_3^- \sim C_6H_5COO^- > NO_2^- > H_2PO_4^- > NO_3^- > HSO_4^-$ for oxygen-containing anions and $F^- > Cl^- > Br^-$ for halide ions. It was found that the binding energies depend on their hydrogen-bond distances of their binding atoms. It was also found that the complexes of receptor **1** and the studied anions are formed via two-point hydrogen-bonding interactions.

1. Introduction

Anions play an important role in several fields such as biology [1], the environment [2], catalysis [3] and potential medical application [4]. Thus the design of molecular sensors for anion recognition and sensing are interesting of chemists for many years, especially, in the research field of supramolecular chemistry [5]. The major need for designing is both sensitive and selective sensors for anions [6,7]. Hosts containing a variety of donor (D) groups, D–H, such as ureas [8–11], amines [12], amides [13,14] and thioamides [15] have been widely investigated. Urea based receptors have been used more extensively for anion detection [16,17]. Receptors containing one or more urea subunits have been designed and tested for anion recognition and sensing over the past years [18]. Moreover, selectivity is also related to the energy of the receptor-anion interaction; in this sense, strong H-bond interactions are established with anions containing the most electronegative atoms. Recently, 1,3-bis(4-nitrophenyl)urea (**1**) complexes with anions and its X-ray structure with acetate and hydrogen carbonate have been obtained [19]. The complex of receptor **1** with fluoride ion was found to be the most stable complex. Molecular structures of pyrrole derivatives, their interactions with halide ions [20–22] and azophenol thioureas, calix[4]arenes and their complexations with dicarboxylate anions [23,24] were studied by theoretical calculations [20–24].

Although the synthesis and anion binding ability of urea containing nitrophenyl **1** have been developed, the theoretical studies to gain clearer information i.e., geometrical structure, binding energy, molecular orbital and charge transfer, on the origin of molecular recognition affinity have never been considered. In this work, the binding energies and thermodynamic properties of the 1,3-bis(4-nitrophenyl)urea complexes with anions F^-, Cl^-, Br^-, NO_2^-, NO_3^-, HCO_3^-, HSO_4^-, $H_2PO_4^-$, CH_3COO^- and $C_6H_5COO^-$ have therefore been theoretically investigated using the density functional theory method.

2. Computational method

Density functional theory (DFT) has been employed to optimize the structures of 1,3-bis(4-nitrophenyl)urea (**1**) and its complexes with anions F^-, Cl^-, Br^-, NO_2^-, NO_3^-, HCO_3^-, HSO_4^-, $H_2PO_4^-$, CH_3COO^- and $C_6H_5COO^-$. The DFT calculations have been performed using the Becke's three-parameter exchange functional with the Lee–Yang–Parr correlation functional (B3LYP) [25]. All calculations have been performed using the MO computations at the B3LYP/6-311+G(d,p) level of theory [26]. The vibrational frequency computations have been carried out at 298.15 K and 1 atm. Stationary points have been fully optimized and characterized by vibrational frequency calculations, which also provided zero point vibrational energies (ZPVE) [27]. The standard enthalpy ΔH^0_{298} and Gibbs free energy changes ΔG^0_{298} of the reactions have been derived from the frequency calculations at the B3LYP/6-311+G(d,p) level.

* Corresponding author. Tel.: +66 2218 7644; fax: +66 2254 1309.
E-mail address: vithaya.r@chula.ac.th (V. Ruangpornvisuti).

0166-1280/$ - see front matter © 2009 Elsevier B.V. All rights reserved.
doi:10.1016/j.theochem.2009.02.010

The natural bond orbital (NBO) analysis implemented in Gaussian 03 program [28] is applied through a series of intermolecular interactions under the above system to evaluate the NBO charges. All calculations were performed with the Gaussian 03 program [28]. The MOLDEN 4.2 program [29] was utilized to display the molecular structure, monitor the geometrical parameters and observe the molecular geometry convergence via the Gaussian output file. The molecular graphics of all related species were generated with the MOLEKEL 4.3 program [30].

3. Results and discussion

3.1. Molecular structures and energies

The B3LYP/6-311+G(d,p) optimized structures of the receptor **1** and its complexes with anions F^-, Cl^-, Br^-, NO_2^-, NO_3^-, HCO_3^-, HSO_4^-, $H_2PO_4^-$, CH_3COO^- and $C_6H_5COO^-$ and their binding free energies are shown in Fig. 1. It was found that the molecular symmetries of the receptor **1** and its complexes with F^-, Cl^-, Br^-, NO_2^-, NO_3^- and $C_6H_5COO^-$ ions are C_{2v} point group but its complexes with HCO_3^-, HSO_4^-, $H_2PO_4^-$ and CH_3COO^- belong to C_s, C_s, C_2 and C_s symmetries, respectively. The selected geometrical parameters for the receptor **1** and its complexes with anions are shown in Table 1. Geometrical parameters of the B3LYP/6-311+G(d,p)-optimized molecule for the complexes with HCO_3^- and CH_3COO^- ions were found to be somewhat different from their corresponding X-ray crystallographic data [19]. It was found that each of these structures of the complexes were formed via two-point hydrogen-bonds.

Relation between the binding free energy (ΔG) of the receptor **1** with anionic guests and their hydrogen-bond distances is shown in Fig. 2(a). It shows that trends on correlation between the binding energies of the receptor **1** with these anions and their hydrogen-bond distances are linearly related depending on anionic type; the above and bottom lines in Fig. 2(a) are for the halide and oxygen-containing anions, respectively. The linear relations for the halide and oxygen-containing anions can be confirmed with the correlation coefficients of 0.992 (r^2, above line) and 0.887 (bottom line), respectively. Due to the thermodynamic formula $\Delta G = -RT \log K$, the negative binding free energy ($-\Delta G$) has to correlate with the log K of the association process and its correlation coefficient must approach to unity. The plots of the negative binding free energy against the experimental values of log K [19] of the systems of two halide ions (top) and of oxygen-containing anions (bottom) are shown in Fig. 2(b) and the weak correlation between $-\Delta G$ and Log K for the system of the oxygen-containing anions ($r^2 = 0.518$) was obtained. Nevertheless, the system of the two halide ions could not be concluded because only two data points were applied.

The hydrogen-bond distances for the halide complexes are within the range of 1.520–2.306 Å and the oxoanionic complexes are within the range of 1.697–2.269 Å. Their hydrogen-bond characteristics should be remarked by their complexation according to the different binding ions. Hydrogen-bond characteristics of the complexes with the halide ions and the oxygen-containing ions are as NH···X, (X = F^-, Cl^- or Br^-) and NH···O, respectively. It was found that the calculated hydrogen-bond distances of the complexes with $HCO_3^-$and CH_3COO^- ions are somewhat different from their corresponding X-ray data [19]; the bond distances of the $HCO_3^-$and CH_3COO^- are 1.729 and 1.697 Å for computation and 1.913 and 1.819 Å for experiment, respectively. This may be caused by the difference of their molecular strain, electrostatic and polarity environments. Moreover, the counter ion such a tetrabutyl ammonium ion which is included in the X-ray structure was not included in the structure optimization. The binding energies, enthalpies and Gibbs free energies of the complexations between the receptor **1** and the anions obtained from the B3LYP/6-311+G(d,p) calculations are listed in Table 2. In the halide system, the **1**/F^- is the most stable complex (ΔE = −79.62 kcal/mol) which is in good agreement with the experiment as reported by Boiocchi group [19]. It was concluded that the complexation abilities of these complexes strongly depend on both intermolecular hydrogen-bond distance and the type of anion. For the system of oxoanionic complex, relative stabilities are in decreasing order: **1**/CH_3COO^- > **1**/HCO_3^- ∼ **1**/$C_6H_5COO^-$ > **1**/NO_2^- > **1**/$H_2PO_4^-$ > **1**/NO_3^- >

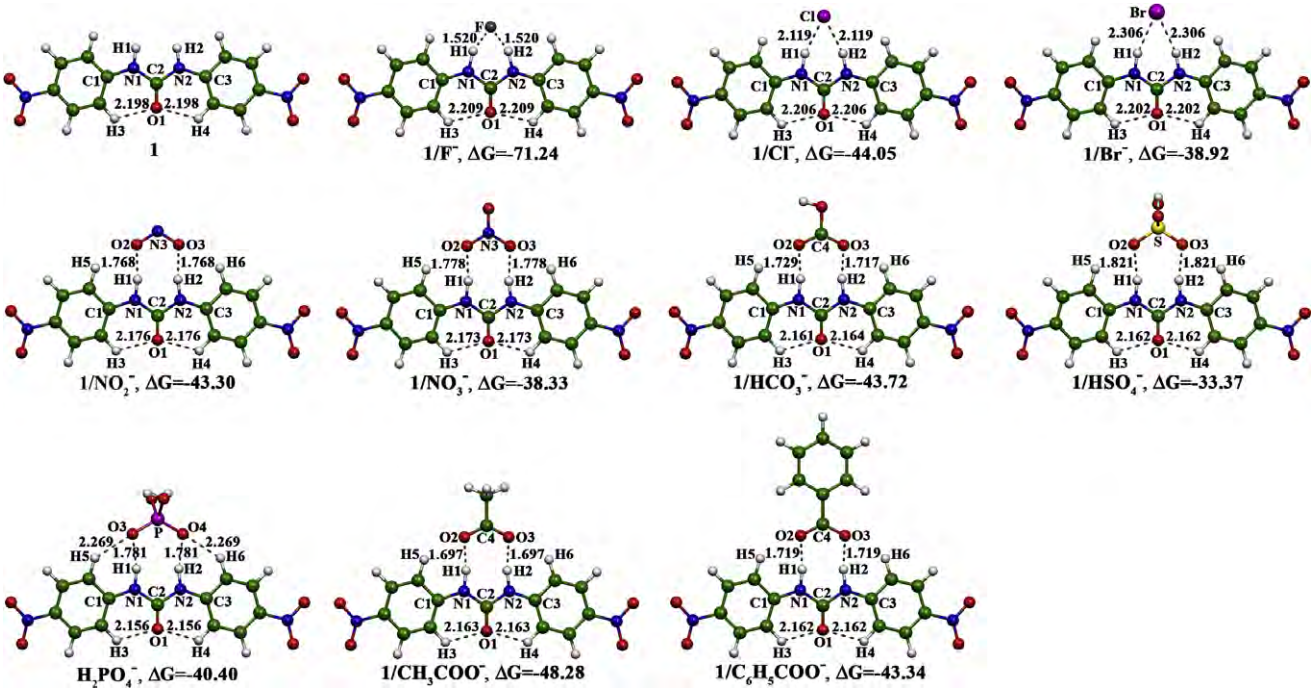

Fig. 1. The B3LYP/6-311+G(d,p) optimized structures of the receptor **1** and its complexes with anionic guests. The hydrogen-bond distances and binding free energies (ΔG) are in angstrom and kcal/mol, respectively.

Table 1
Geometrical data for receptor **1** and its complexes with anionic guests computed at the B3LYP/6-311+G(d,p)) level.

Parameter[a]	**1**	Complexes of the receptor **1**											
		NO_2^-	NO_3^-	HCO_3^-		HSO_4^-	$H_2PO_4^-$	CH_3COO^-		$C_6H_5COO^-$	F^-	Cl^-	Br^-
	Calc	Calc	Calc	Calc	Exp[b]	Calc	Calc	Calc	Exp[b]	Calc	Calc	Calc	Calc
Bond distance (Å)													
C1—N1	1.403	1.384	1.387	1.384	1.397	1.389	1.388	1.383	1.387	1.384	1.371	1.380	1.382
N1—H1	1.009	1.042	1.035	1.044	0.902	1.029	1.036	1.050	0.927	1.046	1.069	1.039	1.036
N1—C2	1.391	1.387	1.387	1.388	1.361	1.387	1.387	1.387	1.366	1.387	1.388	1.387	1.387
C2—O1	1.213	1.224	1.223	1.225	1.228	1.223	1.224	1.225	1.217	1.225	1.226	1.223	1.222
C2—N2	1.391	1.387	1.387	1.386	1.373	1.387	1.387	1.386	1.372	1.387	1.388	1.387	1.387
N2—H2	1.009	1.042	1.035	1.045	0.898	1.029	1.036	1.050	0.907	1.046	1.069	1.039	1.036
N2—C3	1.403	1.384	1.387	1.385	1.395	1.389	1.388	1.383	1.389	1.384	1.371	1.380	1.382
O1—H3	2.198	2.176	2.173	2.161	2.269	2.162	2.156	2.163	2.207	2.162	2.209	2.206	2.202
O1—H4	2.198	2.176	2.173	2.164	2.259	2.162	2.156	2.163	2.217	2.162	2.209	2.206	2.202
H1—O2	–	1.768	1.778	1.729	1.897	1.821	1.782	1.697	1.847	1.719	–	–	–
H2—O3	–	1.768	1.778	1.717	1.930	1.821	1.782	1.697	1.794	1.719	–	–	–
H5—O2	–	2.402	2.390	2.357	2.574	2.324	2.270	2.342	2.614	2.354	–	–	–
H6—O3	–	2.402	2.390	2.347	2.472	2.324	2.270	2.341	2.491	2.354	–	–	–
O2—Y	–	1.258	1.271	1.260	1.247	1.485	1.509	1.262	1.237	2.354	–	–	–
O3—Y	–	1.258	1.271	1.245	1.240	1.485	1.509	1.262	1.242	1.261	–	–	–
H1—X	–	–	–	–	–	–	–	–	–	–	1.520	2.119	2.306
H2—X	–	–	–	–	–	–	–	–	–	–	1.520	2.119	2.306
Bond angle (°)													
C1—N1—C2	128.1	127.4	127.4	127.0	127.6	127.2	126.9	127.0	126.7	127.0	127.9	128.1	128.1
C1—N1—H1	114.3	114.9	114.8	114.3	110.5	114.1	113.7	114.4	114.3	114.5	119.4	116.6	116.2
N1—C2—O1	124.0	124.5	124.4	124.1	123.6	123.9	123.8	124.2	123.3	124.2	125.5	124.9	124.8
N1—C2—N2	112.0	111.1	111.3	111.7	112.5	112.1	112.4	111.5	113.1	111.6	109.0	110.2	110.5
C2—N2—C3	128.1	127.4	127.4	127.0	127.9	127.2	126.9	127.0	126.6	127.0	127.9	128.1	128.1
C2—N2—H2	114.3	117.7	114.8	118.7	116.8	118.7	119.4	118.6	119.2	118.6	112.7	115.3	115.7
N1—H1—O2	–	171.9	171.4	172.1	169.7	169.5	169.0	171.8	173.9	171.8	–	–	–
N2—H2—O3	–	171.9	171.4	171.9	166.8	169.6	169.0	171.8	170.7	171.8	–	–	–
H1—O2—Y	–	121.0	118.9	112.9	118.1	119.0	112.6	114.9	113.1	114.8	–	–	–
H2—O3—Y	–	121.0	118.9	113.7	166.8	119.1	112.6	114.9	117.7	114.8	–	–	–
O2—Y—O3	–	115.3	118.2	128.2	126.1	110.8	119.6	125.0	123.5	125.3	–	–	–
N1—H1—X	–	–	–	–	–	–	–	–	–	–	156.8	162.5	164.0
N2—H2—X	–	–	–	–	–	–	–	–	–	–	156.8	162.5	164.0
H1—X—H2	–	–	–	–	–	–	–	–	–	–	71.9	54.1	50.1
Dihedral angle (°)													
C1—N1—C2—O1	0.0	0.0	0.0	0.0	7.0	0.2	2.8	0.0	5.4	0.0	0.0	0.0	0.0
C1—N1—C2—N2	180.0	180.0	180.0	180.0	174.1	179.7	177.2	180.0	173.7	180.0	180.0	180.0	180.0
N1—C2—N2—C3	180.0	180.0	180.0	180.0	175.4	179.7	177.2	180.0	176.3	180.0	180.0	180.0	180.0
O1—C2—N1—H1	180.0	180.0	180.0	180.0	179.1	180.0	175.2	180.0	177.8	180.0	180.0	180.0	180.0
O1—C2—N2—H2	180.0	180.0	180.0	180.0	175.8	179.9	175.2	180.0	177.3	180.0	180.0	180.0	180.0
O1—C2—N2—C3	0.0	0.0	0.0	0.0	5.8	0.2	2.8	0.0	2.9	0.0	0.0	0.0	0.0
C1—N1—H1—O2	–	0.0	0.1	0.1	85.3	4.3	7.6	0.0	17.7	0.0	–	–	–
C3—N2—H2—O3	–	0.1	0.1	0.0	45.9	4.4	7.6	0.2	56.1	0.0	–	–	–
N1—H1—O2—Y	–	180.0	180.0	180.0	99.3	178.9	173.6	179.9	139.3	180.0	–	–	–
N2—H2—O3—Y	–	180.0	180.0	180.0	162.0	178.8	173.6	179.9	116.2	180.0	–	–	–
C1—N1—H1—X	–	–	–	–	–	–	–	–	–	–	180.0	180.0	180.0
C3—N2-H2—X	–	–	–	–	–	–	–	–	–	–	180.0	180.0	180.0

[a] X = F^-, Cl^- or Br^-, Y = N3, C4, S or P, atomic numbering is shown in Fig. 1.
[b] Taken from Ref. [19].

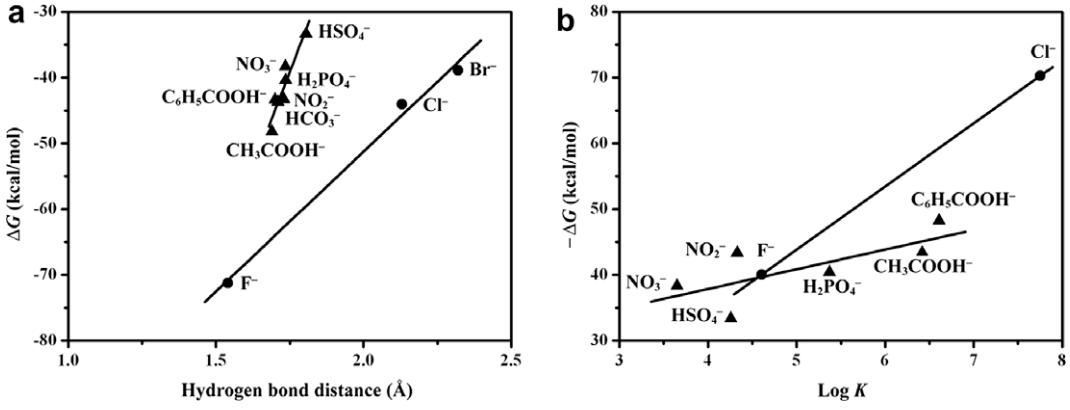

Fig. 2. Relation between (a) the binding free energy (ΔG) of the receptor **1** with anionic guests and their hydrogen-bond distance and (b) the negative binding free energy and the experimental values of log *K*.

Table 2
Energetics and thermodynamic properties of complexations of receptor **1** and anions computed at the B3LYP/6-311+G(d,p) level.

Host/guest complexes	ΔE^{a}	ΔH^{o}_{298} [a]	ΔG^{o}_{298} [a]	Log K^{b}
1/F^-	−79.62	−80.42	−71.24	7.38
1/Cl^-	−52.21	−52.78	−44.05	4.55
1/Br^-	−47.02	−47.45	−38.92	–
1/NO_2^-	−54.76	−55.02	−43.30	4.33
1/NO_3^-	−48.67	−48.65	−38.33	3.65
1/HCO_3^-	−55.80	−55.92	−43.72	–
1/HSO_4^-	−45.24	−45.16	−33.37	4.26
1/$H_2PO_4^-$	−52.28	−52.24	−40.40	5.37
1/CH_3COO^-	−60.47	−60.60	−48.24	6.61
1/$C_6H_5COO^-$	−55.68	−55.68	−43.34	6.42

[a] In kcal/mol.
[b] The experimental values in MeCN solution at 298.51 K, taken from Ref. [19].

Table 3
The orbital energies E_{LUMO}, E_{HOMO} and frontier molecular orbital energy gap, $\Delta E_{HOMO-LUMO}$ of the receptor **1** and its complexes with anions computed at the B3LYP/6-311+G(d,p) level.

Host/guest	E_{LUMO} [a]	E_{HOMO} [a]	$\Delta E_{HOMO-LUMO}$ [a]
1	−3.020	−7.129	4.109
1/F^-	−0.463	−3.701	3.238
1/Cl^-	−0.626	−3.701	3.075
1/Br^-	−0.680	−3.347	2.667
1/NO_2^-	−0.599	−3.320	2.721
1/NO_3^-	−0.653	−4.136	3.483
1/HCO_3^-	−0.544	−3.918	3.374
1/HSO_4^-	−0.680	−4.163	3.483
1/$H_2PO_4^-$	−0.544	−3.973	3.429
1/CH_3COO^-	−0.463	−3.810	3.347
1/$C_6H_5COO^-$	−0.544	−3.918	3.374

[a] In eV.

1/HSO_4^- while for the halide complexes, the relative stabilities are in decreasing order: **1**/F^- > **1**/Cl^- > **1**/Br^-.

3.2. Frontier molecular orbital energies

The energies of the highest occupied molecular orbital (HOMO) E_{HOMO}, the lowest unoccupied molecular orbital (LUMO) E_{LUMO} and the frontier molecular orbital energy gaps ($\Delta E_{HOMO-LUMO}$) of receptor **1** and its complexes computed at the B3LYP/6-311+G(d,p) level are given in Table 3. Based on the energy gaps, relative reactivities of all the complexes are higher than the free receptor. The relative reactivities of the halide and oxoanionic complexes are in orders: **1**/Br^- (2.667 eV) >

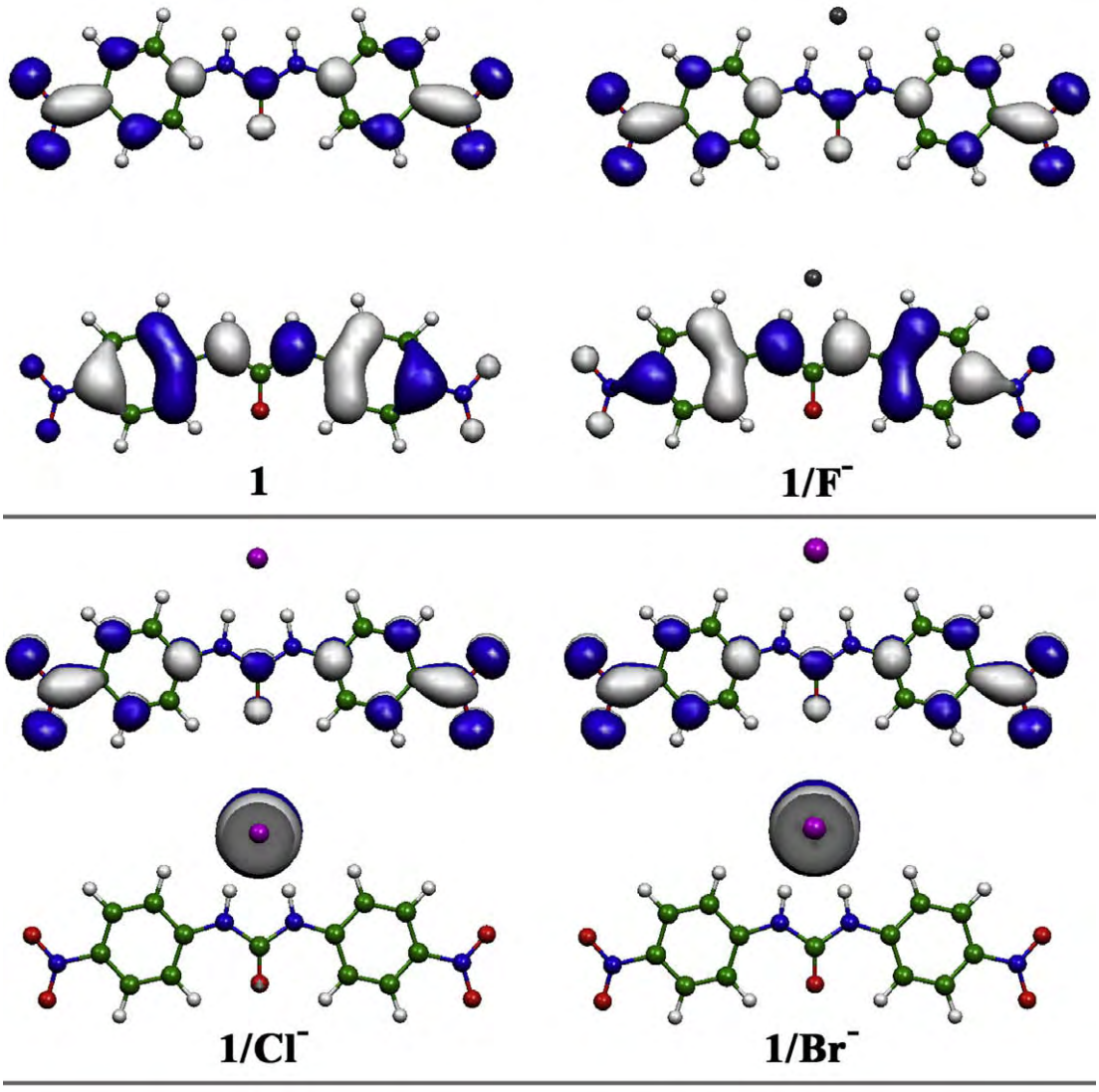

Fig. 3. Plots of the LUMOs (top) and HOMOs (bottom) orbitals at an isosurface value of 0.03 au of the free forms of the receptor **1** and its halide complexes.

1/Cl^- (3.075 eV) > **1**/F^- (3.238 eV) and **1**/NO_2^- > **1**/CH_3COO^- > **1**/HCO_3^- ≈ **1**/$C_6H_5COO^-$ > **1**/$H_2PO_4^-$ > **1**/NO_3^- ≈ **1**/HSO_4^-, respectively. The HOMOs and LUMOs for halide and oxoanionic complexes are illustrated in Figs. 3 and 4, respectively. It was found that the HOMO and LUMO of the free receptor **1** are very similar to the **1**/F^- complex (upper of Fig. 3) and the **1**/Cl^- is also very similar to the **1**/Br^- complex. The similarity of HOMO and LUMO of the free receptor **1** and the **1**/F^- complex is due to the fluoride electron easily transfers to the amide protons (H_N) of the receptor **1**; this process corresponds to the charge of the F^- ion (−0.809e) which is smaller than those of the Cl^- ion (−0.831e) and Br^- ion (−0.838e) as shown in Table 4. The HOMOs of the **1**/Cl^- and **1**/Br^- complexes (Fig. 3) show electron locations in the Cl^- and Br^- ions. For the oxoanionic complexes, the HOMOs

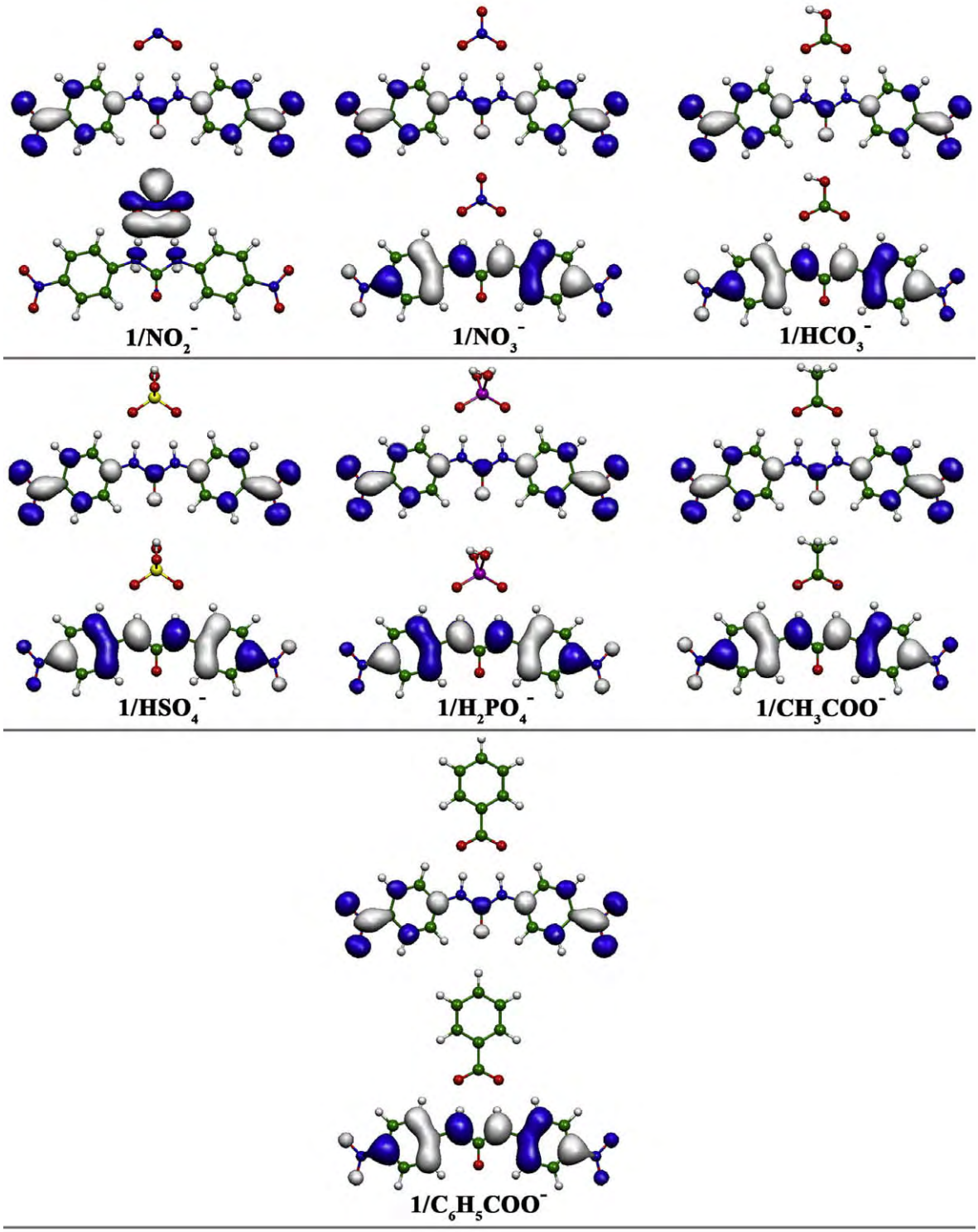

Fig. 4. Plots of the LUMOs (top) and HOMOs (bottom) orbitals at an isosurface value of 0.03 au of the oxoanionic complexes.

Table 4
Selected NBO charges (in e) of atoms of the optimized structures of the receptor **1** and its complexes with anions computed at the B3LYP/6-311+G(d,p) level.

Host/guest[a]	N1	N2	H1[b]	H2[b]	X[c]	O2[d]	O3[d]
1	−0.61	−0.61	0.38	0.38	–	–	–
1/F^-	−0.63	−0.63	0.46	0.46	−0.81	–	–
1/Cl^-	−0.64	−0.64	0.44	0.44	−0.83	–	–
1/Br^-	−0.65	−0.65	0.44	0.44	−0.84	–	–
1/NO_2^-	−0.64	−0.64	0.44	0.44	–	−0.56 (−0.58)	−0.56 (−0.59)
1/NO_3^-	−0.64	−0.64	0.44	0.44	–	−0.57 (−0.56)	−0.57 (−0.56)
1/HCO_3^-	−0.63	−0.64	0.45	0.45	–	−0.82 (−0.83)	−0.78 (−0.80)
1/HSO_4^-	−0.63	−0.63	0.45	0.45	–	−1.00 (−0.97)	−1.00 (−0.97)
1/$H_2PO_4^-$	−0.63	−0.63	0.46	0.46	–	−1.17 (−1.13)	−1.17 (−1.13)
1/CH_3COO^-	−0.64	−0.64	0.45	0.45	–	−0.79 (−0.81)	−0.79 (−0.81)
1/$C_6H_5COO^-$	−0.64	−0.64	0.45	0.45	–	−0.78 (−0.78)	−0.78 (−0.78)

[a] Atomic numbering is shown in Fig. 1.
[b] The amide protons.
[c] Here X represents the F^-, Cl^- or Br^- ions.
[d] NBO charges for O2 and O3 atoms of isolated anions are shown in parentheses.

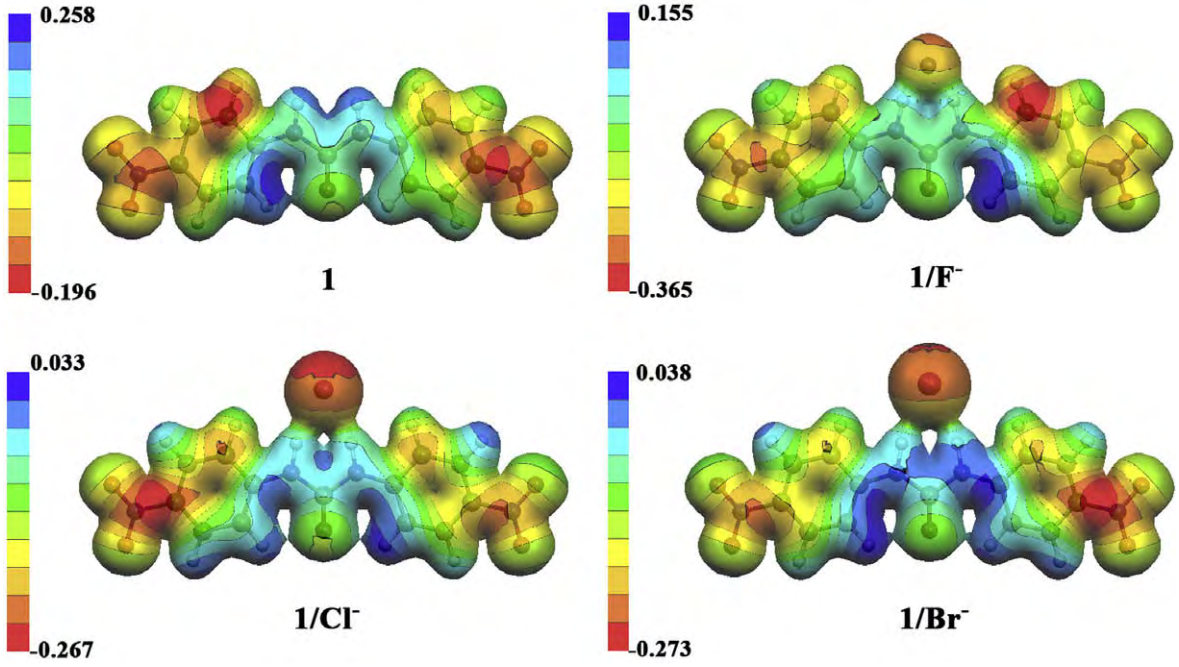

Fig. 5. Plots of the molecular electrostatic potential (in au) presented over electronic isodensity, ρ of 0.05 eÅ^{-3} of the receptor **1** and its halide complexes.

and LUMOs are very similar except the HOMO of the **1**/NO_2^- (see Fig. 4) of which the energy gap is the smallest and smaller than the second value by 0.626 eV. The HOMO of the **1**/NO_2^- complex shows its electron is located in nitrite ion.

3.3. Electrostatic potential surface

The electrostatic potential surfaces of the receptor **1** and its anionic complexes derived from the B3LYP/6-311+G(d,p) computations are shown in Figs. 5 and 6, respectively. The electrostatic potential (in au) of the receptor **1** and its halide and oxoanionic complexes are illustrated in Figs. 5 and 6, respectively for electronic isodensity values greater than ρ = 0.05 eÅ^{-3}. The electronic isodensity surface of the receptor **1** shows strongly positive charge on both amide protons (H_N) with intense blue. All the complexes show a decrease of the positive charges of their amide protons as can be seen from the lowering of the intensity of blue color.

4. Conclusions

Complexations of the 1,3-bis(4-nitrophenyl)urea complexes with F^-, Cl^-, Br^-, NO_2^-, NO_3^-, HCO_3^-, HSO_4^-, $H_2PO_4^-$, CH_3COO^- and $C_6H_5COO^-$ ions were studied using the B3LYP/6-311+G(d,p) calculations. The calculated hydrogen-bond distances of the complexes with HCO_3^- and CH_3COO^- ions are somewhat different from their corresponding X-ray data. The complexation abilities of these complexes strongly depend on both intermolecular hydrogen-bond distance and the type of anion; two types of the studied anions were found as the halide and the oxygen-containing anionic types. The relative stabilities for the systems of the halide and oxoanionic complexes are in decreasing orders: **1**/F^- > **1**/Cl^- > **1**/Br^- and **1**/CH_3COO^- > **1**/HCO_3^- ~ **1**/$C_6H_5COO^-$ > **1**/NO_2^- > **1**/$H_2PO_4^-$ > **1**/NO_3^- > **1**/HSO_4^-, respectively. The relative reactivities of the halide and oxoanionic complexes are in orders: **1**/Br^- > **1**/Cl^- > **1**/F^- and **1**/NO_2^- > **1**/CH_3COO^- > **1**/HCO_3^- ≈ **1**/$C_6H_5COO^-$ > **1**/$H_2PO_4^-$ > **1**/NO_3^- ≈ **1**/HSO_4^-, respectively. The receptor **1** association with F^- was found

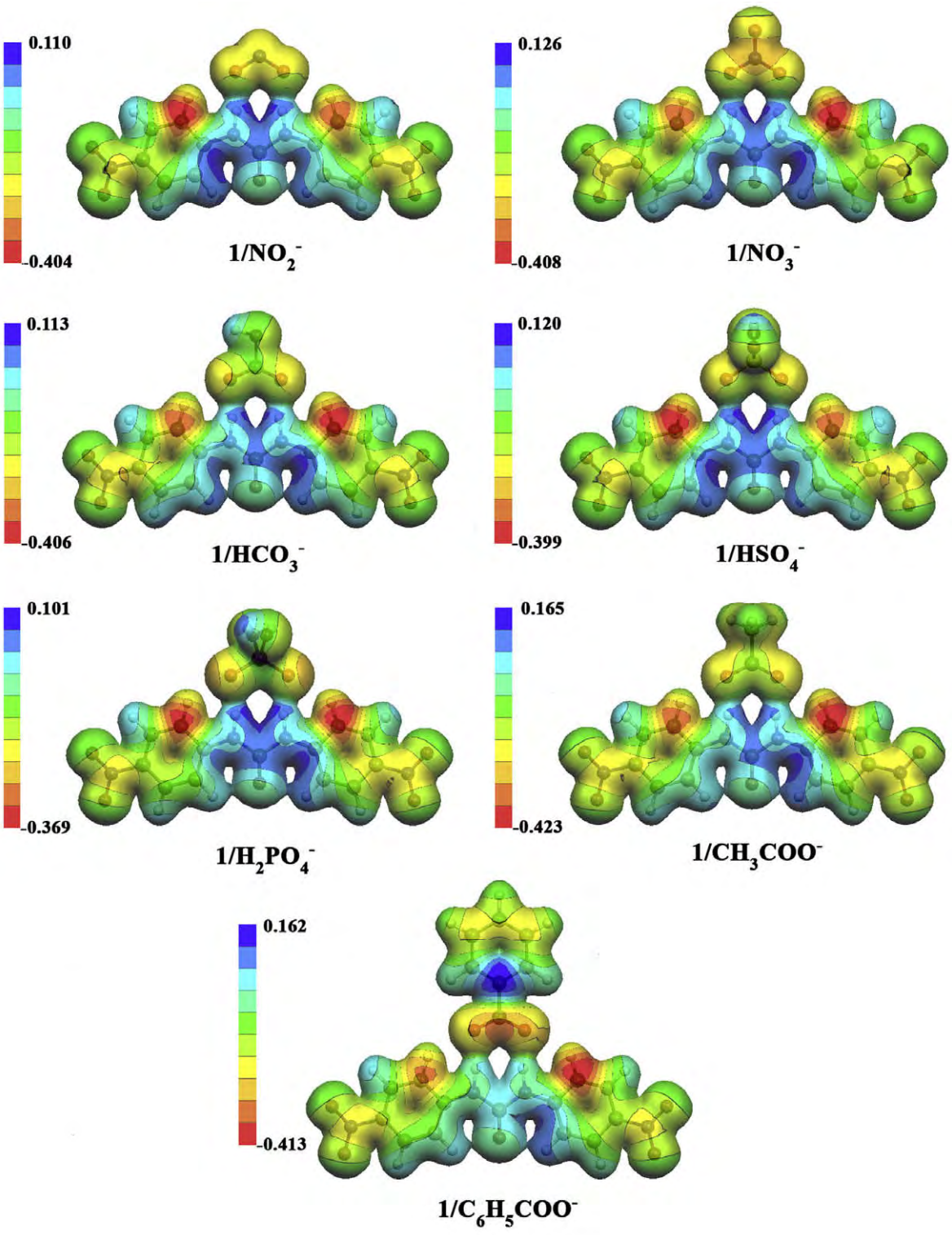

Fig. 6. Plots of the molecular electrostatic potential (in au) presented over electronic isodensity, ρ of 0.05 eÅ^{-3} of the oxoanionic complexes.

to be the most stable complex for which the binding free energy is a high value of −71.24 kcal/mol.

Acknowledgements

The authors gratefully acknowledge the Research Affairs, Mahasarakham University, and the Postgraduate Education and Research in Chemistry (PERCH) program, Thailand, for financial support of this research and the facility provided by Supramolecular Chemistry Research Unit, Department of Chemistry, Faculty of Science, Mahasarakham University. The partial support from the Thailand Research Fund for financial support (Grant No. BRG5180016) is also acknowledged.

References

[1] S. Mangani, M. Ferraroni, in: A. Bianchi, K. Bowman-James, E. Garcia-España (Eds.), Supramolecular Chemistry of Anions, Wiley-VCH, New York, 1997.
[2] J.M. Holloway, R.A. Dahlgren, B. Hansen, W.H. Casey, Nature 395 (1998) 785.
[3] J. Scheele, P. Timmerman, D.N. Reinhoudt, Chem. Commun. (1998) 2613.
[4] J.L. Sessler, P.I. Sansom, A. Andrievski, V. Král, in: A. Bianchi, K. Bowman-James, E. Garcia-España (Eds.), Supramolecular Chemistry of Anions, Wiley-VCH, New York, 1997.
[5] J.M. Lehn, Supramolecular Chemistry, Concepts and Perspectives, VCH, Weinheim, Germany, 1995.
[6] A. Bianchi, K. Bowman-James, E. García-España (Eds.), Supramolecular Chemistry of Anions, Wiley-VCH, New York, 1997.
[7] P.A. Gale, Coord. Chem. Rev. 240 (2003) 191.
[8] S.K. Kim, J. Yoon, Chem. Commun. (2002) 770.
[9] E.J. Cho, B.J. Ryu, Y.J. Lee, K.C. Nam, Org. Lett. 7 (2005) 2607.
[10] S.J. Brooks, P.A. Gale, M.E. Light, Chem. Commun. (2006) 4344.
[11] V. Amendola, D. Esteban-goämez, L. Fabbrizzi, M. Licchelli, Acc. Chem. Res. 39 (2006) 343.
[12] M.A. Hossain, J.A. Liljegren, D. Powell, K. Bowman-James, Inorg. Chem. 43 (2004) 3751.
[13] C.R. Bondy, S.J. Loeb, Coord. Chem. Rev. 240 (2003) 77.
[14] C.R. Bondy, P.A. Gale, S.J. Loeb, Chem. Comm. 8 (2001) 729.
[15] T. Zielińskia, J. Jurczak, Tetrahedron 61 (2005) 4081.
[16] K. Ghosh, T. Sen, Tetrahedron Lett. 49 (2008) 7204.
[17] S.M.S. Chauhan, T. Bisht, B. Garg, Tetrahedron Lett. 49 (2008) 6646.
[18] T. Gunnlaugsson, M. Glynn, G.M. Tocci, P.E. Kruger, F.M. Pfeffer, Coord. Chem. Rev. 250 (2006) 3094.
[19] M. Boiocchi, L.D. Boca, G.D. Esteban, L. Fabbrizzi, M. Licchelli, E. Monzani, J. Am. Chem. Soc. 126 (2004) 16507.
[20] K. Navakhun, V. Ruangpornvisuti, J. Mol. Struct. (THEOCHEM) 772 (2006) 23.
[21] K. Navakhun, V. Ruangpornvisuti, J. Mol. Struct. (THEOCHEM) 806 (2007) 145.
[22] K. Navakhun, V. Ruangpornvisuti, J. Mol. Struct. (THEOCHEM) 864 (2008) 26.
[23] V. Ruangpornvisuti, J. Mol. Struct. (THEOCHEM) 686 (2004) 47.
[24] V. Ruangpornvisuti, B. Wanno, J. Mol. Model. 13 (2007) 65.
[25] A.D. Becke, J. Chem. Phys. 98 (1993) 5648.
[26] C. Lee, W. Yang, R.G. Parr, Phys. Rev. B 37 (1988) 785.
[27] J.W. Ochterski, Thermochemistry in Gaussian, Gaussian Inc., Pittsburgh, PA, 2000.
[28] M.J. Frisch et al., Gaussian 03, Revision D02, Gaussian Inc., Wallingford, CT, 2006.
[29] G. Schaftenaar, Molden 4.2, CAOS/CAMM Center, Nijmegen Toernooiveld, Nijmegen, Netherlands, 1991.
[30] P. Flükiger, H.P. Lüthi, S. Portmann, J. Weber, Molekel 4.3, Swiss Center for Scientific Computing, Manno (Switzerland), 2000.

ภาคผนวก B

Reprint บทความเรื่อง “Molecular structures of 8,8'–dithioureido–2,2'–binaphthalene derivatives and their anions recognition: an ONIOM investigation”

Struct Chem (2009) 20:767–780
DOI 10.1007/s11224-009-9466-4

ORIGINAL RESEARCH

Molecular structures of 8,8′-dithioureido-2,2′-binaphthalene derivatives and their anions recognition: an ONIOM investigation

Sirichai Piyaauksornsak · Totsaporn Tangthongkul · Raina Wanbayor · Banchob Wanno · Vithaya Ruangpornvisuti

Received: 26 February 2009 / Accepted: 20 April 2009 / Published online: 6 May 2009

Abstract The structures of 8,8′-bis(3-phenylthioureidomethyl)-2,2′-binaphthalene (**1**), 8,8′-bis(3-butylthioureidomethyl)-2,2′-binaphthalene (**2**) and their complexes with anionic guests such as carboxylate ions (acetate, oxalate, malonate, succinate, glutarate, adipate, pimelate, suberate, and azelate), inorganic oxygen-containing anions (nitrate, sulfate, bicarbonate, hydrogen phosphate, and dihydrogen phosphate), and halide ions (fluoride, chloride, and bromide) were obtained using the ONIOM approach. The binding abilities of receptors **1** and **2** to anionic species in terms of binding energy, thermodynamic properties, and selectivity coefficient were obtained at the ONIOM(B3LYP/6-31G(d):AM1) and BSSE-corrected B3LYP/6-31G(d)//ONIOM(B3LYP/6-31G(d):AM1) levels of theory. The multipoint hydrogen bonding between receptors (either the receptor **1** or **2**) and anionic guests were found. The hydrogen phosphate is the most preferable ion to bind with either the receptor **1** or **2**.

Keywords 8,8′-Dithioureido-2,2′-binaphthalene · Carboxylate · Halide · Anions · Host–guest · Selectivity · ONIOM · DFT · BSSE

S. Piyaauksornsak · T. Tangthongkul · R. Wanbayor · V. Ruangpornvisuti (✉)
Department of Chemistry, Faculty of Science and Center for Petroleum, Petrochemicals and Advanced Materials, Chulalongkorn University, Bangkok 10330, Thailand
e-mail: vithaya.r@chula.ac.th

B. Wanno
Department of Chemistry, Faculty of Science, Mahasarakham University, Mahasarakham 44150, Thailand

Introduction

The organic anion receptors which contain chromophore part are basically used for chromogenic sensors for detection of biological anions. An anion receptor such as thiourea-based chromophores with *p*-nitrophenyl groups is found to be an excellent chromogenic anion receptor for monocarboxylate such as acetate [1]. Anion recognition of two binding-sites receptors lead to discovery of useful sensors not only for dicarboxylates but also monocarboxylates. Chromogenic azophenol-thiourea-based anion sensors developed for the selective colorimetric detection of acetate and other anions [2–4], chromogenic indoaniline-thiourea-based receptors as fluoride detection sensors [5] and anthracene urea, thiourea compounds and their effective chromogenic anion sensors [6] were studied. And fluorescent and luminescent chemosensors for detection of anions have been developed for dicarboxylate recognition [7]. Tripodal urea receptors were synthesized and their binding properties with large terephthalate and trimesylate anions in polar aprotic solvents were investigated using NMR and luminescence titration methods and their association constants were reported [8]. The urea or thiourea groups incorporated receptors as anion recognition were studied in system of various solvents [9–11]. Previous theoretical work, the binding energies and thermodynamic properties of the 1,3-bis(4-nitrophenyl)urea complexes with halide anions and oxygen-containing anions were studied [12]. The recognition of carboxylate and dicarboxylates by azophenol-thiourea derivatives were first investigated by the IMOMO method and the oxalate is the most favorite ion to form complexes with both receptors of azophenol-thiourea derivatives [13]. Since determination of the binding and complexation energies of the complexes of the *p-tert*-butylsulfonylcalix[4]arene [14], *p-tert*-butylthiacalix[4]arene

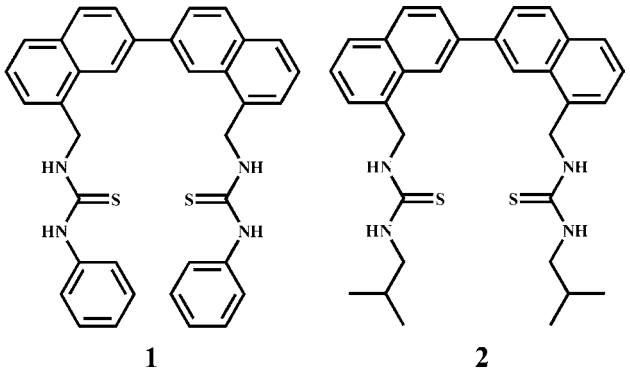

Scheme 1 Receptors **1** (8,8′-bis(3-phenylthioureidomethyl)-2,2′-binaphthalene) and **2** (8,8′-bis(3-butylthioureidomethyl)-2,2′-binaphthalene)

[15] and tetraamino-*tert* -butylthiacalix[4]arene [16] derivatives with zinc(II) cation were theoretically carried out, the complexes of these receptors with organic anions should be therefore investigated, particularly the calix[4]arene derivative functionalized by amino group. The binding abilities of the tetraamino-*tert*-butylthiacalix[4]arene derivatives to zinc (II) cation [16, 17] and the tetraamino-*tert*-butylthiacalix[4]arene and tetraamino-tert-butylcalix[4]arene receptors binding to carboxylate and dicarboxylate guests were studied [18].

As organic anions such as acetate, oxalate, malonate, and succinate are important biological anions, detection of these species is very useful data for medical and biological topics. Since 8,8′-dithioureido-2,2′-binaphthalene derivatives [19, 20] were synthesized and their anion recognition were studied using UV–Vis spectroscopic method, the binding properties of many interesting anionic guests on these receptors should therefore be investigated using molecular modeling as the efficient tool. To better understanding of binding properties of 8,8′-dithioureido-2,2′-binaphthalene derivatives, their interaction with various anionic guests have been theoretically investigated. In this work, 8,8′-bis(3-phenylthioureidomethyl)-2,2′-binaphthalene (**1**), 8,8′-bis(3-butylthioureidomethyl)-2,2’-binaphthalene (**2**) shown in Scheme 1 and anionic guests such as acetate, oxalate, malonate, succinate, glutarate, adipate, pimelate, suberate, azelate, nitrate, sulfate, bicarbonate, hydrogen phosphate, dihydrogen phosphate, fluoride, chloride, and bromide have therefore been investigated.

Computational details

Geometries of the host–guest complexes and their host and guest components were optimized using the hybrid density functional B3LYP [21, 22] method and the two-layered ONIOM(MO:MO) approach [23, 24] using B3LYP/6-31G(d) as high level and semiempirical AM1 [25] and PM3 [26] as low level. The real and model systems used in the two-layer ONIOM(MO:MO) calculations for the hosts and host–guest interaction models are shown in Fig. 1. The reliability of the two-layer ONIOM calculations at the integrated level, ONIOM(B3LYP/6-31G(d):AM1) and ONIOM(B3LYP/6-31G(d):PM3) approaches was well examined [16–18, 27] and discussed in references [28, 29]. In this work, the reliability of the ONIOM(B3LYP/6-31G(d):AM1) and ONIOM(B3LYP/6-31G(d):PM3) was examined by geometry optimizations of the complexes of receptors **1** and **2** with oxalate guest compared with their target geometry optimized at the B3LYP/6-31G(d) level. Geometries of **1**/oxalate and **2**/oxalate as the host–guest complexes were calculated at the AM1, ONIOM(B3LYP/6-31G(d):AM1) and ONIOM(B3LYP/6-31G(d):PM3) levels and compared with the target B3LYP/6-31G(d) geometry as shown in Fig. 2 and Tables 1 and 2. The ONIOM(B3LYP/6-31G(d):AM1) calculation of the system examined provides reasonable results at a relatively low cost for the present host–guest interactions. The two-layer ONIOM(B3LYP/6-31G(d):AM1) was therefore used for geometry optimization throughout this work. All calculations were performed using the GAUSSIAN 03 program [30] and their structures were visualized using the MOLEKEL 4.3 program [31].

Binding energy between guest and host ($\Delta E_{\text{binding}}$), preorganization energies of host $\left(\Delta E^{\text{host}}_{\text{preorg.}}\right)$, guest

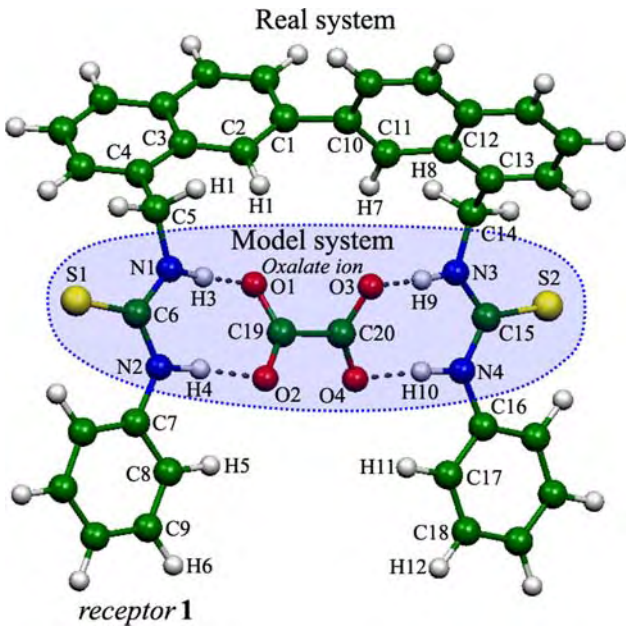

Fig. 1 The two-layer ONIOM model for the **1**/oxalate complex. The atoms in shade area of the complex structure are treated as the high-level layer using at the B3LYP/6–31G(d) level while the rest of the molecular cluster is treated as the low-level layer using at the semi-empirical levels (AM1 or PM3). Atomic numbering for the **1**/oxalate complex defined as a representative complex structure

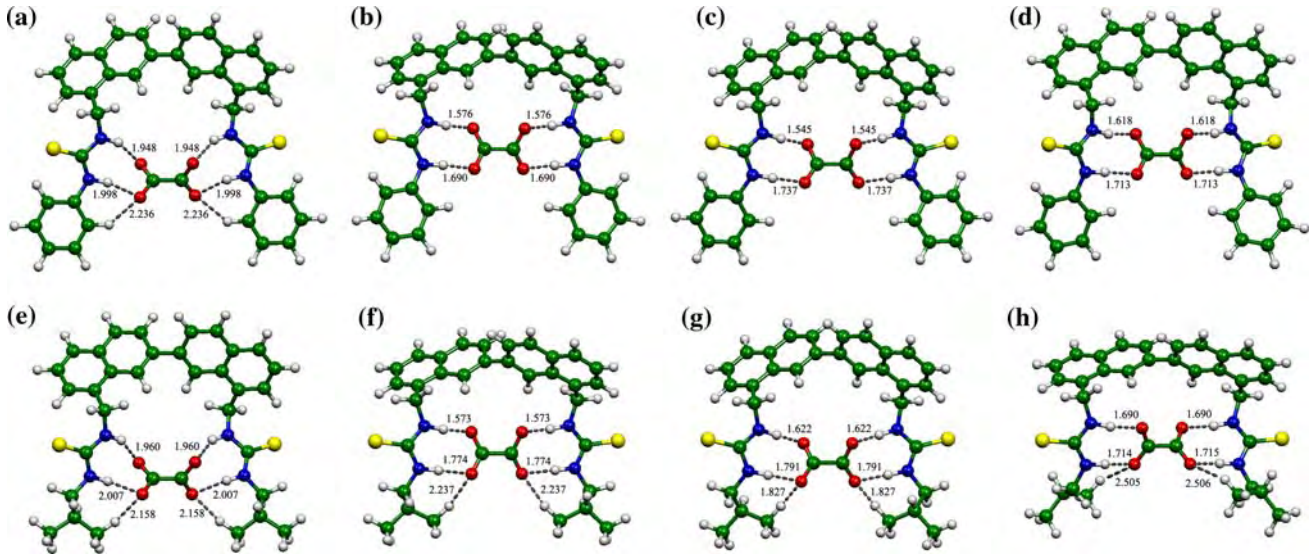

Fig. 2 The optimized structures of the **1**/oxalate complex at the **a** AM1, **b** ONIOM(B3LYP/6-31G(d):AM1), **c** ONIOM(B3LYP/6-31G(d):PM3), **d** B3LYP/6-31G(d), **2**/oxalate at the **e** AM1, **f**ONIOM(B3LYP/6-31G(d):AM1), **g** ONIOM(B3LYP/6-31G(d):PM3) and **h** B3LYP/6-31G(d). The bond lengths are in Å

$\left(\Delta E^{\text{guest}}_{\text{preorg.}}\right)$ and complexation energy of host–guest complex $\left(\Delta E_{\text{complex}}\right)$ based on the ONIOM(B3LYP/6-31G(d):AM1) approach are defined as following formulae:

$$\begin{aligned}\Delta E_{\text{binding}} &= E[\text{ONIOM(B3LYP/6-31G(d):AM1)}](\text{host}-\text{guest complex})\\ &\quad - E[\text{ONIOM (B3LYP/6-31G(d):AM1)}](\text{isolated host})\\ &\quad - E[\text{B3LYP/6-31G(d)}](\text{isolated guest})\end{aligned} \tag{1}$$

$$\begin{aligned}\Delta E^{\text{host}}_{\text{preorg.}} &= E[\text{ONIOM(B3LYP/6-31G(d):AM1)}](\text{complexed host})\\ &\quad - E[\text{ONIOM (B3LYP/6-31G(d):AM1)}](\text{isolated host})\end{aligned} \tag{2}$$

$$\Delta E^{\text{guest}}_{\text{preorg}} = E[\text{B3LYP/6-31G(d)}](\text{complexed guest}) - E[\text{B3LYP/6-31G(d)}](\text{isolated guest}) \tag{3}$$

$$\begin{aligned}\Delta E_{\text{complex}} &= E[\text{ONIOM(B3LYP/6-31G(d):AM1)}](\text{host}-\text{guest complex})\\ &\quad - E[\text{ONIOM (B3LYP/6-31G(d):AM1)}](\text{complexed host})\\ &\quad - E[\text{B3LYP/6-31G(d)}](\text{complexed guest})\end{aligned} \tag{4}$$

$$\Delta E_{\text{binding}} = \Delta E^{\text{host}}_{\text{preorg.}} + \Delta E^{\text{guest}}_{\text{preorg.}} + \Delta E_{\text{complex}} \tag{5}$$

$$\Delta E_{\text{binding}} = \Delta E^{\text{total}}_{\text{preorg.}} + \Delta E_{\text{complex}} \tag{6}$$

To estimate the basis set superposition error (BSSE) for the energies of host–guest complex formation at the B3LYP/6-31G(d)//ONIOM(B3LYP/6-31G(d):AM1) level, counterpoise (CP) calculations were performed using the Boys–Bernardi's CP scheme [32–37]. The BSSE energies of the host–guest complex formation were used to compute the energies of BSSE corrected binding $\left(\Delta E^{\text{BSSE}}_{\text{binding}}\right)$ and complexation $\left(\Delta E^{\text{BSSE}}_{\text{complex}}\right)$. The total preorganization energy with BSSE correction $\left(\Delta E^{\text{BSSE}}_{\text{preorg.}}\right)$ is therefore obtained by Eq. 7.

$$\Delta E^{\text{BSSE}}_{\text{preorg.}} = \Delta E^{BSSE}_{binding} - \Delta E^{BSSE}_{complex} \tag{7}$$

The enthalpy ΔH^{298} and Gibbs free energy changes ΔG^{298} of all complexation reactions have been derived from the frequency computations at ONIOM(B3LYP/6-31G(d):AM1) level of theory. The equilibrium constant, K of binding process at 298.15 and 1 atmosphere was computed using thermodynamic relation of $\Delta G^{298} = -\text{RT ln } K$.

The binding selectivity of 8,8′-dithioureido-2,2′-binaphthalene receptor to guest B with respect to guest A

Table 1 Geometrical data for the **1**/oxalate complex optimized at the AM1, ONIOM(B3LYP/6-31G(d):AM1), ONIOM(B3LYP/6-31G(d):PM3), and B3LYP/6-31G(d) levels of theory

Parameter[a]	AM1	(B3LYP/6-31G(d):AM1)	(B3LYP/6-31G(d):PM3)	B3LYP/6-31G(d)
Host				
Bond distance (Å)				
C1–C10	1.465	1.469	1.473	1.496
C1–C2	1.379	1.379	1.372	1.385
C2–C3	1.425	1.426	1.424	1.430
C3–C4	1.427	1.429	1.428	1.436
C4–C5	1.510	1.507	1.500	1.523
C2–H1	1.103	1.105	1.103	1.085
C5–H2	1.128	1.129	1.113	1.095
C5–N1	1.431	1.447	1.489	1.449
N1–H3	1.016	1.080	1.095	1.061
N1–C6	1.382	1.354	1.349	1.347
C6–S1	1.629	1.729	1.752	1.720
C6–N2	1.383	1.374	1.369	1.372
N2–H4	1.035	1.072	1.066	1.055
N2–C7	1.401	1.412	1.446	1.396
C7–C8	1.424	1.422	1.403	1.414
C8–H5	1.111	1.107	1.100	1.087
Bond angle (°)				
C1–C2–C3	121.081	120.797	120.585	121.461
C1–C2–H1	119.429	119.959	121.091	118.865
C2–C3–C4	123.126	122.832	122.160	123.647
C3–C4–C5	122.254	121.610	121.087	123.077
C4–C5–N1	115.687	114.243	112.324	113.786
C5–N1–H3	117.370	116.837	117.905	113.440
C5–N1–C6	122.694	121.428	121.609	125.666
N1–C6–N2	115.312	111.774	112.315	111.182
C6–N2–H4	117.436	118.694	118.055	114.006
N2–C6–S1	124.341	126.041	125.028	125.777
N2–C7–C8	117.110	127.469	117.411	115.523
Dihedral angle (°)				
C2–C1–C10–C11	61.991	97.830	85.665	66.308
C3–C4–C5–N1	−107.011	−88.085	−104.896	−105.115
C4–C5–N1–C6	−94.968	−117.347	−105.721	−115.062
C5–N1–C6–N2	−178.426	−177.409	−168.353	−163.940
N1–C6–N2–C7	169.141	−177.995	−172.605	−168.603
C6–N2–C7–C8	−153.824	−177.142	176.897	−169.959
Guest				
Bond distance (Å)				
C19–O1	1.279	1.266	1.270	1.267
C19–O2	1.272	1.263	1.261	1.263
C19–C20	1.517	1.560	1.554	1.554
Bond angle (°)				
O1–C19–O2	118.227	126.370	126.100	126.077
Dihedral angle (°)				
O1–C19–C20–O3	75.387	38.395	52.005	41.365

Table 1 continued

Parameter[a]	AM1	(B3LYP/ 6-31G(d):AM1)	(B3LYP/ 6-31G(d):PM3)	B3LYP/ 6-31G(d)
Host/Guest				
Bond distance (Å)				
H3···O1[b]	1.949	1.576	1.545	1.618
H4···O2[b]	1.998	1.690	1.737	1.713
H5···O2[b]	2.236	2.446	2.842	2.405
Bond angle (°)				
N1–H3···O1	151.512	176.190	176.981	166.664
N2–H4···O2	146.032	174.543	175.017	173.266
Dihedral angle (°)				
N1–H3···O1–C19	−93.365	133.777	113.864	115.230
N2–H4···O2–C19	−150.295	−174.421	−110.381	−144.518

[a] Atomic labeling is shown in Fig. 1

[b] Hydrogen bond

has been derived from the selectivity coefficient $\left(K_B^A\right)$ [38] which is defined as an equilibrium constant of ion exchange between ions A and B. Since exchange is a chemical reaction as Eq. 8, it can be treated like any other mass action expression.

$$AX + B \rightleftharpoons BX + A \tag{8}$$

Therefore, the selectivity coefficient can be defined as $K_B^A = \frac{[BX][A]}{[AX][B]}$. If the complexations of BX and AX are observed, their stability constants based on Eqs. 9 and 10 can be expressed as $K_A = \frac{[AX]}{[X][A]}$ and $K_B = \frac{[BX]}{[X][B]}$.

$$X + B \rightleftharpoons BX \tag{9}$$

$$X + A \rightleftharpoons AX \tag{10}$$

The selectivity coefficient can be therefore written as $K_B^A = \frac{K_B}{K_A}$. If the value of the selectivity coefficient K_B^A is larger than one, this implies that B is preferred over A and if K_B^A is smaller than one, then A is preferred over B.

Results and discussion

To examine the reliability of the two-layer ONIOM(MO:MO) method, the geometries of the **1**/oxalate complex were optimized at four different levels of theory. Its geometries optimized at the AM1, B3LYP/6-31G(d), ONIOM(B3LYP/6-31G(d):AM1), and ONIOM(B3LYP/6-31G(d):PM3) levels of theory are shown in Fig. 3 and their corresponding geometrical data are tabulated in Table 1. As the hydrogen bonds of the four different levels of theory for the **1**/oxalate and **2**/oxalate complexes have been compared, its ONIOM(B3LYP/6-31G(d):AM1)-optimized hydrogen-bond distances are in good agreement with the B3LYP/6-31G(d)-optimized geometrical data, as shown in Tables 1 and 2, respectively. The ONIOM(B3LYP/6-31G(d):AM1)-optimized geometry of the **1**/oxalate complex is very similar to the target B3LYP/6-31G(d)-optimized geometry (Fig. 3) and its geometrical data are correspondingly confirmed, see Table 1. As the reliability test of the ONIOM(MO:MO) approach for this host–guest system, the ONIOM(B3LYP/6-31G(d):AM1) is therefore to be the most reliable one with respect to the full B3LYP/6-31G(d) level of theory.

Complexation of 8,8′-bis(3-phenylthioureidomethyl)-2,2′-binaphthalene (receptor **1**)

The receptor **1** can form stable complexes with all anionic guests. The relative stabilities of the receptor **1** complexes with carboxylates, inorganic oxygen-containing anions, and halide ions are in decreasing orders: oxalate > malonate > succinate > glutarate > adipate > pimelate > suberate > azelate >acetate, $HPO_4^{2-} > SO_4^{2-} > HCO_3^- > H_2PO_4^- \approx NO_3^-$ and $F^- \gg Cl^- \approx Br^-$, respectively. The ONIOM(B3LYP/6-31G(d):AM1)-optimized structures of the complexes of receptor **1** with carboxylate and inorganic anions are show in Figs. 4 and 5, respectively. The multipoint hydrogen bonding between the receptor **1** and anionic guests were found; for carboxylate and dicarboxylate ions and for inorganic and halide anions are shown in Figs. 4 and 5, respectively. The selectivity coefficients of the receptor **1** toward anions with respect to hydrogen phosphate (the most stable complex with **1**) in Table 3 indicate that the receptor **1** is able to well recognize the hydrogen phosphate among all anionic species. The order of the relative stabilities of the receptor **1** complexes with F^- and Cl^- ($F^- > Cl^-$) is in agreement with the experiment [20], see Table 3. For the system of carboxylate anionic species, the total preorganization energy due to the

Table 2 Geometrical data for the **2**/oxalate complex optimized at the AM1, ONIOM(B3LYP/6-31G(d):AM1), ONIOM(B3LYP/6-31G(d):PM3), and B3LYP/6-31G(d) levels of theory

Parameter[a]	AM1	(B3LYP/6-31G(d):AM1)	(B3LYP/6-31G(d):PM3)	B3LYP/6-31G(d)
Host				
Bond distance (Å)				
C1–C10	1.465	1.469	1.473	1.492
C1–C2	1.379	1.380	1.372	1.384
C2–C3	1.425	1.426	1.423	1.424
C3–C4	1.427	1.429	1.428	1.437
C4–C5	1.511	1.508	1.500	1.526
C2–H1	1.103	1.106	1.103	1.083
C5–H2	1.128	1.129	1.113	1.096
C5–N1	1.429	1.445	1.486	1.450
N1–H3	1.015	1.079	1.075	1.055
N1–C6	1.382	1.356	1.357	1.352
C6–S1	1.639	1.736	1.740	1.733
C6–N2	1.370	1.359	1.353	1.351
N2–H4	1.025	1.056	1.066	1.053
N2–C7	1.436	1.447	1.487	1.447
C7–C8	1.539	1.539	1.535	1.545
C9–H6	1.125	1.122	1.125	1.094
Bond angle (°)				
C1–C2–C3	121.096	120.817	120.606	121.754
C1–C2–H1	119.473	119.882	121.137	118.027
C2–C3–C4	123.126	122.866	122.121	122.997
C3–C4–C5	122.394	121.737	121.120	122.292
C4–C5–N1	115.830	114.578	112.579	113.452
C5–N1–H3	117.812	117.036	118.894	116.104
C5–N1–C6	122.677	121.471	121.884	124.984
N1–C6–N2	116.766	113.501	112.574	113.583
C6–N2–H4	120.160	120.874	120.913	117.807
N2–C6–S1	121.875	123.513	123.483	123.004
N2–C7–C8	113.039	113.919	110.288	113.865
Dihedral angle (°)				
C2–C1–C10–C11	59.975	101.242	88.368	117.044
C3–C4–C5–N1	−106.927	−86.288	−104.283	−84.110
C4–C5–N1–C6	−92.233	−111.174	−102.737	−95.207
C5–N1–C6–N2	−178.243	−179.193	−169.144	172.337
N1–C6–N2–C7	175.570	−175.846	−171.516	−179.641
C6–N2–C7–C8	158.529	121.739	138.478	90.710
Guest				
Bond distance (Å)				
C19–O1	1.278	1.267	1.265	1.267
C19–O2	1.273	1.261	1.268	1.265
C19–C20	1.519	1.571	1.556	1.551
Bond angle (°)				
O1–C19–O2	118.468	126.557	126.302	126.134
Dihedral angle (°)				
O1–C19–C20–O3	80.458	25.829	52.352	−65.241

Table 2 continued

Parameter[a]	AM1	(B3LYP/6-31G(d):AM1)	(B3LYP/6-31G(d):PM3)	B3LYP/6-31G(d)
Host/Guest				
Bond distance (Å)				
H3···O1[b]	1.960	1.573	1.622	1.690
H4···O2[b]	2.007	1.774	1.791	1.714
H6···O2[b]	2.158	2.237	1.827	2.505
Bond angle (°)				
N1–H3···O1	150.673	176.100	178.848	172.746
N2–H4···O2	148.261	178.457	175.186	172.812
Dihedral angle (°)				
N1–H3···O1–C19	−98.203	162.954	−95.108	−155.659
N2–H4···O2–C19	−138.861	−137.754	−112.127	141.476

[a] Atomic labeling is shown in Fig. 1

[b] Hydrogen bond

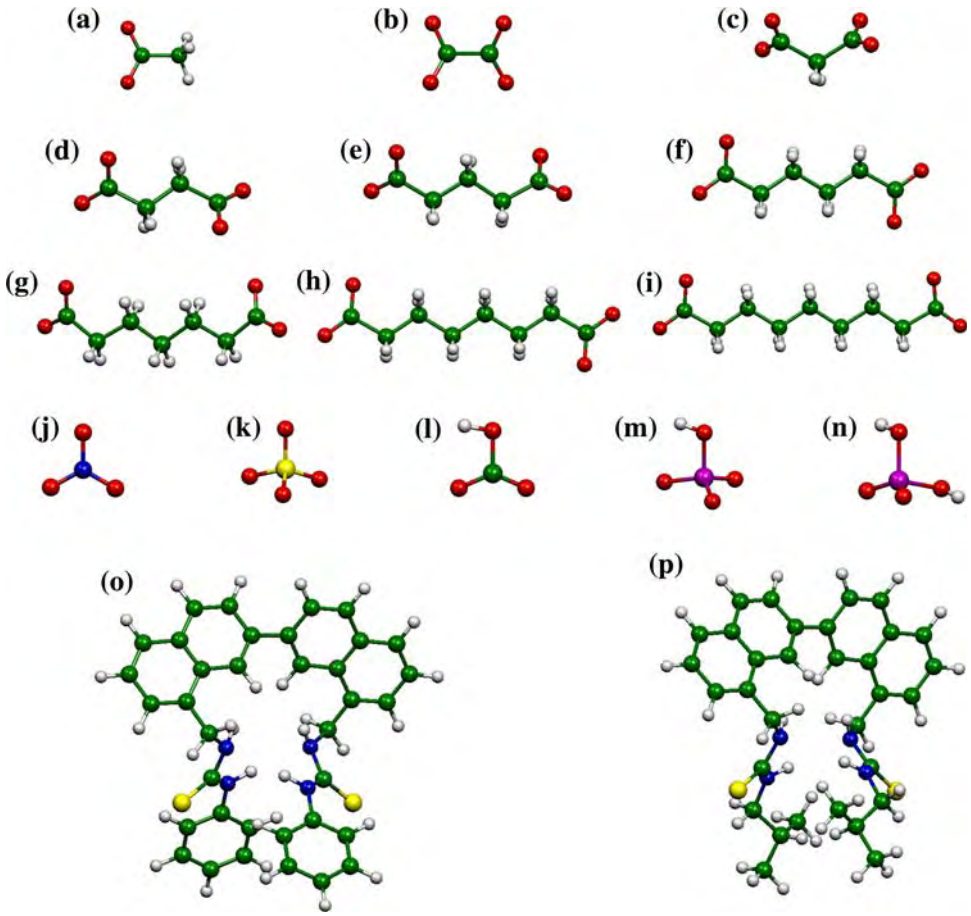

Fig. 3 B3LYP/6-31G(d)-optimized geometries of free forms of the anionic guests **a** acetate, **b** oxalate, **c** malonate, **d** succinate, **e** glutarate, **f** adipate, **g** pimelate, **h** suberate, **i** azelate, **j** nitrate, **k** sulphate, **l** hydrogen carbonate, **m** hydrogen phosphate, **n** dihydrogen phosphate and the ONIOM(B3LYP/6-31G(d):AM1)-optimized structures of **o** the receptor **1**, and **p** receptor **2**

complexation $\left(\Delta E^{\text{total}}_{\text{preorg.}} = 13.51\,\text{kcal/mol}\right)$ of the receptor **1** and the acetate anion of which the preorganization energies are, respectively, $\Delta E^{\text{receptor 1}}_{\text{preorg.}} = 11.66$ kcal/mol and $\Delta E^{\text{acetate}}_{\text{preorg.}} = 1.85$ kcal/mol is the smallest value as listed in Table 4. Plot of the preorganization energies of the receptor **1** and carboxylate anionic species against sizes of carboxylate ionic guests, obtained at the ONIOM(B3LYP/6-31G(d):AM1) level of theory are shown in Fig. 6a.

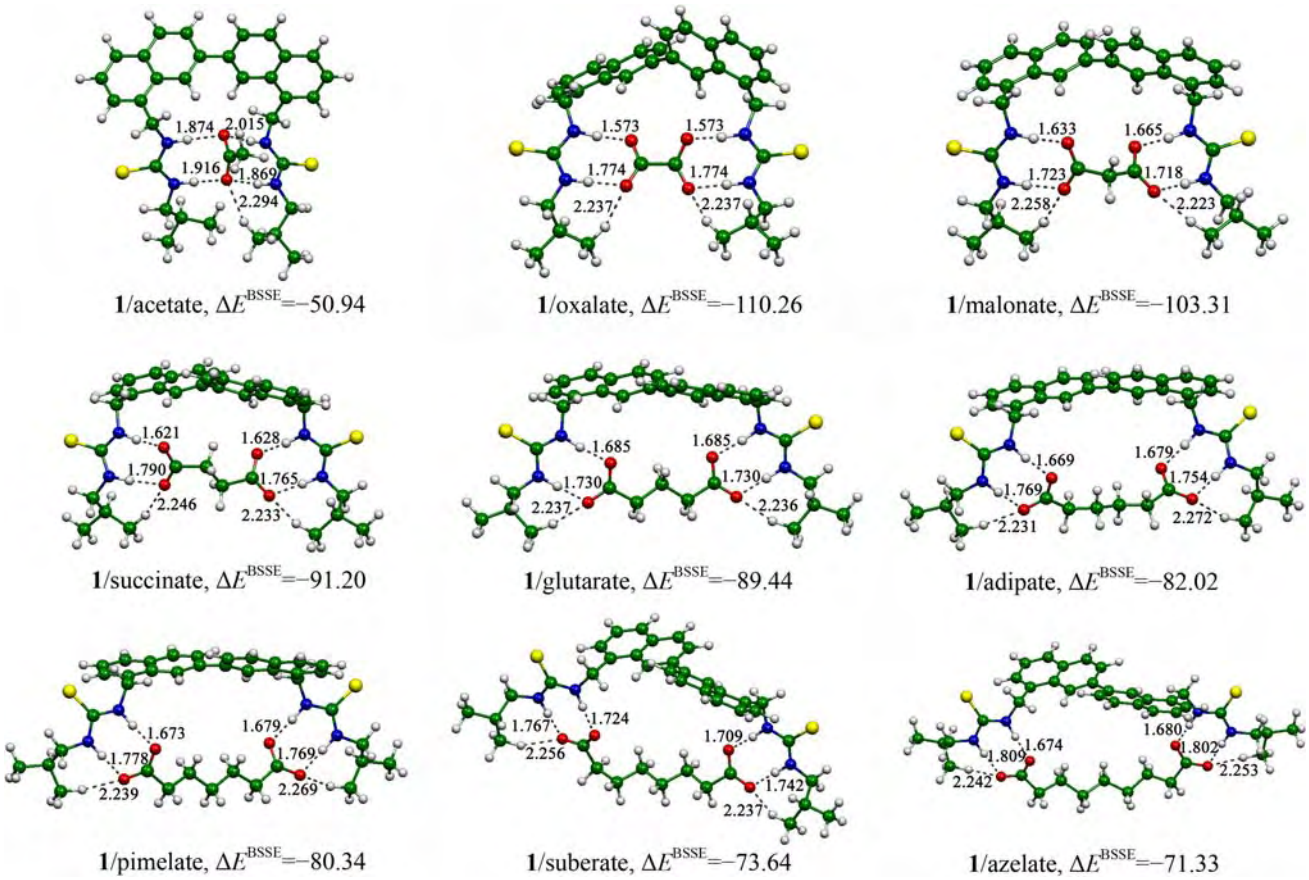

Fig. 4 The ONIOM(B3LYP/6-31G(d):AM1)-optimized structures of receptor **1** complexes with carboxylate and dicarboxylate guests. Binding energies, ΔE^{BSSE} computed at the B3LYP/6-31G(d)//ONIOM(B3LYP/6-31G(d):AM1 with BSSE correction are in kcal/mol. The bond lengths are in Å

Binding energies with and without BSSE correction, BSSE corrected preorganization energies of complexations of the receptor **1** with the various anionic species derived at the B3LYP/6-31G(d)//ONIOM(B3LYP/6-31G(d):AM1) level of theory are shown in Table 5. It shows that the BSSE corrected binding energy of the **1**/HPO_4^{2-} complex is the most stable species. The relative stabilities of complexes of the receptor **1** obtained at the B3LYP/6-31G(d)//ONIOM(B3LYP/6-31G(d):AM1) calculations either with or without BSSE correction are in the same orders: oxalate > malonate > succinate > glutarate > adipate > pimelate > suberate > azelate > acetate for carboxylates, $HPO_4^{2-} > SO_4^{2-} > HCO_3^- > H_2PO_4^- \approx NO_3^-$ for inorganic oxygen-containing anions and $F^- \gg Cl^- \approx Br^-$ for halide ions. The binding energies of the receptor **1** with all anionic species obtained form the BSSE-corrected B3LYP/6-31G(d)//ONIOM(B3LYP/6-31G(d):AM1) calculation are more accurate than the energies computed at the ONIOM (B3LYP/6-31G(d):AM1) level by 13.3–38.1%.

Complexation of 8,8′-bis(3-butylthioureidomethyl)-2,2′-binaphthalene (receptor **2**)

The relative stabilities of complexes of the receptor **2** with carboxylates, inorganic oxygen-containing anions, and halide ions are in the same order as the receptor **1** system, namely: oxalate > malonate > succinate > glutarate > adipate > pimelate > suberate > azelate > acetate, $HPO_4^{2-} > SO_4^{2-} > HCO_3^- > NO_3^- \approx H_2PO_4^-$ and $F^- \gg Br^- \approx Cl^-$, respectively. The ONIOM(B3LYP/6-31G(d):AM1)-optimized structures of the receptor **2** complexes with carboxylate and inorganic anionic species are show in Figs. 7 and 8, respectively. The multipoint hydrogen bonding between the receptor **2** and anionic guests were found; for carboxylate and dicarboxylate ions and for inorganic and halide anions are shown in Figs. 7 and 8, respectively.

Table 6 also shows that the receptor **2** complex with hydrogen phosphate ion is the most stable complex. The order of the relative stabilities of the receptor **2**

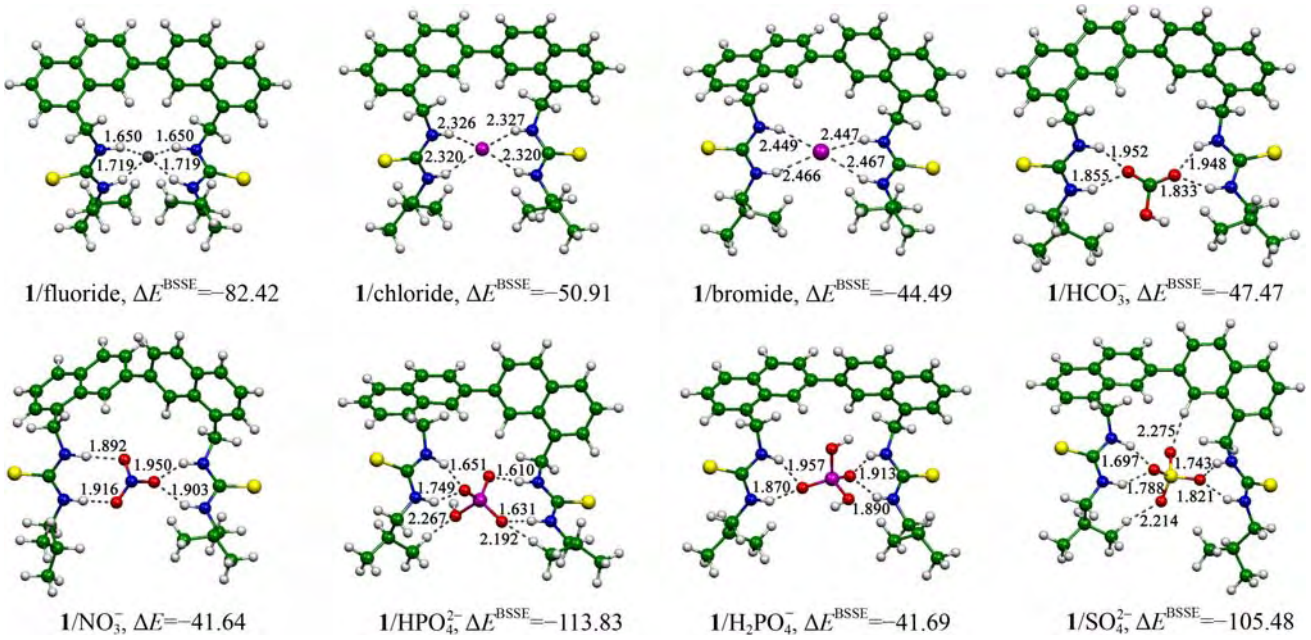

Fig. 5 The ONIOM(B3LYP/6-31G(d):AM1)-optimized structures of receptor **1** complexes with halide ions, carbonate, nitrate, phosphate, and sulfate ions. Binding energies, ΔE^{BSSE} computed at the B3LYP/6-31G(d)//ONIOM(B3LYP/6-31G(d):AM1 with BSSE correction are in kcal/mol. The bond lengths are in Å

Table 3 Binding energies, enthalpies and free energies of complexation of the receptor **1** with various anionic guests

Guest	$\Delta E_{\mathrm{binding}}$ [a]	ΔH^{298} [a]	ΔG^{298} [a]	$K_{\mathrm{B}}^{\mathrm{acetate}}$ [b]	K_{298} [c]
Acetate	−67.14	−67.06	−54.81	1.80×10^{8}	1.17×10^{6}
Oxalate	−140.87	−140.40	−128.53	2.00×10^{62}	–
Malonate	−128.51	−128.73	−114.22	6.46×10^{51}	–
Succinate	−115.95	−116.24	−101.10	1.55×10^{42}	–
Glutarate	−111.32	−111.46	−96.85	1.19×10^{39}	–
Adipate	−100.52	−99.72	−87.17	9.64×10^{31}	–
Pimelate	−98.12	−97.83	−83.65	2.50×10^{29}	–
Suberate	−90.70	−89.76	−78.00	1.82×10^{25}	–
Azelate	−88.20	−87.79	−74.33	3.71×10^{22}	–
NO_3^-	−55.25	−54.84	−44.46	4.67×10^{0}	–
SO_4^{2-}	−128.80	−128.69	−116.46	2.83×10^{53}	–
HCO_3^-	−61.54	−61.22	−50.77	1.99×10^{5}	–
HPO_4^{2-}	−139.98	−139.88	−126.16	3.68×10^{60}	–
$H_2PO_4^-$	−55.81	−55.74	−43.55	1.00×10^{0}	–
F^-	−133.05	−133.66	−125.15	6.70×10^{59}	1.42×10^{6}
Cl^-	−58.74	−58.67	−53.32	1.45×10^{7}	2.31×10^{3}
Br^-	−60.94	−60.86	−54.76	1.65×10^{8}	–

[a] In kcal/mol, derived from the ONIOM(B3LYP/6-31G(d):AM1) energies with ZPVE correction

[b] Selectivity coefficient of guests with respect to dihydrogen phosphate

[c] In MeCN determined by UV–vis spectroscopy, taken from Ref. [20]

complexes with F^- and Cl^- ($F^- > Cl^-$) is in agreement with the experiment [20], see Table 6. For the system of carboxylate anionic species, the total preorganization energy due to the complexation $\left(\Delta E_{\mathrm{preorg.}}^{\mathrm{total}} = 2.57 \text{ kcal/mol}\right)$ of the receptor **2** and the glutarate anion of which the preorganization energies are, respectively, $\Delta E_{\mathrm{preorg.}}^{\mathrm{receptor\ 2}} = 2.57$ kcal/mol and $\Delta E_{\mathrm{preorg.}}^{\mathrm{glutarate}} \approx 0$ kcal/mol is the smallest value as listed in Table 7. This informs that the glutarate structure has no change or has hardly changed during association with the receptor **2**. Plot of the preorganization energies of the receptor **2** and carboxylate anionic species against sizes of carboxylate ionic guests, obtained at the ONIOM(B3LYP/6-31G(d):AM1) level of theory are shown in Fig. 6b.

Binding energies with and without BSSE correction, BSSE corrected preorganization energies of complexations of the receptor **2** with the various anionic species derived at the B3LYP/6-31G(d)//ONIOM(B3LYP/6-31G(d):AM1) level of theory are shown in Table 8. It shows that the BSSE corrected binding energy of the **2**/HPO_4^{2-} complex is the most stable species. The relative stabilities of complexes of the receptor **2** obtained at the B3LYP/6-31G(d)//ONIOM(B3LYP/6-31G(d):AM1) calculations either with or without BSSE correction are in the same order: oxalate > malonate > succinate > glutarate > adipate > pimelate > suberate > azelate > acetate. For the stabilities

Table 4 Preorganization energies of the receptor **1** (host), carboxylates (guest) and their complexes, complexation energies and their corresponding thermodynamics derived from the ONIOM (B3LYP/6-31G(d):AM1) calculations

Host:guest	Host			Guest			$\Delta E_{preorg.}^{total}$ [a]	$\Delta E_{complex}$ [a]
	$\Delta E_{preorg.}^{host}$ [a]	ΔH^{298} [a]	ΔG^{298} [a]	$\Delta E_{preorg.}^{guest}$ [b]	ΔH^{298} [b]	ΔG^{298} [b]		
1/acetate	11.66	10.43	13.71	1.85	1.30	2.89	13.51	−80.65
1/oxalate	14.80	12.66	19.26	0.39	0.40	−0.02	15.19	−156.05
1/malonate	14.66	13.04	17.47	1.75	1.22	2.37	16.41	−144.93
1/succinate	12.43	10.76	15.87	4.56	3.52	6.14	16.99	−132.95
1/glutarate	12.34	10.68	15.63	1.79	0.74	3.79	14.13	−125.45
1/adipate	13.05	11.96	14.91	4.72	5.21	3.00	17.77	−118.29
1/pimelate	13.46	12.37	15.55	3.04	3.01	2.54	16.50	−114.62
1/suberate	13.30	12.30	14.92	7.12	7.06	6.57	20.42	−111.12
1/azelate	13.60	12.64	15.02	7.32	6.67	8.50	20.92	−109.13
$1/NO_3^-$	5.72	4.56	7.98	0.37	0.37	−0.27	6.09	−61.34
$1/SO_4^{2-}$	15.66	13.67	19.73	2.53	2.52	1.06	18.19	−146.99
$1/HCO_3^-$	7.21	6.03	8.86	1.53	1.50	1.55	8.74	−70.27
$1/HPO_4^{2-}$	18.13	16.09	22.32	4.22	4.35	3.99	22.35	−162.34
$1/H_2PO_4^-$	6.73	5.47	8.43	3.14	2.98	3.31	9.87	−65.68
$1/F^-$	13.96	12.17	17.49	0.00	0.00	0.00	13.96	−147.01
$1/Cl^-$	8.08	6.99	9.56	0.00	0.00	0.00	8.08	−66.82
$1/Br^-$	9.02	7.92	11.04	0.00	0.00	0.00	9.02	−69.97

[a] In kcal/mol, derived at the ONIOM (B3LYP/6-31G(d):AM1) level with ZPVE correction

[b] In kcal/mol, derived at the B3LYP/6-31G(d) level with ZPVE correction

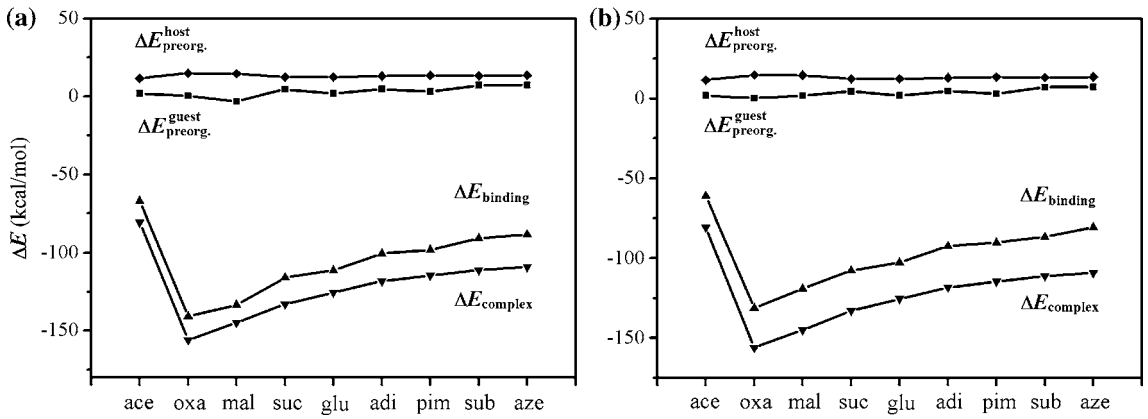

Fig. 6 Plots of binding, complexation and preorganization energies of complex systems of **a** the receptor **1** and **b** receptor **2**, against the size of the carboxylate ions, based on the ONIOM(B3LYP/6-31G(d):AM1) method

of the receptor **2** complexes with inorganic oxygen-containing and halide anions are in orders: $HPO_4^{2-} > SO_4^{2-} \gg HCO_3^- > H_2PO_4^- \approx NO_3^-$ and $F^- \gg Cl^- > Br^-$, respectively. The binding energies of the receptor **2** with all anionic species obtained form the BSSE-corrected B3LYP/6-31G(d)//ONIOM(B3LYP/6-31G(d):AM1) calculation are more accurate than the energies computed at the ONIOM(B3LYP/6-31G(d):AM1) level by 15.7–33.1%.

Conclusions

The binding energies of the receptors **1** and **2** with carboxylate guests (acetate, oxalate, malonate, succinate, glutarate, adipate, pimelate, suberate, azelate), inorganic oxygen-containing anions (nitrate, sulfate, bicarbonate, hydrogen phosphate, dihydrogen phosphate), and halide ions (fluoride, chloride and bromide), preorganization and

Table 5 Binding energies of complexation of the receptor **1** with various anionic species and their BSSE corrected values

Host:guest	$\Delta E_{binding}$ [a]	$\Delta E_{complex}$ [a]	BSSE[b]	$\Delta E^{BSSE}_{binding}$ [c]	$\Delta E^{BSSE}_{complex}$ [c]	$\Delta E^{BSSE}_{preorg.}$ [c]
1/acetate	−67.14	−80.65	16.20	−50.94	−131.59	80.65
1/oxalate	−140.87	−156.05	30.61	−110.26	−266.31	156.05
1/malonate	−128.51	−144.93	25.20	−103.31	−248.24	144.93
1/succinate	−115.95	−132.95	24.75	−91.20	−224.15	132.95
1/glutarate	−111.32	−125.45	21.88	−89.44	−214.89	125.45
1/adipate	−100.52	−118.29	18.50	−82.02	−200.31	118.29
1/pimelate	−98.12	−114.62	17.78	−80.34	−194.96	114.62
1/suberate	−90.70	−111.12	17.06	−73.64	−184.76	111.12
1/azelate	−88.20	−109.13	16.87	−71.33	−180.46	109.13
$1/NO_3^-$	−55.25	−61.34	13.61	−41.64	−102.98	61.34
$1/SO_4^{2-}$	−128.80	−146.99	23.32	−105.48	−252.47	146.99
$1/HCO_3^-$	−61.54	−70.27	14.07	−47.47	−117.74	70.27
$1/HPO_4^{2-}$	−139.98	−162.34	26.15	−113.83	−276.17	162.34
$1/H_2PO_4^-$	−55.81	−65.68	14.12	−41.69	−107.37	65.68
$1/F^-$	−133.05	−147.01	50.63	−82.42	−229.43	147.01
$1/Cl^-$	−58.74	−66.82	7.83	−50.91	−117.73	66.82
$1/Br^-$	−60.94	−69.97	16.45	−44.49	−114.46	69.97

[a] The energies at the ONIOM(B3LYP/6-31G(d):AM1) level

[b] The BSSE energies at the B3LYP/6-31G(d)//ONIOM(B3LYP/6-31G(d):AM1) level

[c] The BSSE corrected energies at the B3LYP/6-31G(d)//ONIOM(B3LYP/6-31G(d):AM1) level

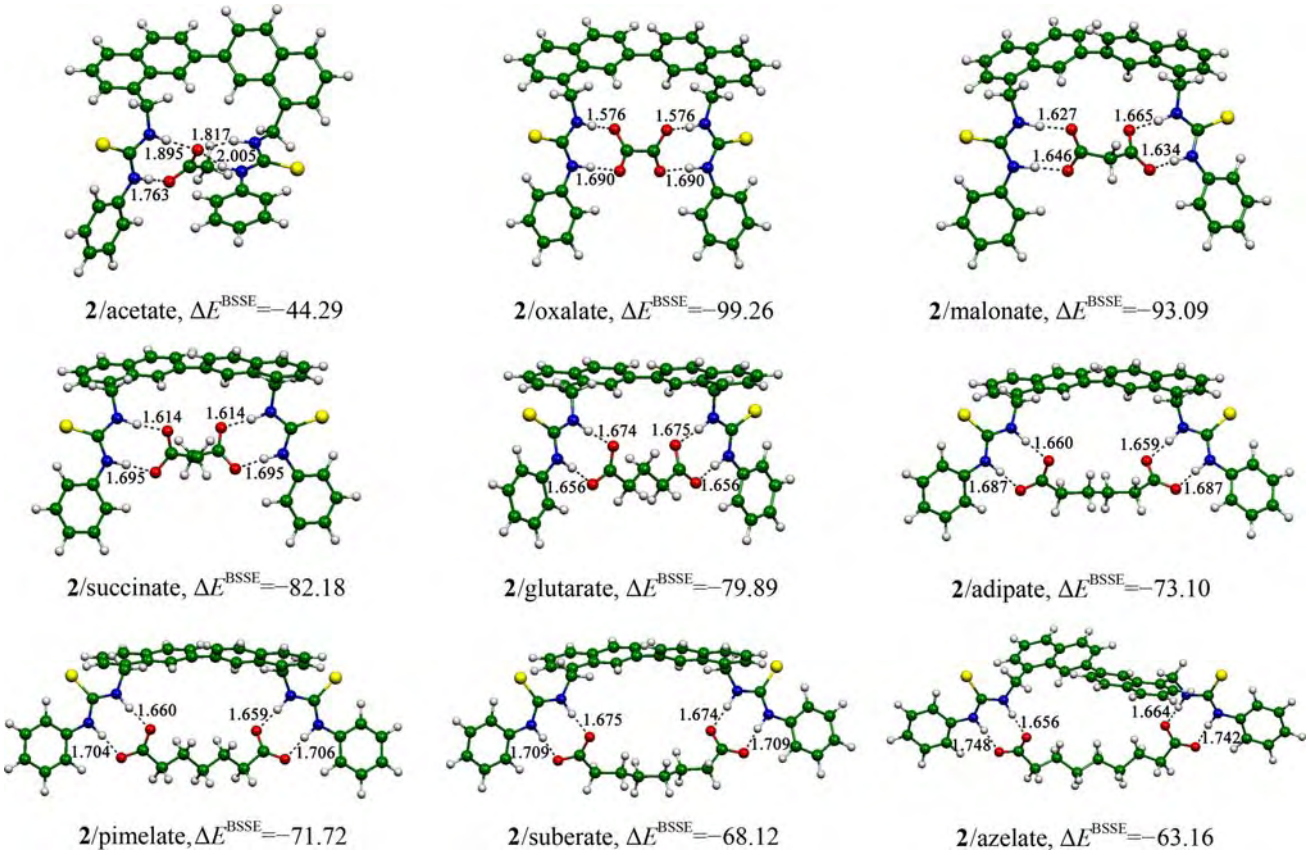

Fig. 7 The ONIOM(B3LYP/6-31G(d):AM1)-optimized structures of receptor **2** complexes with carboxylate and dicarboxylate guests. Binding energies, ΔE^{BSSE} computed at the B3LYP/6-31G(d)//ONIOM(B3LYP/6-31G(d):AM1 with BSSE correction are in kcal/mol. The bond lengths are in Å

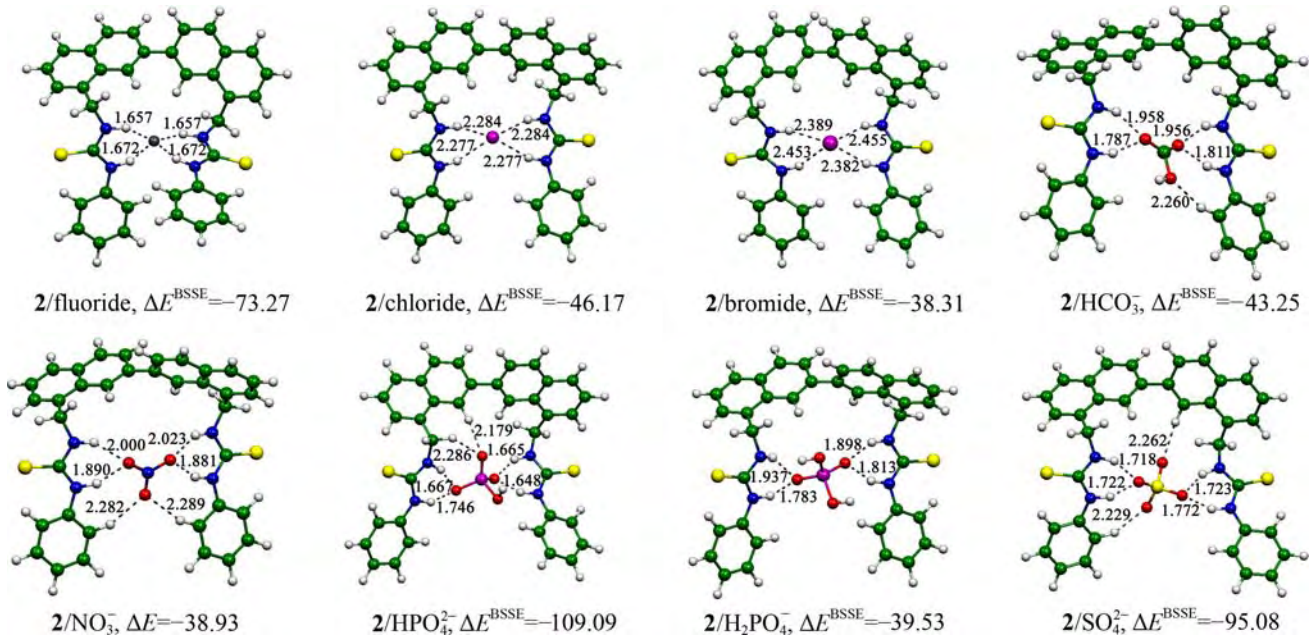

Fig. 8 The ONIOM(B3LYP/6-31G(d):AM1)-optimized structures of receptor **2** complexes with halide ions, carbonate, nitrate, phosphate, and sulfate ions. Binding energies, ΔE^{BSSE} computed at the B3LYP/6-31G(d)//ONIOM(B3LYP/6-31G(d):AM1 with BSSE correction are in kcal/mol. The bond lengths are in Å

Table 6 Binding energies, enthalpies, and free energies of complexation of the receptor **2** with various anionic species

Guest	$\Delta E_{binding}$ [a]	ΔH^{298} [a]	ΔG^{298} [a]	$K_B^{acetate}$ [b]	K_{298} [c]
Acetate	−61.14	−60.58	−48.95	2.62×10^4	1.21×10^5
Oxalate	−131.21	−130.83	−119.48	1.32×10^{56}	–
Malonate	−119.10	−118.83	−106.65	5.16×10^{46}	–
Succinate	−107.61	−107.41	−94.30	4.62×10^{37}	–
Glutarate	−102.60	−102.25	−90.20	4.52×10^{34}	–
Adipate	−92.17	−90.86	−80.69	4.86×10^{27}	–
Pimelate	−90.07	−89.29	−77.20	1.34×10^{25}	–
Suberate	–86.50	–85.07	–75.49	7.45×10^{23}	–
Azelate	–80.52	–79.65	−68.29	3.89×10^{18}	–
NO_3^-	−53.31	−52.41	−45.35	5.99×10^1	–
SO_4^{2-}	−120.47	−119.98	−109.37	5.15×10^{48}	–
HCO_3^-	−58.00	−57.24	−48.16	6.92×10^3	–
HPO_4^{2-}	−134.96	−134.44	−122.90	4.24×10^{58}	–
$H_2PO_4^-$	−52.78	−51.89	−42.93	1.00×10^0	–
F^-	−126.32	−126.35	−120.80	1.23×10^{57}	3.81×10^5
Cl^-	−54.75	−54.27	−50.05	1.67×10^5	3.60×10^3
Br^-	−57.26	−56.67	−52.80	1.72×10^7	–

[a] In kcal/mol, derived from the ONIOM(B3LYP/6-31G(d):AM1) energies with ZPVE corrections

[b] Selectivity coefficient of guests with respect to dihydrogen phosphate

[c] In MeCN determined by UV–vis spectroscopy, taken from Ref. [20]

complexation energies of their complexes were obtained using the ONIOM(B3LYP/6-31G(d):AM1) and BSSE-corrected B3LYP/6-31G(d)//ONIOM calculations. The ONIOM(B3LYP/6-31G(d):AM1) thermodynamic quantities, preorganization energies, complexation energies of these complexes, and anion binding abilities of their receptors in terms of selectivity coefficient were obtained. The relative stabilities of the complexes of either receptor **1** or **2** with carboxylate guests are in the same order: oxalate > malonate > succinate > glutarate > adipate > pimelate > suberate > azelate > acetate. The relative stabilities of complexes of the receptor **1** with inorganic oxygen-containing anions and halide ions are, respectively, in orders: $HPO_4^{2-} > SO_4^{2-} > HCO_3^- > NO_3^- \approx H_2PO_4^-$ and $F^- \gg Br^- \approx Cl^-$ at the ONIOM(B3LYP/6-31G(d):AM1) level and in orders: $HPO_4^{2-} > SO_4^{2-} > HCO_3^- > H_2PO_4^- \approx NO_3^-$ and $F^- \gg Cl^- \approx Br^-$ at the BSSE-corrected B3LYP/6-31G(d)//ONIOM (B3LYP/6-31G(d):AM1) level. For the relative stabilities of complexes of the receptor **2** with inorganic oxygen-containing anions and halide ions are, respectively, in orders: $HPO_4^{2-} > SO_4^{2-} > HCO_3^- > NO_3^- \approx H_2PO_4^-$ and $F^- \gg Br^- \approx Cl^-$ at the ONIOM(B3LYP/6-31G(d):AM1) level and in orders: $HPO_4^{2-} > SO_4^{2-} \gg HCO_3^- > H_2PO_4^- \approx NO_3^-$ and $F^- \gg Cl^- > Br^-$ at the BSSE-corrected B3LYP/6-31G(d)//ONIOM(B3LYP/6-31G(d):

Table 7 Preorganization energies of the receptor **2** (host), carboxylates (guest) and their complexes, complexation energies and their corresponding thermodynamics derived from the ONIOM (B3LYP/6-31G(d):AM1) calculations

Host:guest	Host			Guest			$\Delta E_{\text{preorg.}}^{\text{total}}$ [a]	$\Delta E_{\text{complex}}$ [a]
	$\Delta E_{\text{preorg.}}^{\text{host}}$ [a]	ΔH^{298} [a]	ΔG^{298} [a]	$\Delta E_{\text{preorg.}}^{\text{guest}}$ [b]	ΔH^{298} [b]	ΔG^{298} [b]		
2/acetate	10.44	10.13	11.80	1.52	0.97	2.56	11.96	−73.10
2/oxalate	13.39	12.34	14.05	1.09	1.08	0.71	14.48	−145.69
2/malonate	13.07	11.95	14.05	1.57	1.04	2.17	14.64	−133.75
2/succinate	11.21	10.01	13.03	2.62	1.57	4.38	13.83	−121.44
2/glutarate	2.57	3.75	−2.78	0.00	0.00	0.00	2.57	−105.17
2/adipate	11.92	11.35	11.52	4.30	4.80	2.48	16.22	−108.38
2/pimelate	12.34	11.77	12.31	2.70	2.10	3.95	15.04	−105.11
2/suberate	3.23	4.31	−2.07	2.48	3.50	0.09	5.71	−92.20
2/azelate	12.57	12.09	12.20	6.85	6.21	8.04	19.42	−99.94
$2/NO_3^-$	7.54	7.44	5.18	0.31	0.30	−0.34	7.85	−61.15
$2/SO_4^{2-}$	16.02	14.93	17.55	2.22	2.21	0.75	18.24	−138.70
$2/HCO_3^-$	0.00	0.58	−2.17	0.00	0.00	0.00	0.00	−57.97
$2/HPO_4^{2-}$	17.29	16.13	18.80	3.07	3.16	2.91	20.36	−155.32
$2/H_2PO_4^-$	2.57	3.75	−2.77	0.00	0.00	0.00	2.57	−55.35
$2/F^-$	13.15	11.85	14.76	0.00	0.00	0.00	13.15	−139.46
$2/Cl^-$	7.79	7.08	8.36	0.00	0.00	0.00	7.79	−62.54
$2/Br^-$	7.09	6.39	7.68	0.00	0.00	0.00	7.09	−64.35

[a] In kcal/mol, derived at the ONIOM (B3LYP/6-31G(d):AM1) level with ZPVE correction

[b] In kcal/mol, derived at the B3LYP/6-31G(d) level with ZPVE correction

Table 8 Binding energies of complexation of the receptor **2** with various anionic guests and their BSSE corrected values

Host:guest	$\Delta E_{\text{binding}}$ [a]	$\Delta E_{\text{complex}}$ [a]	BSSE [b]	$\Delta E_{\text{binding}}^{\text{BSSE}}$ [c]	$\Delta E_{\text{complex}}^{\text{BSSE}}$ [c]	$\Delta E_{\text{preorg.}}^{\text{BSSE}}$ [c]
2/acetate	−61.14	−73.10	16.85	−44.29	−117.39	73.10
2/oxalate	−131.21	−145.69	31.95	−99.26	−244.95	145.69
2/malonate	−119.10	−133.75	26.01	−93.09	−226.84	133.75
2/succinate	−107.61	−121.44	25.43	−82.18	−203.62	121.44
2/glutarate	−102.60	−105.17	22.71	−79.89	−185.06	105.17
2/adipate	−92.17	−108.38	19.07	−73.10	−181.48	108.38
2/pimelate	−90.07	−105.11	18.35	−71.72	−176.83	105.11
2/suberate	−86.50	−92.20	18.38	−68.12	−160.32	92.20
2/azelate	−80.52	−99.94	17.36	−63.16	−163.10	99.94
$2/NO_3^-$	−53.31	−61.15	14.38	−38.93	−100.08	61.15
$2/SO_4^{2-}$	−120.47	−138.70	25.39	−95.08	−233.78	138.70
$2/HCO_3^-$	−58.00	−57.97	14.75	−43.25	−101.22	57.97
$2/HPO_4^{2-}$	−134.96	−155.32	25.87	−109.09	−264.41	155.32
$2/H_2PO_4^-$	−52.78	−55.35	13.25	−39.53	−94.88	55.35
$2/F^-$	−126.32	−139.46	53.05	−73.27	−212.73	139.46
$2/Cl^-$	−54.75	−62.54	8.58	−46.17	−108.71	62.54
$2/Br^-$	−57.26	−64.35	18.95	−38.31	−102.66	64.35

[a] The energies at the ONIOM(B3LYP/6-31G(d):AM1) level

[b] The BSSE energies at the B3LYP/6-31G(d)//ONIOM(B3LYP/6-31G(d):AM1) level

[c] The BSSE corrected energies at the B3LYP/6-31G(d)//ONIOM(B3LYP/6-31G(d):AM1) level

AM1) level. The multipoint hydrogen bonding between receptors (either the receptor **1** or **2**) and anionic guests were found.

Acknowledgment The authors gratefully acknowledge the Thailand Research Fund for financial support (Grant no. BRG5180016).

References

1. Kato R, Nishizawa S, Hayashita T, Teramae N (2001) Tetrahedron Lett 42:5053–5056. doi:10.1016/S0040-4039(01)00916-9
2. Lee DH, Lee KH, Hong J-I (2001) Org Lett 3:5–8. doi:10.1021/ol006690t
3. Lee DH, Lee HY, Lee KH, Hong J-I (2001) Chem Commun (Camb) 1188–1189. doi:10.1039/b102187g
4. Lee DH, Lee HY, Hong J-I (2002) Tetrahedron Lett 43:7273–7276. doi:10.1016/S0040-4039(02)01455-7
5. Jiménez D, Martínez-Máñez R, Sancenón F, Soto J (2002) Tetrahedron Lett 43:2823–2825. doi:10.1016/S0040-4039(02)00363-5
6. Piatek P, Jurczak J (2002) Chem Commun (Camb) 20:2450–2451. doi:10.1039/b207335h
7. Gunnlaugsson T, Davis AP, O'Brien JE, Glynn M (2002) Org Lett 4:2449–2452. doi:10.1021/ol026004l
8. Fan A, Hong HK, Valiyaveettil S, Vittal JJ (2002) J Supramol Chem 2:247–254. doi:10.1016/S1472-7862(03)00079-0
9. Baerrigter H, Grave L, Nissink WM, Chrisstoffels LAJ, Vander Maas JH, Verboom W, de Jong F, Reindoudt DN (1998) Org Chem 63:4174–4180. doi:10.1021/jo972127l
10. Fan E, Van Arman SA, Kincaid D, Hamilton AD (1993) J Am Chem Soc 115:369–370. doi:10.1021/ja00054a066
11. Lee KH, Hong J-I (2000) Tetrahedron Lett 41:6083–6087. doi:10.1016/S0040-4039(00)00966-7
12. Wanno B, Rakrai W, Keawwangchai S, Morakot N, Morakot N, Nunthaboot N, Ruangpornvisuti V (2009) J Mol Struct THEOCHEM 902:33–40. doi:10.1016/j.theochem.2009.02.010
13. Ruangpornvisuti V (2004) J Mol Struct THEOCHEM 686:47–55. doi:10.1016/j.theochem.2004.08.007
14. Wanno B, Sang-aroon W, Tuntulani T, Pulpoka B, Ruangpornvisuti V (2003) J Mol Struct THEOCHEM 629:137–150. doi:10.1016/S0166-1280(03)00135-0
15. Ruangpornvisuti V (2004) J Mol Struct THEOCHEM 683:103–113. doi:10.1016/j.theochem.2004.06.022
16. Wanno B, Ruangpornvisuti V (2004) J Mol Struct THEOCHEM 685:57–71. doi:10.1016/j.theochem.2004.06.016
17. Wanno B, Ruangpornvisuti V (2006) J Mol Struct 787:76–89. doi:10.1016/j.molstruc.2005.11.006
18. Wanno B, Ruangpornvisuti V (2007) J Mol Model 13:65–77
19. Kondo S, Nagamine M, Yano Y (2003) Tetrahedron Lett 44:8801–8804. doi:10.1016/j.tetlet.2003.09.207
20. Kondo S, Sato M (2006) Tetrahedron 62:4844–4850. doi:10.1016/j.tet.2006.03.002
21. Becke AD (1988) Phys Rev A 38:3098–3100. doi:10.1103/PhysRevA.38.3098
22. Lee C, Yang W, Parr RG (1988) Phys Rev B 37:385–789
23. Maseras F, Morokuma K (1995) J Comput Chem 16:1170–1179. doi:10.1002/jcc.540160911
24. Humbel S, Sieber S, Morokuma K (1996) J Chem Phys 105:1959–1967. doi:10.1063/1.472065
25. Dewar MJS, Reynolds CH (1986) J Comput Chem 2:140–143. doi:10.1002/jcc.540070206
26. Stewart JJP (1989) Comput Chem 10:209–220. doi:10.1002/jcc.540100208
27. Dapprich S, Komaromi I, Byun KS, Morokuma K, Frisch MJ (1999) J Mol Struct THEOCHEM 461:1–21. doi:10.1016/S0166-1280(98)00475-8
28. Remko M, Walsh OA, Richards WG (2001) J Phys Chem A 105:6926–6931. doi:10.1021/jp010637k
29. Remko M (2002) J Phys Chem A 106:5005–5010. doi:10.1021/jp020300y
30. Frisch MJ, Trucks GW, Schlegel HB, Scuseria GE, Robb MA, Cheeseman JR Montgomery JA Jr, Vreven T, Kudin KN, Burant JC, Millam JM, Iyengar SS, Tomasi J, Barone V, Mennucci B, Cossi M, Scalmani G, Rega N, Petersson GA, Nakatsuji H, Hada M, Ehara M, Toyota K, Fukuda R, Hasegawa J, Ishida M, Nakajima T, Honda Y, Kitao O, Nakai H, Klene M, Li X, Knox JE, Hratchian HP, Cross JB, Adamo C, Jaramillo J, Gomperts R, Stratmann RE, Yazyev O, Austin AJ, Cammi R, Pomelli C, Ochterski JW, Ayala PY, Morokuma K, Voth GA, Salvador P, Dannenberg JJ, Zakrzewski VG, Dapprich S, Daniels AD, Strain MC, Farkas O, Malick DK, Rabuck AD, Raghavachari K, Foresman JB, Ortiz JV, Cui Q, Baboul AG, Clifford S, Cioslowski J, Stefanov BB, Liu G, Liashenko A, Piskorz P, Komaromi I, Martin RL, Fox DJ, Keith T, Al-Laham MA, Peng CY, Nanayakkara A, Challacombe M, Gill PMW, Johnson B, Chen W, Wong MW, Gonzalez C, Pople JA (2003) Gaussian 03, Revision B.03, Gaussian, Inc., Pittsburgh, PA
31. Flükiger P, Lüthi HP, Portmann S, Weber J (2000) MOLEKEL 4.3: Swiss Center for Scientific Computing, Manno (Switzerland)
32. Boys SF, Bernadi F (1970) Mol Phys 19:553–566. doi:10.1080/00268977000101561
33. Mayer I, Surjan PR (1992) Chem Phys Lett 191:497–499. doi:10.1016/0009-2614(92)85415-7
34. Turi L, Dannenberg JJ (1993) J Phys Chem 97:2488–2490. doi:10.1021/j100113a002
35. Simon S, Duran M, Dannenberg JJ (1999) J Phys Chem A 103:1640–1643. doi:10.1021/jp9842188
36. Hamza A, Vibok A, Halasz GJ, Mayer I (2000) J Mol Struct THEOCHEM 427:501–502
37. Makowski M, Raczyska ED, Chmurzyski L (2001) J Phys Chem A 105:869–874. doi:10.1021/jp002458t
38. Long Y, Liu Y, Lei L, Nie L, Yao S (2001) Analyst (Lond) 126:1090–1094. doi:10.1039/b101478l

ภาคผนวก C

Reprint บทความเรื่อง “A DFT study of structures of dipicolyl urea isomers and their recognition with carboxylic acids and their carboxylate anions”

Research Article

Journal of Physical Organic Chemistry

Received: 8 August 2009, Revised: 30 January 2010, Accepted: 3 March 2010, Published online in Wiley InterScience: 2010

(www.interscience.wiley.com) DOI 10.1002/poc.1711

A DFT study of structures of dipicolyl urea isomers and their recognition with carboxylic acids and their carboxylate anions

Boosayarat Tomapatanaget[a] and Vithaya Ruangpornvisuti[a]*

Four isomers of dipicolyl urea were obtained and the intramolecular hydrogen-bonded structure was found to be the most stable isomer. Energetics, thermodynamic properties, rate constants, and association constants of their isomerizations computed using the B3LYP/6-31+G(p,d) method were obtained. Complexes of all isomers of dipicolyl urea with formic acid, acetic acid, benzoic acid, oxalic acid, and their deprotonated species were investigated. Energetics, thermodynamic properties, and rate constants of their associations were obtained. Stabilities of all complexes in terms of association constants of the most stable species were determined. Copyright © 2010 John Wiley & Sons, Ltd.

Supporting information may be found in the online version of this paper.

Keywords: DFT; dipicolyl urea compound; molecular structure; recognition; selectivity

INTRODUCTION

Review articles for the supramolecular compounds containing amide functional groups as anion receptors[1] and amide-based ligands for anion coordination[2] were summarized. Fluorescence switch-on sensor for copper (II) by an amide linked lower rim 1,3-bis(2-picolyl)amine derivative of calix[4]arene in aqueous methanol[3] and phenanthroline complexes bearing diamide–anion[4] were studied. Many theoretical studies of anion receptors namely 1,3-bis(4-nitrophenyl)urea derivative,[5] 3,4-dichloro-2,5-diamido-substituted pyrrole,[6] 3,4-dichloro-2,5-diamido-substituted pyrrole derivatives,[7] 3,4-dichloro-2,5-diamidopyrrole,[8] non-rigid bis-(2,5-diamidopyrrole),[9] azophenol–thiourea derivatives,[10] 8,8′-dithioureido-2,2′-binaphthalene derivatives,[11] tetraamino-*tert*-butylthiacalix[4]arene, and tetraamino-*tert*-butylcalix[4]arene[12] were done. *N*-nitrophenyl benzamide derivatives for cyanide colorimetric detection[13] and synthesis and anion-binding properties of new disulfonamide-based receptors[14] were studied.

In this work, the dipicolyl urea isomers, their energetics, thermodynamic properties, rate constants, and association constants of their isomerization have been determined using the B3LYP/6-31+G(p,d) level. Association energies, thermodynamic properties, rate and association constants of their complexes with formic acid, acetic acid, benzoic acid, oxalic acid, and their deprotonated ions have been obtained.

COMPUTATIONAL DETAILS

Structures of dipicolyl urea isomers, formic acid, formate ion, acetic acid, acetate ion, benzoic acid, benzoate ion, oxalic acid, oxalate ions, and related species were optimized using density functional theory (DFT) method. DFT calculations have been performed with the Becke's three parameter hybrid functional[15] with the Lee–Yang–Parr correlation functional,[16] B3LYP method[17] with 6-31+G(d,p) basis set.[18,19] All structures and their reactions were studied in gas phase unless otherwise specified. The optimization of structures of dipicolyl urea isomers in aqueous solution, the solvent effect using the conductor-like polarizable continuum model (CPCM)[20,21] with UAKS cavity model[22] as employed in the previous work,[23,24] was carried out. All calculations were performed with the Gaussian 03 program.[22] The molecular graphics for all species were generated with the MOLEKEL 4.3 program.[25]

The standard enthalpy ΔH^o_{298} and Gibbs free energy changes ΔG^o_{298} of isomerization of dipicolyl urea isomers, association of their complexes, and their conversion reactions have been derived from the frequency calculations at the B3LYP/6-31+G(d,p) level of theory. The vibrational frequency scale factor and zero-point vibrational energies (ZPVE) were scaled by the empirical factors 0.9627 and 0.9857,[26] respectively. The rate constant k(T), based on transition state theory, was computed from the activation energy, $\Delta^{\ddagger}E$ using Eqn (1).[27]

$$k(T) = \kappa \frac{k_B T}{h} \frac{Q_{TS}}{Q_{REA}} \exp\left(\frac{-\Delta^{\ddagger}E}{RT}\right) = \kappa A \exp\left(\frac{-\Delta^{\ddagger}E}{RT}\right) \quad (1)$$

where k_B is the Boltzmann's constant, h is Plank's constant, T is the absolute temperature, and R is the gas constant. Q_{TS} and Q_{REA}

* *Correspondence to: V. Ruangpornvisuti, Department of Chemistry, Faculty of Science and Center for Petroleum, Petrochemicals and Advanced Materials, Chulalongkorn University, Bangkok 10330, Thailand*
E-mail: vithaya.r@chula.ac.th

a *B. Tomapatanaget, V. Ruangpornvisuti*
Department of Chemistry, Faculty of Science and Center for Petroleum, Petrochemicals and Advanced Materials, Chulalongkorn University, Bangkok 10330, Thailand

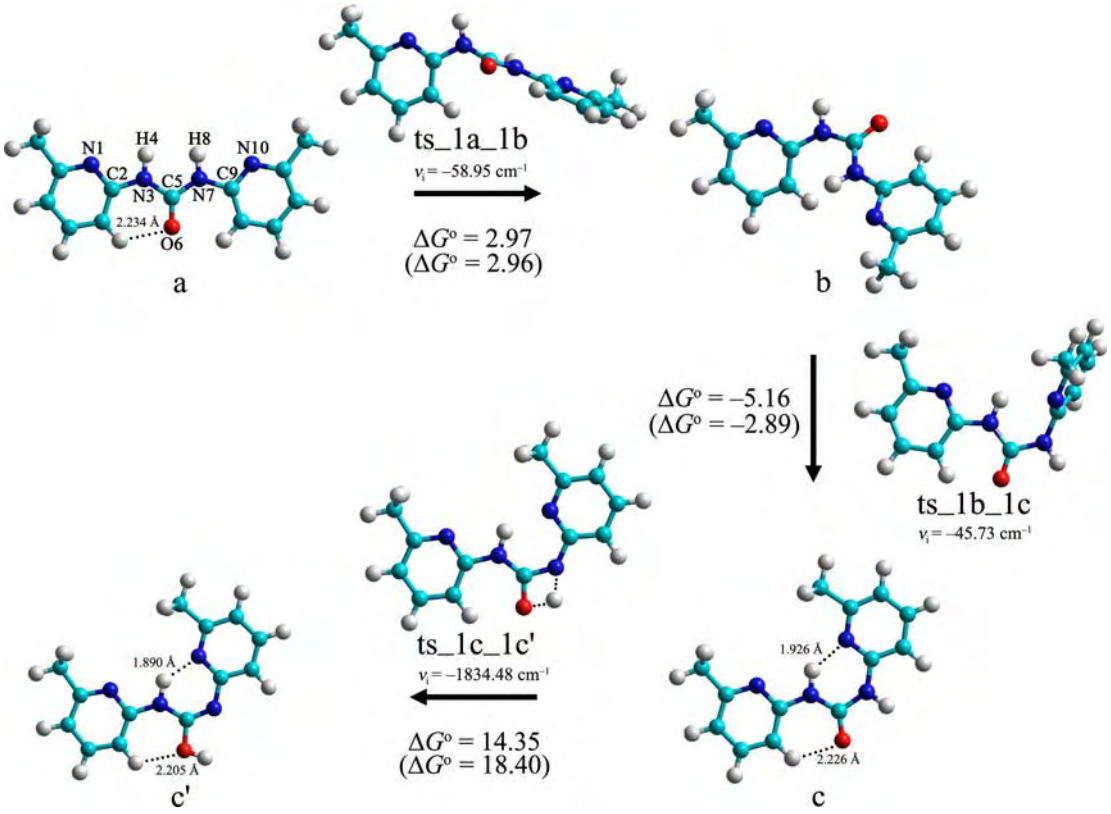

Figure 1. Isomerization of the receptor **1** via three transition states. Reaction free energies are in kcal/mol

are the partition functions of the transition state and the reactant of dipicolyl urea isomer, respectively. These partition functions are defined as the product of the translational, rotational, vibrational, and electronic partition functions. These partition functions were obtained from their frequency calculations using the GAUSSIAN 03 program.[22] The tunneling coefficient (κ) can be computed with the Wigner method[28–30] as $\kappa = 1 + 1/24(h\nu_i/k_BT)^2$ where ν_i is the imaginary frequency

Table 1. Selected vibration frequencies of isomers of receptor **1** involved with their binding atoms of the B3LYP/6-31+G(d,p) computed vibration modes and their energy gaps

Species	IR frequency[a]	IR Intensity[b]	Energy gap[c]
1a	$\delta_{C-N-H} = 1504.40$, in plane	1147.98	0.27
	$\nu_{C=O} + \delta_{C-N-H} + \delta_{C-N-H}' = 1696.58$	205.86	
	ν_{N-H}(asym) = 3461.37	11.18	
	ν_{N-H}(sym) = 3475.34	62.36	
1b	$\nu_{C=O} + \delta_{C-N-H} + \delta_{C-N-H}' = 1692.92$	531.50	0.22
	$\nu_{N-H}' = 3463.91$[d]	53.76	
	$\nu_{N-H} = 3479.11$[d]	72.64	
1c	$\nu_{C=O} + \delta_{C-N-H} + \delta_{C-N-H}' = 1695.18$	529.35	0.33
	$\nu_{N-H}' = 3254.81$[e]	473.82	
	$\nu_{N-H} = 3499.46$[d]	55.11	
1c′	$\delta_{C-O-H} = 1169.51$	197.53	0.14
	$\nu_{N-H} = 3178.69$[e]	398.39	
	$\nu_{O-H} = 3624.84$	96.40	

[a] In cm^{-1}, the computed *IR* vibration frequencies were scaled by 0.9627.[26]
[b] In kg/mol.
[c] In eV.
[d] NH bond does not form intramolecular hydrogen bond.
[e] NH bond forms intramolecular hydrogen bond.

Table 2. Reaction energies, thermodynamic properties, rate constants and association constants of isomerizations of receptor 1, computed at the B3LYP/6-31+G(d,p) level of theory

Reaction	$\Delta^{\ddagger}E^{a,b}$	$k_{298}{}^{c}$	ΔE^{a}	$\Delta H_{298}{}^{d}$	$\Delta G_{298}{}^{d}$	K_{298}
In gas phase						
1a → **ts_1a_1b** → **1b**	9.16 (6.07)	2.30×10^{5} (3.47×10^{7})	3.09	3.05	2.97	6.65×10^{-3}
1b → **ts_1b_1c** → **1c**	3.54 (9.12)	4.08×10^{9} (7.14×10^{5})	−5.58	−5.67	−5.16	6.04×10^{3}
1c → **ts_1c_1c′** → **1c′**	37.34 (22.96)	8.11×10^{-15} (2.74×10^{-4})	14.38	14.33	14.35	3.01×10^{-11}
In aqueous[e]						
1a → **1b**	—	—	4.62	5.15	2.96	6.78×10^{-3}
1b → **1c**	—	—	−3.27	−3.96	−2.89	1.31×10^{2}
1c → **1c′**	—	—	16.58	16.58	18.40	3.24×10^{-14}

[a] Energy with ZPVE corrections scaled by the empirical factor 0.9857, in kcal/mol.
[b] Activation energies for forward and backward (in parenthesis) reactions.
[c] Forward and backward (in parenthesis) rate constants, in s^{-1}.
[d] In kcal/mol.
[e] In aqueous solution, derived from the CPCM calculations ($\varepsilon = 78.37$) at the B3LYP/6-31+G(d,p) level.

that accounts for the vibration motion along the reaction path. The pre-exponential factor (A) is defined as $A = k_B T/h\ Q_{TS}/Q_{REA}$. The association constant K at 298.15 K (K_{298}) and 1 atm is computed using a thermodynamic equation $\Delta G^0 = -RT\ln K$.

The binding selectivity of receptor **1** to guest B with respect to guest A has been derived from the selectivity coefficient (K_B^A)[31] which is defined as an equilibrium constant of ion exchange between ions A and B. Since exchange is a chemical reaction as

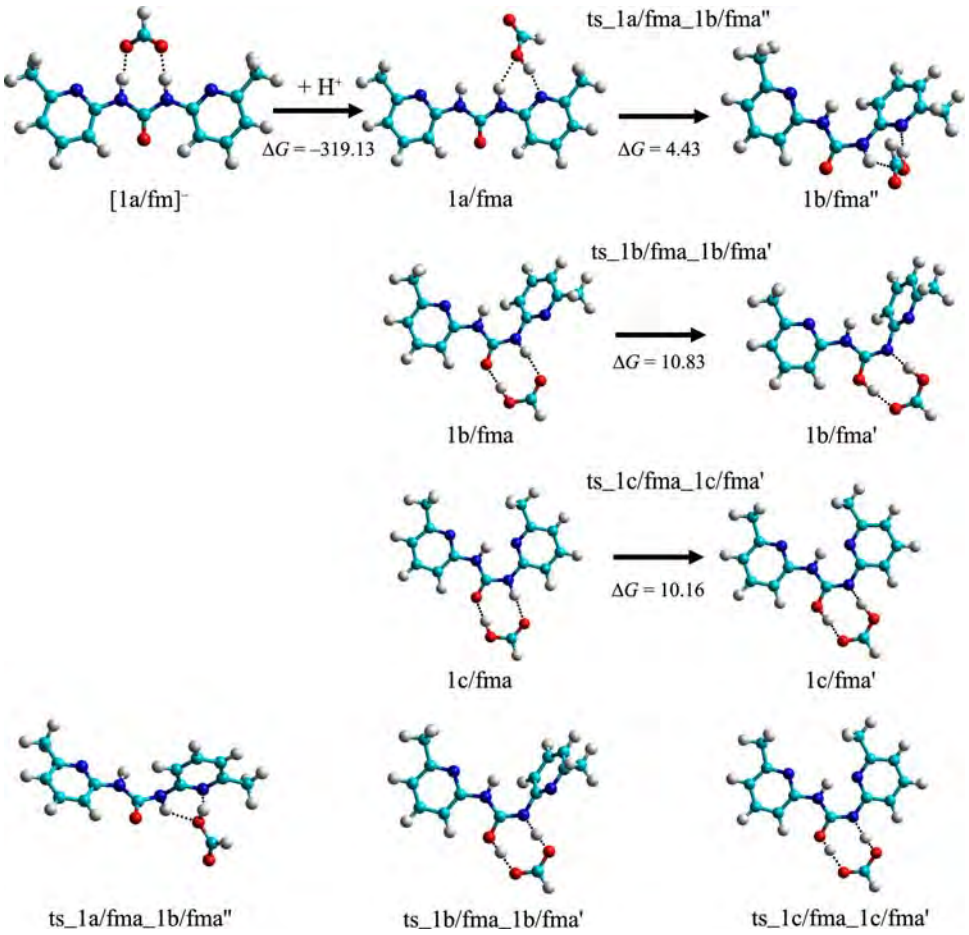

Figure 2. Association mechanism of complexes of **1** with formic acid, their transformations and protonation of formate ion. The free energy of reaction is in kcal/mol

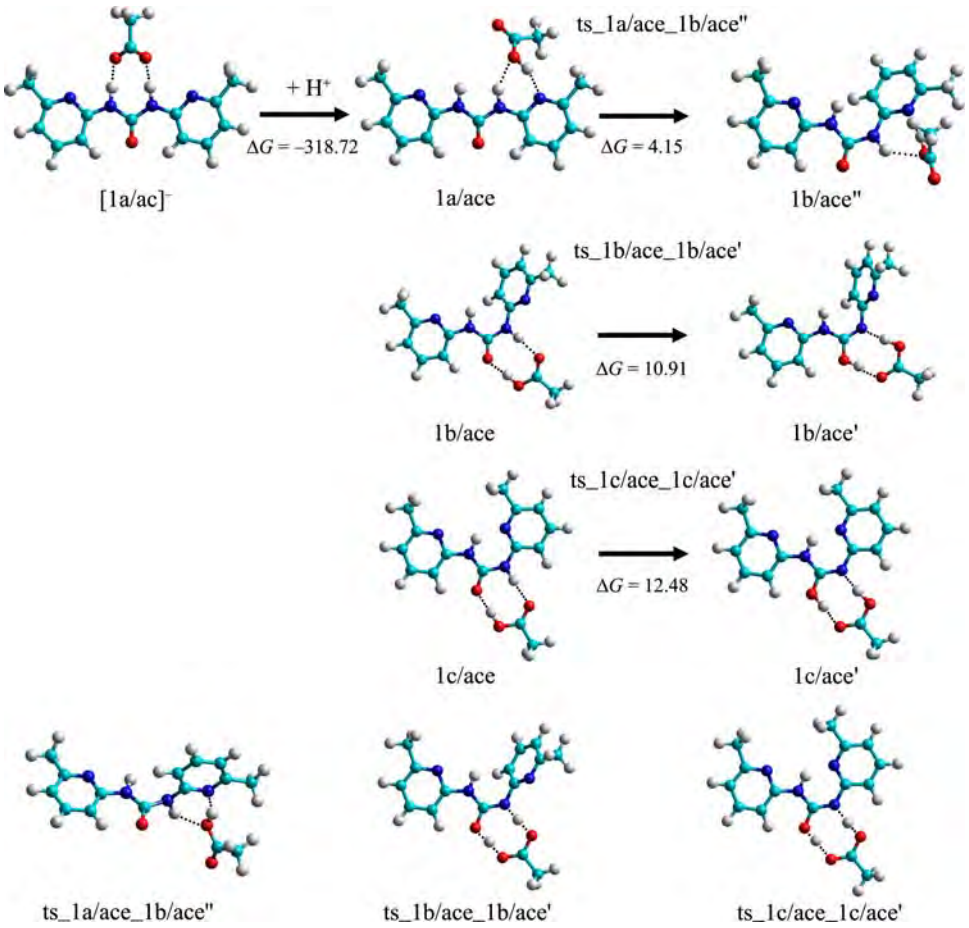

Figure 3. Association mechanism of complexes of **1** with acetic acid, their transformations and protonation of acetate ion. The free energy of reaction is in kcal/mol

Eqn (1), it can be treated like any other mass action expression.

$$AX + B \leftrightarrow BX + A \quad (1)$$

Therefore, the selectivity coefficient can be defined as $K_B^A = [BX][A]/[AX][B]$. If the complexations of BX and AX are observed, their stability constants based on Eqns (2) and (3) can be expressed as $K_A = [AX]/[X][A]$ and $K_B = [BX]/[X][B]$.

$$X + B \leftrightarrow BX \quad (2)$$

$$X + A \leftrightarrow AX \quad (3)$$

The selectivity coefficient can be therefore written as $K_B^A = K_B/K_A$. If the value of the selectivity coefficient K_B^A is larger than 1, this implies that B is preferred over A and if K_B^A is smaller than 1 then A is preferred over B.

RESULTS AND DISCUSSION

Isomers of dipicolyl urea

The B3LYP/6-31+G(d,p) optimized structures of isomers of receptor **1** as **1a**, **1b**, **1c**, and **1c′** including atomic numbering scheme are shown in Fig. 1. It shows that the isomerization occurs via three transition states, **ts_1a_1b**, **ts_1b_1c**, and **ts_1c_1c′**, sequentially. The rotational transition states, **ts_1a_1b** and **ts_1b_1c** describe the interconversion of their corresponding reactant and product through rotation around the N3—C5 and C2—N3 bonds, respectively. The single imaginary frequencies for the transition states **ts_1a_1b** and **ts_1b_1c** are respectively −58.95 and −45.73 cm^{-1} which are low frequencies but **ts_1c_1c′** is the proton-transfer transition state of which imaginary frequency is high (−1834.48 cm^{-1}). All the isomers are planar structure except for the isomer **1b**. **1c** is the most stable isomer which is stabilized by its intermolecular hydrogen-bond, N1···H8 but the **1c′** is the least stable isomer because its N3 atom prefers to bond with H4 as amide nitrogen rather than imine form. The standard Gibbs free energy for the **1b** to **1c** transformation exhibits its spontaneous reaction.

The potential energy profile of the transformation of receptor **1**, in terms of relative energy, is shown in Fig. S1, Supporting Information. The relative stabilities of these isomers are in orders: **1c** > **1a** > **1b** > **1c′** in gas phase and **1a** > **1c** > **1b** > **1c′** in aqueous solution. Nevertheless, energy difference between **1a** and **1c** is small (2.49 kcal/mol in gas phase and 1.36 kcal/mol in aqueous solution). Selected B3LYP/6-31+G(d,p)-computed vibration modes of isomers of the receptor **1** namely their acceptor (H_{NH}) and donor (O_C) atoms are shown in Table 1. The C═O stretch vibrations for **1a**, **1b**, and **1c**, combined with C—H—N bending modes, are 1696.58, 1692.92, and 1695.18 cm^{-1}, respectively. Table 1 shows that frequencies of stretching vibration of N—H bond which does not form intramolecular hydrogen bond, such as $\nu_{N—H}$ (asym) =

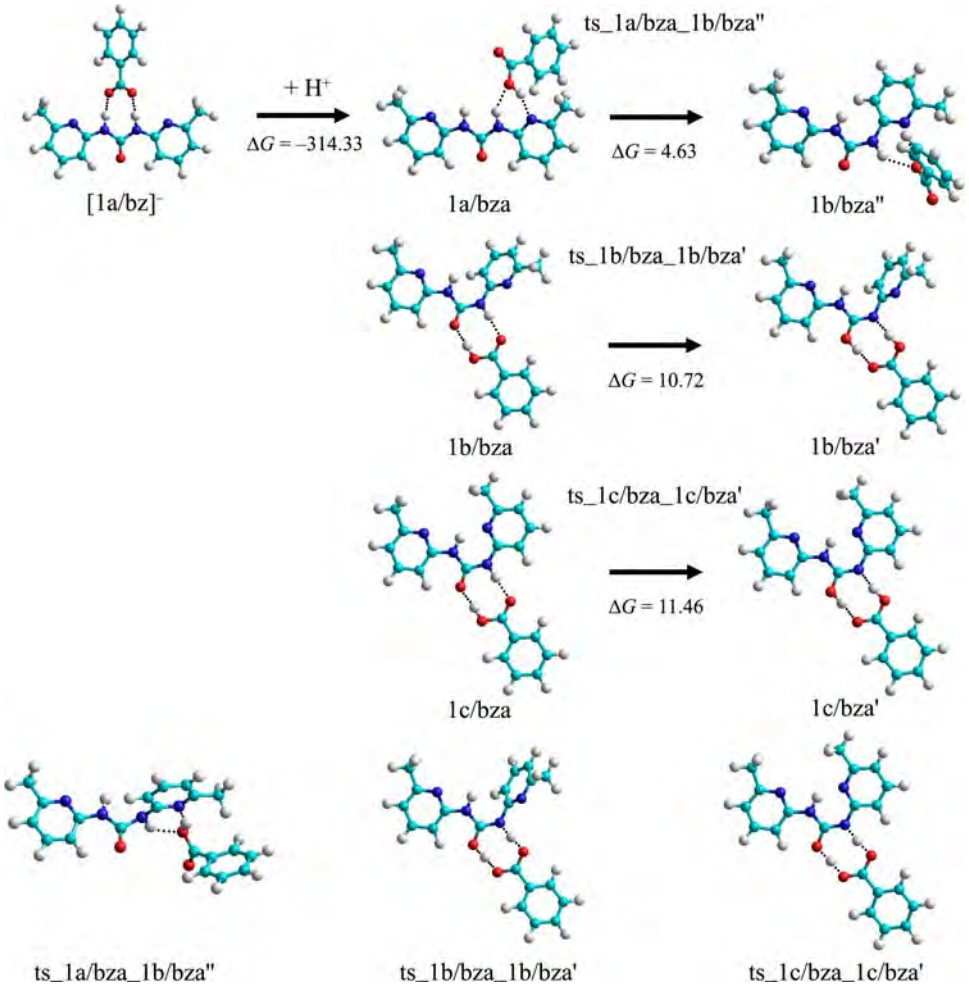

Figure 4. Association mechanism of complexes of **1** with benzoic acid, their transformations and protonation of benzoate ion. The free energy of reaction is in kcal/mol

3461.37 cm^{-1}, $\nu_{N—H}$ (sym) = 3475.34 cm^{-1} of **1a**, $\nu_{N—H}'$ = 3463.91 cm^{-1}, $\nu_{N—H}$ = 3479.11 cm^{-1} of **1b**, $\nu_{N—H}$ = 3499.46 cm^{-1} of **1c**, are higher than frequencies of stretching vibration of N—H bond which form intramolecular hydrogen bond such as $\nu_{N—H}'$ = 3254.81 cm^{-1} of **1c** and $\nu_{N—H}$ = 3178.69 cm^{-1} of **1c′**. As the chemical reactivity of compound is the inverse of its energy gap as given in Table 1, the reactivities of these isomers in gas phase are therefore in orders: **1c′** >> **1b** > **1a** >> **1c**. This means that trend for **1a** forming complex with some guest is more preferable than **1c** but is not much different.

Reaction energies, thermodynamic properties, rate constants, and association constants of isomerizations of the receptor 1, computed at the B3LYP/6-31+G(d,p) level of theory, are shown in Table 2. It shows that **1b** to **1c** transformation is the thermodynamically preferred reaction with $K_{298} = 6.04 \times 10^3$ which corresponds to its forward and backward rate constants of $k_{298}^{fw} = 4.08 \times 10^9$ and $k_{298}^{bw} = 7.14 \times 10^5\ s^{-1}$, respectively. Due to the **1c** → **1c′** reaction step, its forward and backward rate constants are very small and its reaction is non-spontaneous process.

The selected geometrical parameters and NBO charges for isomers of the receptor **1** are shown in Table S1, Supporting Information. It shows that the **1c** isomer corresponds to the X-ray structure[32] and its geometric parameters exhibit good agreement with the X-ray data. The NBO charges of nitrogen and oxygen atoms of these isomers are kept as high negative values.

Dipicolyl urea complexes with carboxylic acid/carboxylate anion

The B3LYP/6-31+G(d,p) optimized structures of isomers of **1** complexes with formic acid (fma), acetic acid (ace), benzoic acid (bza), and oxalic acid (oxa) are shown in Figs 2–5, respectively. The relative energies of complexes are shown in Table S2, Supporting Information. The relative stabilities for the complexes with formic, acetic, benzoic, and oxalic acids are in orders: **1c**/fma > **1b**/fma > **1c**/fma′ > **1a**/fma > **1b**/fma″ > **1b**/fma′, **1c**/aca > **1b**/aca > **1c**/aca′ > **1a**/aca > **1b**/aca″ > **1b**/aca′, **1c**/bza > **1b**/bza > **1c**/bza′ > **1a**/bza > **1b**/bza′ > **1b**/bza″, and **1c**/oxa > **1b**/oxa > **1a**/oxa > **1b**/oxa″ > **1b**/oxa′, respectively. The most stable complexes with fma, ace, bza, and oxa are the complexes of the isomer **1c**. The association energies, thermodynamic properties, rate constants, and equilibrium constants of **1** complexes with fma, ace, bza, oxa, and their anions, computed at the B3LYP/6-31 + G(d,p) level are shown in Table 3. Magnitudes of the equilibrium constant of complexations of isomers **1a**, **1b**, **1b′**, **1b″**, **1c**, and **1c′** with the carboxylic acids are in orders: **1a**/

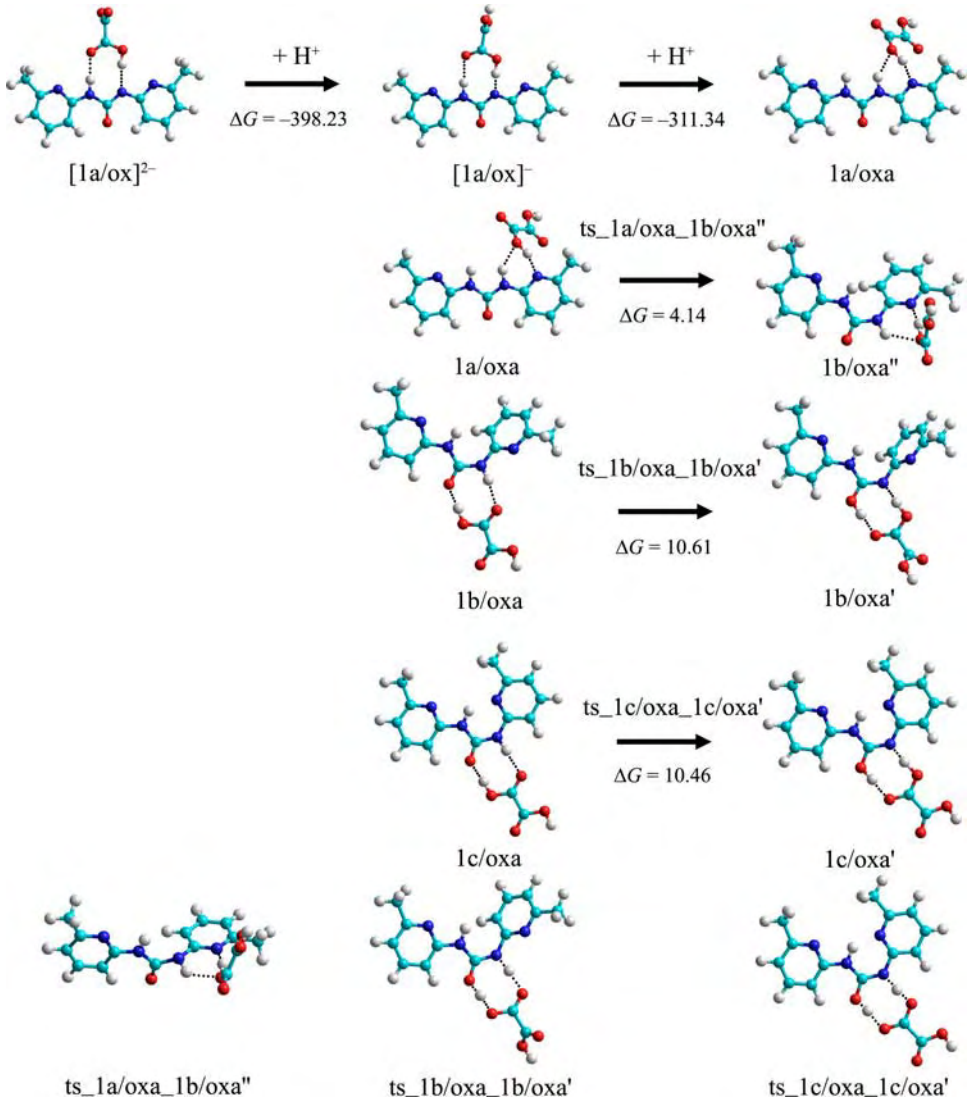

Figure 5. Association mechanism of complexes of **1** with oxalic acid, their transformations and protonation of oxalate ion. The free energy of reaction is in kcal/mol

Table 3. Reaction energies, thermodynamic properties and association constants of **1** complexes with carboxylic acids and carboxylate ions, computed at the B3LYP/6-31+G(d,p) level of theory

Reaction	$\Delta E^{a,b}$	$\Delta H_{298}{}^{b}$	$\Delta G_{298}{}^{b}$	K_{298}
Formic acid/Formate ion:				
1a + fma → **1a**/fma	−6.09	−5.81	4.11	9.68×10^{-4}
1b + fma → **1b**/fma	−12.24	−12.16	−1.37	1.01×10^{1}
1b′ + fma → **1b**/fma′	−1.40	−1.50	9.46	1.16×10^{-7}
1b″ + fma → **1b**/fma″	−4.13	−3.72	5.57	8.27×10^{-5}
1c + fma → **1c**/fma	−15.33	−15.36	−3.97	8.13×10^{2}
1c′ + fma → **1c**/fma′[c]	−19.97	−20.52	−8.17	9.70×10^{5}
1a + fm^- → [**1a**/fm]$^{-}$[d]	−26.68	−26.61	−16.40	1.05×10^{12}
[**1a**/fm]$^-$ + H^+ → **1a**/fma	−319.01	−318.55	−319.13	—[e]
Acetic acid/Acetate ion:				
1a + aca → **1a**/aca	−3.80	−3.50	7.21	5.15×10^{-6}
1b + aca → **1b**/aca	−11.90	−11.61	−1.08	6.15×10^{0}

(*Continues*)

Table 3. (Continued)

Reaction	$\Delta E^{a,b}$	$\Delta H_{298}{}^{b}$	$\Delta G_{298}{}^{b}$	K_{298}
1b′ + aca → **1b**/aca′	−1.30	−1.20	9.83	6.21×10^{-8}
1b″ + aca → **1b**/aca″	−1.57	−1.12	8.39	7.05×10^{-7}
1c + aca → **1c**/aca	−15.05	−14.88	−3.66	4.83×10^{2}
1c′ + aca → **1c**/aca′[c]	−17.97	−18.47	−5.54	1.15×10^{4}
1a + ac$^-$ → [**1a**/ac]$^-$[d]	−28.15	−27.93	−17.88	1.27×10^{13}
[**1a**/ac]$^-$ + H$^+$ → **1a**/aca	−320.04	−319.76	−318.72	—[e]
Benzoic acid/Benzoate ion:				
1a + bza → **1a**/bza	−2.23	−1.72	8.77	3.71×10^{-7}
1b + bza → **1b**/bza	−12.27	−11.88	−1.12	6.60×10^{0}
1b′ + bza → **1b**/bza′	−1.87	−1.65	9.60	9.12×10^{-8}
1b″ + bza → **1b**/bza″	−0.32	0.25	10.44	2.24×10^{-8}
1c + bza → **1c**/bza	−15.36	−15.06	−3.73	5.42×10^{2}
1c′ + bza → **1c**/bza′[c]	−18.59	−18.44	−6.63	7.20×10^{4}
1a + bz$^-$ → [**1a**/bz]$^-$[d]	−25.10	−24.76	−14.42	3.71×10^{10}
[**1a**/bz]$^-$ + H$^+$ → **1a**/bza	−314.74	−314.34	−314.33	—[e]
Oxalic acid/Oxalate ion:				
1a + oxa → **1a**/oxa	−9.62	−8.85	2.45	1.61×10^{-2}
1b + oxa → **1b**/oxa	−13.98	−13.17	−2.73	9.96×10^{1}
1b′ + oxa → **1b**/oxa′	−3.66	−2.96	7.88	1.67×10^{-6}
1b″ + oxa → **1b**/oxa″	−8.35	−7.53	3.62	2.22×10^{-3}
1c + oxa → **1c**/oxa[b]	−16.92	−16.24	−5.01	4.73×10^{3}
1c′ + oxa → **1c**/oxa′[f]	—	—	—	—
1a + ox^{2-} → [**1a**/ox]$^{2-}$[g]	−65.34	−64.21	−56.50	2.65×10^{41}
1a + ox$^-$ → [**1a**/ox]$^-$[g]	−24.34	−23.34	−14.93	8.86×10^{10}
[**1a**/ox]$^{2-}$ + H$^+$ → [**1a**/ox]$^-$	−398.30	−398.08	−398.23	—[e]
[**1a**/ox]$^-$ + H$^+$ → **1a**/ox	−312.11	−311.99	−311.34	—[e]

[a] Energy with ZPVE corrections scaled by the empirical factor 0.9857, in kcal/mol.
[b] In kcal/mol.
[c] The most stable species of complex with acidic form.
[d] The most stable species of complex with anionic form.
[e] Very large values.
[f] Unstable complex.
[g] The most stable species of complex with anionic form which is formed via proton transfer process.

oxa >> **1a**/fma >> **1a**/aca > **1a**/bza, **1b**/oxa > **1b**/fma > **1b**/bza > **1b**/aca, **1b**/oxa″ > **1b**/fma″ > **1b**/oxa′ > **1b**/aca″ > **1b**/fma′ > **1b**/bza′, **1b**/aca′ > **1b**/bza″, **1c**/fma′ > **1c**/bza′ > **1c**/aca > **1c**/oxa > **1c**/fma > **1c**/bza > **1c**/aca, respectively. It was found that the complex **1c**/oxa′ is not stable because the hydroxyl proton of **1c**′ is preferably transferred to carbonyl oxygen of the oxalic acid and its carboxylic proton is simultaneously transferred to amide nitrogen and stabilized as the **1c**/oxa complex. It was also found that complexations of **1a**, **1c**, and **1c**′ with four carboxylic acids are thermodynamically preferred reaction steps. The magnitudes of equilibrium constants of complexations between **1a** and monoanionic species of the carboxylic acids are very large and in order: [**1a**/ac]$^-$ > [**1a**/fm]$^-$ > [**1a**/ox]$^-$ > [**1a**/bz]$^-$.

Selectivity coefficients of **1** complexes with carboxylic acids based on their most stable species are listed in Table S3 which shows that the relative selectivities of the receptor **1c** are in order: oxa > fma > bza > aca. As the receptor **1c** mainly prefers to form complex with oxalic acid, this can be complied that receptor **1** selectively recognizes the oxalic acid (Fig. 6). Throughout the paper, anionic form of the formic acid (fma), acetic acid (ace),

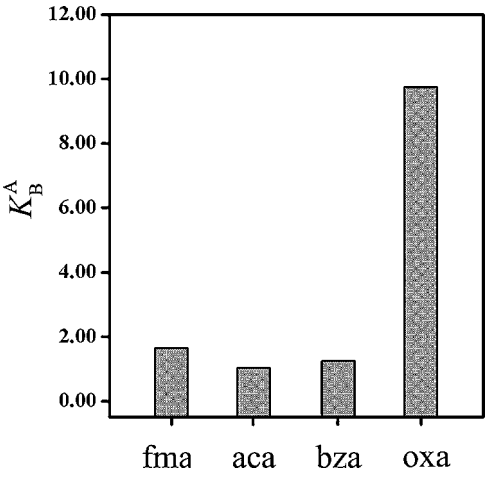

Figure 6. Relation of selectivity coefficient of complexes **1** and carboxylic acid guests

Table 4. Reaction energies, thermodynamic properties, rate constants and equilibrium constants of **1** complexes with carboxylic acids, computed at the B3LYP/6-31+G(d,p) level of theory.

Reaction	$\Delta^{\ddagger}E^{a,b}$	$k_{298}{}^{c}$	$\Delta E^{a,b}$	$\Delta H_{298}{}^{b}$	$\Delta G_{298}{}^{b}$	K_{298}
Complexes with formic acid:						
1a/fma → ts_**1a**/fma _**1b**/fma″ → **1b**/fma″	9.23	3.06×10^{5}	5.05	5.14	4.43	5.68×10^{-4}
1b/fma → ts_**1b**/fma_**1b**/fma′ → **1b**/fma′	8.95	1.14×10^{6}	10.85	10.65	10.83	1.15×10^{-8}
1c/fma → ts_**1c**/fma_**1c**/fma′ → **1c**/fma′	10.59	3.39×10^{4}	9.74	9.17	10.16	3.59×10^{-8}
Complexes with acetic acid:						
1a/aca → ts_**1a**/aca_**1b**/aca″ → **1b**/aca″	9.48	1.26×10^{6}	5.32	5.44	4.15	9.11×10^{-4}
1b/aca → ts_**1b**/aca_**1b**/aca′ → **1b**/aca′	8.80	3.48×10^{5}	10.61	10.41	10.91	1.01×10^{-8}
1c/aca → ts_**1c**/aca_**1c**/aca′ → **1c**/aca′	9.51	8.16×10^{13}	11.46	10.74	12.48	7.14×10^{-10}
Complexes with benzoic acid:						
1a/bza → ts_**1a**/bza_**1b**/bza″ → **1b**/bza″	9.40	1.27×10^{5}	5.00	5.02	4.63	4.01×10^{-4}
1b/bza → ts_**1b**/bza_**1b**/bza′ → **1b**/bza′	8.99	1.22×10^{6}	10.40	10.23	10.72	3.15×10^{-8}
1c/bza → ts_**1c**/bza_**1c**/bza′ → **1c**/bza′	9.46	1.74×10^{5}	11.15	10.95	11.46	4.00×10^{-9}
Complexes with oxalic acid:						
1a/oxa → ts_**1a**/oxa_**1b**/oxa″ → **1b**/oxa″	8.93	4.41×10^{5}	4.36	4.37	4.14	9.16×10^{-4}
1b/oxa → ts_**1b**/oxa_**1b**/oxa′ → **1b**/oxa′	12.03	1.80×10^{3}	10.32	10.21	10.61	1.68×10^{-8}
1c/oxa → ts_**1c**/oxa_**1c**/oxa′ → **1c**/oxa′[d]	8.18	3.01×10^{6}	12.87	9.66	10.46	2.15×10^{-8}
Complexes with oxalate ion:						
$[$**1a**/ox$]^{2-}$ → ts_$[$**1a**/ox$]^{2-}$_$[$**1a**/ox$]^{2-}$ → $[$**1a**/ox$]^{2-}$[e]	5.18	1.96×10^{7}	0.00	0.00	0.00	1.00×10^{0}
$[$**1a**/ox$]^{-}$ → ts_$[$**1a**/ox$]^{-}$_$[$**1a**/ox$]^{-}$ → $[$**1a**/ox$]^{-}$[e]	28.47	2.94×10^{-8}	0.00	0.00	0.00	1.00×10^{0}

[a] Energy with ZPVE corrections scaled by the empirical factor 0.9857, in kcal/mol.
[b] In kcal/mol.
[c] In s^{-1}.
[d] Unstable complex.
[e] Autoconversion reaction.

benzoic acid (bza), and oxalic acid (oxa), respectively, denoted as fm^{-}, ac^{-}, bz^{-}, and (ox^{-} and ox^{2-}) are used as shown in Table 3. As the most stable species of **1** complexes with these anions are in the form of **1a** isomer, the protonation of complexes in the form of **1a** isomer is therefore investigated. Proton affinities of monoprotonated complexes of these carboxylic acids are in order: $[$**1a**/fm$]^{-} > [$**1a**/ac$]^{-} > [$**1a**/bz$]^{-} > [$**1a**/ox$]^{-}$ which corresponds to their free energies as shown in Table S4. Association energies of these complexes are very high and their complexations are spontaneous reaction. Reaction energies, thermodynamic properties, rate constants, and equilibrium constants of transformation of **1** complexes with carboxylic acids, computed at the B3LYP/6-31+G(d,p) level of theory, are shown in Table 4.

Association mechanisms of **1** complexes with formic acid, acetic acid, benzoic acid, oxalic acid, and their interconversions are shown in Figs 2–5, respectively. The plot of selectivity coefficient against carboxylic acid guests is shown in Fig. 6. It shows that the receptor **1** in the form of isomer **1c** could selectively recognize the oxalic acid in a mixture of carboxylic acids. The relative energies of conversion reactions of formic acid and its deprotonated species, in terms of energy profile, are shown in Fig. 7. It also shows autoconversions of anionic complex species $[$**1a**/ox$]^{-}$ and $[$**1a**/ox$]^{2-}$ via the transition states ts_$[$**1a**/ox$]^{-}$_$[$**1a**/ox$]^{-}$ and ts_$[$**1a**/ox$]^{2-}$_$[$**1a**/ox$]^{2-}$, respectively; also refer to Table 4. Rate constants of the $[$**1a**/ox$]^{2-}$ → ts_$[$**1a**/ox$]^{2-}$_$[$**1a**/ox$]^{2-}$ → $[$**1a**/ox$]^{2-}$ are much more higher than that of the $[$**1a**/ox$]^{-}$ → ts_$[$**1a**/ox$]^{-}$_$[$**1a**/ox$]^{-}$ → $[$**1a**/ox$]^{-}$; their values are 1.96×10^{7} and 2.94×10^{-8} s^{-1}, respectively.

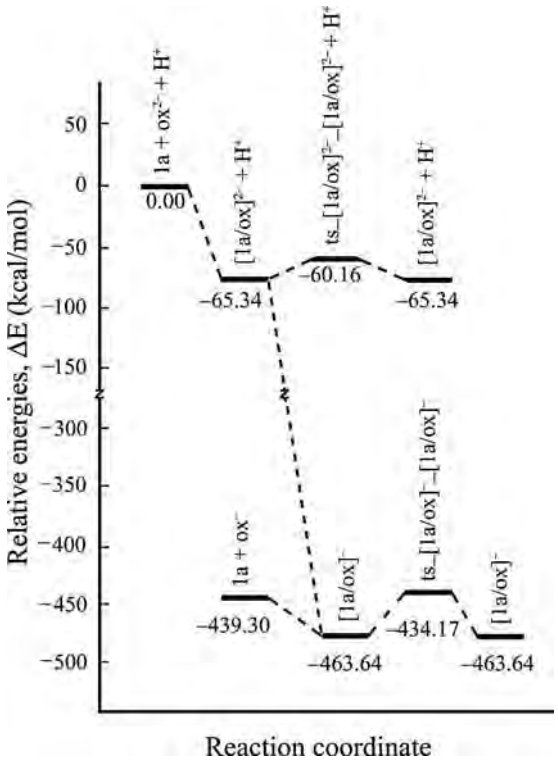

Figure 7. Relative energies for change of oxalic acid/oxalate ions and their complexes with receptor **1**

CONCLUSIONS

Four isomers dipicolyl urea, **1a**, **1b**, **1c**, and **1c′**, were found to be transformed via three transition states, **ts_1a_1b**, **ts_1b_1c**, and **ts_1c_1c′**. The relative stabilities of these isomers are in orders: **1c** > **1a** > **1b** > **1c′** in gas phase and **1a** > **1c** > **1b** > **1c′** in aqueous solution. Transformation of **1b** to **1c** is the thermodynamically preferred reaction with $K_{298} = 6.04 \times 10^3$ which corresponds to its forward and backward rate constants of $k_{298}^{fw} = 4.08 \times 10^9$ and $k_{298}^{bw} = 7.14 \times 10^5\ s^{-1}$, respectively. Structure of the most stable isomer, **1c**, is in good agreement with the X-ray data.

The relative stabilities for the complexes with formic, acetic, benzoic, and oxalic acids are in orders: **1c**/fma > **1b**/fma > **1c**/fma′ > **1a**/fma > **1b**/fma″ > **1b**/fma′, **1c**/aca > **1b**/aca > **1c**/aca′ > **1a**/aca > **1b**/aca″ > **1b**/aca′, **1c**/bza > **1b**/bza > **1c**/bza′ > **1a**/bza > **1b**/bza′ > **1b**/bza″, and **1c**/oxa > **1b**/oxa > **1a**/oxa > **1b**/oxa″ > **1b**/oxa′, respectively. The most stable complexes with fma, ace, bza, and oxa are the complexes of the isomer **1c**. The relative selectivities of the receptor **1c** are in order: oxa > fma > bza > aca. The proton affinities of monoprotonated complexes of these carboxylic acids with **1a** are in order: [**1a**/fm]$^-$ > [**1a**/ac]$^-$ > [**1a**/bz]$^-$ > [**1a**/ox]$^-$. Autoconversions of anionic complex species [**1a**/ox]$^-$ and [**1a**/ox]$^{2-}$ were found and their rate constants are 1.96×10^7 and $2.94 \times 10^{-8}\ s^{-1}$, respectively.

Acknowledgements

The authors gratefully acknowledge the Thailand Research Fund for financial support (grant no. BRG5180016).

REFERENCES

[1] C. R. Bondy, S. J. Loeb, *Coord. Chem. Rev.* **2003**, *240*, 77–99.
[2] S. O. Kang, R. A. Begum, K. Bowman-James, *Angew. Chem. Int. Ed. Engl.* **2006**, *45*, 7882–7894.
[3] R. Joseph, B. Ramanujam, A. Acharya, C. P. Rao, *Tet. Lett.* **2009**, *50*, 2735–2739.
[4] X.-F. Shang, H.-K. Lin, H. Lin, *Trans. Met. Chem.* **2007**, *32*, 38–41.
[5] B. Wanno, W. Rakrai, S. Keawwangchai, N. Morakot, N. Morakot, N. Nunthaboot, V. Ruangpornvisuti, *J. Mol. Struct. (Theochem)* **2009**, *902*, 33–40.
[6] K. Navakhun, V. Ruangpornvisuti, *J. Mol. Struct. (Theochem)* **2006**, *772*, 23–30.
[7] K. Navakhun, V. Ruangpornvisuti, *J. Mol. Struct. (Theochem)* **2007**, *806*, 145–153.
[8] K. Navakhun, V. Ruangpornvisuti, *J. Mol. Struct. (Theochem)* **2008**, *864*, 26–30.
[9] K. Navakhun, V. Ruangpornvisuti, *J. Mol. Struct. (Theochem)* **2009**, *907*, 131–134.
[10] V. Ruangpornvisuti, *J. Mol. Struct. (Theochem)* **2004**, *686*, 47–55.
[11] S. Piyaauksornsak, T. Tangthongkul, R. Wanbayor, B. Wanno, V. Ruangpornvisuti, *Struct. Chem.* **2009**, *20*, 767–780.
[12] V. Ruangpornvisuti, B. Wanno, *J. Mol. Model* **2007**, *13*, 65–77.
[13] Y. Sun, G. Wang, W. Guo, *Tetrahedron* **2009**, *65*, 3480–3484.
[14] O. Mammoliti, S. Allasia, S. Dixon, J. D. Kilburn, *Tetrahedron* **2009**, *65*, 2184–2195.
[15] W. Kohn, L. Sham, *J. Phys. Rev.* **1965**, *140*, A1133–A1138.
[16] A. D. Becke, *J. Chem. Phys.* **1993**, *98*, 5648–5652.
[17] C. Lee, W. Yang, R. G. Parr, *Phys. Rev. B* **1988**, *37*, 785–789.
[18] W. J. Hehre, R. Ditchfield, J. A. Pople, *J. Chem. Phys.* **1972**, *56*, 2257–2261.
[19] M. S. Gordon, *Chem. Phys. Lett.* **1980**, *76*, 163–168.
[20] V. Barone, M. Cossi, J. Tomasi, *J. Comput. Chem.* **1998**, *19*, 404–417.
[21] M. Cossi, V. Barone, *J. Chem. Phys.* **1998**, *109*, 6246–6254.
[22] M. J. Frisch, G. W. Trucks, H. B. Schlegel, G. E. Scuseria, M. A. Robb, J. R. Cheeseman, J. A. Montgomery, Jr., T. Vreven, K. N. Kudin, J. C. Burant, J. M. Millam, S. S. Iyengar, J. Tomasi, V. Barone, B. Mennucci, M. Cossi, G. Scalmani, N. Rega, G. A. Petersson, H. Nakatsuji, M. Hada, M. Ehara, K. Toyota, R. Fukuda, J. Hasegawa, M. Ishida, T. Nakajima, Y. Honda, O. Kitao, H. Nakai, M. Klene, X. Li, J. E. Knox, H. P. Hratchian, J. B. Cross, V. Bakken, C. Adamo, J. Jaramillo, R. Gomperts, R. E. Stratmann, O. Yazyev, A. J. Austin, R. Cammi, C. Pomelli, J. W. Ochterski, P. Y. Ayala, K. Morokuma, G. A. Voth, P. Salvador, J. J. Dannenberg, V. G. Zakrzewski, S. Dapprich, A. D. Daniels, M. C. O. Strain, Farkas, D. K. Malick, A. D. Rabuck, K. Raghavachari, J. B. Foresman, J. V. Ortiz, Q. Cui, A. G. Baboul, S. Clifford, J. Cioslowski, B. B. Stefanov, G. Liu, A. Liashenko, P. Piskorz, I. Komaromi, R. L. Martin, D. J. Fox, T. Keith, M. A. Al-Laham, C. Y. Peng, A. Nanayakkara, M. Challacombe, P. M. W. Gill, B. Johnson, W. Chen, M. W. Wong, C. Gonzalez, J. A. Pople, *Gaussian 03, Revision C.02, Gaussian Inc., Wallingford, 2004.*
[23] W. Sang-Aroon, V. Ruangpornvisuti, *Int. J. Quantum Chem.* **2009**, *108*, 1181–1188.
[24] W. Sang-Aroon, V. Ruangpornvisuti, *J. Mol. Graph. Model.* **2008**, *26*, 982–990.
[25] P. Flükiger, H. P. Lüthi, S. Portmann, J. Weber, *MOLEKEL 4.3, Swiss Center for Scientific Computing, Manno, Switzerland, 2000.*
[26] J. P. Merrick, D. Moran, L. Radom, *J. Phys. Chem. A* **2007**, *111*, 11683–11700.
[27] V. Ruangpornvisuti, *Int. J. Quantum Chem.* **2009**, *109*, 275–284.
[28] E. P. Wigner, *Z. Phys. Chem. B* **1932**, *19*, 203–204.
[29] J. O. Hirschfelder, E. P. Wigner, *J. Chem. Phys.* **1939**, *7*, 616–628.
[30] R. P. Bell, *The Tunnel Effect in Chemistry*, Chapman and Hall, London, **1980**.
[31] Y. Long, Y. Liu, L. Lei, L. Nie, S. Yao, *Analyst* **2001**, *126*, 1090–1094.
[32] S. Goswami, S. Jana, S. Dey, D. Sen, H.-K. Fun, S. Chantrapromma, *Tetrahedron* **2008**, *64*, 6426–6433.

ภาคผนวก D

Manuscript บทความเรื่อง “A DFT investigation of cyclic amide receptors and their recognition with monovalent anions”

A DFT investigation of cyclic amide receptors and their recognition with monovalent anions

Pornpan Chanapiwat [a], Korakot Navakhun [b], Vithaya Ruangpornvisuti [a,*]

[a] *Supramolecular Chemistry Research Unit, Department of Chemistry, Faculty of Science, Chulalongkorn University, Bangkok 10330, Thailand*

[b] *Department of Chemistry and Center of Excellence for Innovation in Chemistry, Faculty of Science, Ramkhamhaeng University, Huamark, Bangkapi, Bangkok 10240, Thailand*

Corresponding authors: Phone: 66–2218–7644, Fax: 66–2254–1309.
E–mail addresses: vithaya.r@chula.ac.th. (V. Ruangpornvisuti)

Abstract

Binding energies of complexes between six cyclic amide receptors and monovalent anions F^-, Cl^-, Br^-, CH_3COO^-, HSO_4^- and $H_2PO_4^-$ and thermodynamic properties of these complexations were obtained at the B3LYP/6–31G(d) level. The binding abilities of these six receptors are in decreasing orders: $F^- > CH_3COO^- > Br^- > H_2PO_4^- > Cl^- > HSO_4^-$ for receptor **1**, $F^- > Br^- > CH_3COO^- > H_2PO_4^- > Cl^- > HSO_4^-$ for receptors **2** and **3**, $F^- > H_2PO_4^- > CH_3COO^- \approx Br^- > Cl^- > HSO_4^-$ for receptor **4**, $F^- > H_2PO_4^- \approx CH_3COO^- \approx Br^- > Cl^- > HSO_4^-$ for receptor **5** and $F^- > H_2PO_4^- > Br^- > CH_3COO^- \approx > Cl^- \approx HSO_4^-$ for receptor **6**.

Keywords cyclic amide receptors, molecular structure, selectivity, recognition; DFT

1. Introduction

Review articles for the supramolecular compounds containing amide functional groups as anion receptors [1] and amide–based ligands for anion coordination [2] were summarized. Fluorescence switch–on sensor for copper (II) by an amide linked lower rim 1,3–bis(2–picolyl)amine derivative of calix[4]arene in aqueous methanol [3] and phenanthroline complexes bearing diamide–anion [4] were studied. Many theoretical studies of anion receptors namely 1,3–bis(4–nitrophenyl)urea derivative[5], non–rigid bis–(2,5–diamidopyrrole) [6], 3,4–dichloro–2,5–diamidopyrrole [7], 3,4–dichloro–2,5–diamido–substituted pyrrole derivatives [8], 3,4–dichloro–2,5–diamido–substituted pyrrole [9], azophenol–thiourea derivatives [10], 8,8′–dithioureido–2,2′–binaphthalene derivatives [11], tetraamino–tert–butylthiacalix[4]arene and tetraamino–tert–butylcalix[4]arene [12] were studied. N–nitrophenyl benzamide derivatives for cyanide colorimetric detection [13] and synthesis and anion–binding properties of new disulfonamide–based receptors [14] were studied.

In this work, the cyclic amide receptors, their energies, thermodynamic properties, rate constants and association constants of their isomerization have been determined using the B3LYP/6–31G(p) level. Association energies, thermodynamic properties, rate and association constants of their complexes with monovalent anions F^-, Cl^-, Br^-, CH_3COO^-, HSO_4^- and $H_2PO_4^-$ have been obtained.

2. Computational details

Structures of cyclic amide receptors, formic acid, formate ion, acetic acid, acetate ion, benzoic acid, benzoate ion, oxalic acid, oxalate ions and related species were optimized using density functional theory (DFT) method. DFT calculations have been performed with the Becke's three parameter hybrid functional [15] with the Lee−Yang−Parr correlation functional [16], B3LYP method [17] with 6−31(d) basis set [18,19]. All structures and their reactions were studied in gas phase unless otherwise specified. All calculations were performed with the Gaussian 03 program [20]. The molecular graphics for all species were generated with the MOLEKEL 4.3 program [21].

The standard enthalpy ΔH^{o}_{298} and Gibbs free energy changes ΔG^{o}_{298} of isomerization of cyclic amide receptors, association of their complexes and their conversion reactions have

been derived from the frequency calculations at the B3LYP/6−31G(d) level of theory. The association constant *K* at 298.15 K (K_{298}) and 1 atm is computed using a thermodynamic equation $\Delta G^{o} = -RT \ln K$.

The binding selectivity of receptor **1** to guest B with respect to guest A has been derived from the selectivity coefficient (K_B^A) [22] which is defined as an equilibrium constant of ion exchange between ions A and B. Since exchange is a chemical reaction as eq. (1), it can be treated like any other mass action expression.

$$AX + B \rightleftharpoons BX + A \quad (1)$$

Therefore, the selectivity coefficient can be defined as $K_B^A = \frac{[BX][A]}{[AX][B]}$. If the complexations of BX and AX are observed, their stability constants based on eqs. (2) and (3) can be expressed as $K_A = \frac{[AX]}{[X][A]}$ and $K_B = \frac{[BX]}{[X][B]}$.

$$X + B \rightleftharpoons BX \quad (2)$$

$$X + A \rightleftharpoons AX \quad (3)$$

The selectivity coefficient can be therefore written as $K_B^A = \frac{K_B}{K_A}$. If the value of the selectivity coefficient K_B^A is larger than one, this implies that B is preferred over A and if K_B^A is smaller than one then A is preferred over B.

3. Results and discussion

The B3LYP/6–31G(d) optimized structures of cyclic amide receptors are shown in Fig. 1 and their complexes with the monovalent anions F^-, Cl^-, Br^-, CH_3COO^-, HSO_4^- and $H_2PO_4^-$ are shown in Figs. 2 to 6. Binding energies and thermodynamic properties of binding between these receptors and anions were determined. Binding energies of receptors are in decreasing orders: $F^- >> CH_3COO^- > Br^- > H_2PO_4^- > Cl^- > HSO_4^-$ for receptor **1**, $F^- >> Br^- > CH_3COO^- > H_2PO_4^- > Cl^- > HSO_4^-$ for receptors **2** and **3**, $F^- >> H_2PO_4^- > CH_3COO^- \approx Br^- > Cl^- > HSO_4^-$ for receptor **4**, $F^- >> H_2PO_4^- \approx CH_3COO^- \approx Br^- > Cl^- > HSO_4^-$ for receptor **5** and $F^- >> H_2PO_4^- > Br^- > CH_3COO^- \approx > Cl^- \approx HSO_4^-$ for receptor **6**.

Selectivity coefficients of receptors to monovalent anions relative to sulfate ion are listed in Table 1 which shows that the relative selectivities of the receptors are in decreasing order: $F^- >> CH_3COO^- > Br^- > Cl^- > H_2PO_4^- > HSO_4^-$ for receptor **1**, $F^- >> Br^- > Cl^- > CH_3COO^- > H_2PO_4^- > HSO_4^-$ for receptor **2**, $F^- >> Br^- > CH_3COO^- > H_2PO_4^- > Cl^- > HSO_4^-$ for receptor**s 3**, **4**, and **5** and $F^- >> Br^- > H_2PO_4^- > Cl^- > CH_3COO^- > HSO_4^-$ for receptor **6**. It can be concluded that receptor **1** electively recognizes acetate anion but receptors **2**, **3**, **4**, **5** and **6** recognize bromine ion as shown in Table 1.

4. Conclusions

Binding energies of receptors are in decreasing orders: $F^- >> CH_3COO^- > Br^- > H_2PO_4^- > Cl^- > HSO_4^-$ for receptor **1**, $F^- >> Br^- > CH_3COO^- > H_2PO_4^- > Cl^- > HSO_4^-$ for receptors **2** and **3**, $F^- >> H_2PO_4^- > CH_3COO^- \approx Br^- > Cl^- > HSO_4^-$ for receptor **4**, $F^- >> H_2PO_4^- \approx CH_3COO^- \approx Br^- > Cl^- > HSO_4^-$ for receptor **5** and $F^- >> H_2PO_4^- > Br^- > CH_3COO^- \approx > Cl^- \approx HSO_4^-$ for receptor **6**. It can be concluded that receptor 1 electively recognizes acetate anion but receptors 2, 3, 4, 5 and 6 recognize bromine ion as shown in Table 1.

Acknowledgements

The authors gratefully acknowledge the Thailand Research Fund for financial support (Grant no. BRG5180016). The Center for Petroleum, Petrochemicals and Advanced Materials, Chulalongkorn University, Bangkok, Thailand is also acknowledged for partial financial support.

References

[1] C. R. Bondy, S. J. Loeb, Amide based receptors for anions, Coord. Chem. Rev. 240 (2003) 77–99.

[2] S.O. Kang, R.A. Begum, K. Bowman–James, Amide–based ligands for anion coordination, Angew. Chem. Int. Ed. 45 (2006) 7882–7894.

[3] R. Joseph, B. Ramanujam, A. Acharya, C.P. Rao, Fluorescence switch–on sensor for Cu^{2+} by an amide linked lower rim 1,3–bis(2–picolyl)amine derivative of calix[4]arene in aqueous methanol, Tet. Lett. 50 (2009) 2735–2739.

[4] X.–F. Shang, H.–K. Lin, H. Lin, Phenanthroline complexes bearing diamide–anion recognition sites, Trans. Met. Chem. 32 (2007) 38–41.

[5] B. Wanno, W. Rakrai, S. Keawwangchai, N. Morakot, N. Morakot, N. Nunthaboot, V. Ruangpornvisuti, A density functional investigation of 1,3–bis(4–nitrophenyl)urea as anion receptor, J. Mol. Struct. Theochem 902 (2009) 33–40.

[6] K. Navakhun, V. Ruangpornvisuti, Non–rigid bis–(2,5–diamidopyrrole) receptor, its deprotonated species and their complexes with fluoride, chloride and hydroxide ions, J. Mol. Struct. (Theochem) 907 (2009) 131–134.

[7] K. Navakhun, V. Ruangpornvisuti, Anion binding of 3,4–dichloro–2,5–diamidopyrrole and anionic self–assembly dimerization of its deprotonated species, J. Mol. Struct. (Theochem) 864 (2008) 26–30.

[8] K. Navakhun, V. Ruangpornvisuti, A DFT study of chloride and hydroxide anions effects on deprotonations of 3,4–dichloro–2,5–diamido–substituted pyrrole derivatives, J. Mol. Struct. (Theochem) 806 (2007) 145–153.

[9] K. Navakhun, V. Ruangpornvisuti, Molecular structures of 3,4–dichloro–2,5–diamido–substituted pyrrole anion dimers, their deprotonation reactions in systems with and without fluoride ion, J. Mol. Struct. (Theochem) 772 (2006) 23–30.

[10] V. Ruangpornvisuti, Recognition of carboxylate and dicarboxylates by azophenol–thiourea derivatives: a theoretical host–guest investigation, J. Mol. Struct. Theochem 686 (2004) 47–55.

[11] S. Piyaauksornsak, T. Tangthongkul, R. Wanbayor, B. Wanno, V. Ruangpornvisuti, Molecular structures of 8,8′–dithioureido–2,2′–binaphthalene derivatives and their anions recognition: an ONIOM investigation, Struct. Chem. (2009), in press.

[12] V. Ruangpornvisuti, B. Wanno, Molecular model for host–guest interaction of tetraamino–tert–butylthiacalix[4]arene and tetraamino–tert–butylcalix[4]arene

receptors with carboxylate and dicarboxylate guests: an ONIOM study, J. Mol. Model. 13 (2007) 65–77.

[13] Y. Sun, G. Wang, W. Guo, Colorimetric detection of cyanide with N–nitrophenyl benzamide derivatives, Tetrahedron, 65 (2009) 3480–3484.

[14] O. Mammoliti, S. Allasia, S. Dixon, J.D. Kilburn, Synthesis and anion–binding properties of new disulfonamide–based receptors, Tetrahedron 65 (2009) 2184–2195.

[15] W. Kohn, L. J. Sham, Self–consistent equations including exchange and correlation effects, Phys. Rev. 140 (1965) A1133–A1138.

[16] A.D. Becke, Density–functional thermochemistry. III. The role of exact exchange, J. Chem. Phys. 98 (1993) 5648–5652.

[17] C. Lee, W. Yang, R.G. Parr, Development of the Colle–Salvetti correlation–energy formula into a functional of the electron density, Phys. Rev. B 37 (1988) 785–789.

[18] W. J. Hehre, R. Ditchfield, J. A. Pople, Self–consistent molecular orbital methods. XII. Further extensions of gaussian–type basis sets for use in molecular orbital studies of organic molecules, J. Chem. Phys. 56 (1972) 2257–2261.

[19] M. S. Gordon, The isomers of silacyclopropane, Chem. Phys. Lett. 76 (1980) 163–168.

[20] M.J. Frisch, et al, Gaussian 03, Revision C.02, Gaussian, Inc., Wallingford CT, 2006 (full reference given in Supplementary data).

[21] P. Flükiger, H.P. Lüthi, S. Portmann and J. Weber, Molekel 4.3, Swiss Center for Scientific Computing, Manno, Switzerland (2000).

[22] Y. Long, Y. Liu, L. Lei, L. Nie, S. Yao, Construction and application of phenytoin anion–selective electrode based on bulk acoustic wave (BAW) sensing technique, Analyst 126 (2001) 1090–1094.

Table 1.

Reaction energies, thermodynamic properties and association constants of complexes of receptors and monovalent anions, computed at the B3LYP/6–31G(d) level of theory

Reaction	ΔE [a]	ΔH_{298} [b]	ΔG_{298} [b]	K_{298}	$\log K_{298}^{HSO_4^-}$
Receptor **1**/anions:					
1 + F^- → **1**/F^-	–131.34	–132.49	–122.56	7.08 x 10^{89}	63.97
1 + Cl^- → **1**/Cl^-	–58.10	–58.62	–49.88	3.71 x 10^{36}	10.69
1 + Br^- → **1**/Br^-	–64.63	–65.19	–55.71	6.97 x 10^{40}	14.97
1 + AcO^- → **1**/AcO^-	–67.65	–67.21	–56.75	4.02 x 10^{41}	15.73
1 + HSO_4^- → **1**/ HSO_4^-	–46.77	–46.08	–35.30	7.53 x 10^{25}	0.00
1 + $H_2PO_4^-$ → **1**/ $H_2PO_4^-$	–60.63	–59.94	–48.90	7.03 x 10^{35}	9.97
Receptor **2**/anions:					
2 + F^- → **2**/F^-	–135.33	–136.39	–127.02	1.30 x 10^{93}	59.71
2 + Cl^- → **2**/Cl^-	–66.73	–67.14	–59.79	6.78 x 10^{43}	10.43
2 + Br^- → **2**/Br^-	–74.79	–76.24	–64.62	2.36 x 10^{47}	13.97
2 + AcO^- → **2**/AcO^-	–67.89	–68.02	–55.72	7.06 x 10^{40}	7.44
2 + HSO_4^- → **2**/ HSO_4^-	–56.98	–56.36	–45.57	2.54 x 10^{33}	0.00
2 + $H_2PO_4^-$ → **2**/ $H_2PO_4^-$	–66.88	–66.52	–54.14	4.86 x 10^{39}	6.28
Receptor **3**/anions:					
3 + F^- → **3**/F^-	–139.36	–140.98	–128.80	2.66 x 10^{94}	59.80
3 + Cl^- → **3**/Cl^-	–66.71	–67.65	–57.52	1.46 x 10^{42}	7.54
3 + Br^- → **3**/Br^-	–73.97	–74.78	–64.61	2.33 x 10^{47}	12.75
3 + AcO^- → **3**/AcO^-	–73.02	–73.42	–60.60	2.66 x 10^{44}	9.80
3 + HSO_4^- → **3**/ HSO_4^-	–59.42	–59.14	–47.23	4.18 x 10^{34}	0.00
3 + $H_2PO_4^-$ → **3**/ $H_2PO_4^-$	–71.35	–71.17	–57.54	1.51 x 10^{42}	7.56
Receptor **4**/anions:					
4 + F^- → **4**/F^-	–139.49	–143.91	–130.66	6.07 x 10^{95}	65.38
4 + Cl^- → **4**/Cl^-	–64.98	–66.21	–54.50	8.90 x 10^{39}	9.55
4 + Br^- → **4**/Br^-	–71.10	–72.29	–60.28	1.56 x 10^{44}	13.79
4 + AcO^- → **4**/AcO^-	–71.12	–71.23	–58.12	4.02 x 10^{42}	12.20
4 + HSO_4^- → **4**/ HSO_4^-	–57.06	–57.56	–41.47	2.54 x 10^{30}	0.00
4 + $H_2PO_4^-$ → **4**/ $H_2PO_4^-$	–73.79	–74.45	–57.17	8.17 x 10^{41}	11.51
Receptor **5**/anions:					
5 + F^- → **5**/F^-	–127.57	–129.27	–116.19	1.51 x 10^{85}	67.26
5 + Cl^- → **5**/Cl^-	–48.32	–49.58	–37.50	3.09 x 10^{27}	9.58
5 + Br^- → **5**/Br^-	–54.84	–55.92	–43.87	1.44 x 10^{32}	14.24
5 + AcO^- → **5**/AcO^-	–53.88	–54.06	–39.68	1.22 x 10^{29}	11.17
5 + HSO_4^- → **5**/ HSO_4^-	–40.01	–40.11	–24.44	8.23 x 10^{17}	0.00
5 + $H_2PO_4^-$ → **5**/ $H_2PO_4^-$	–56.26	–56.87	–39.27	6.10 x 10^{28}	10.87
Receptor **6**/anions:					
6 + F^- → **6**/F^-	– [c]	– [c]	– [c]	–	–
6 + Cl^- → **6**/Cl^-	–55.87	–57.10	–43.68	1.05 x 10^{32}	1.83
6 + Br^- → **6**/Br^-	–61.84	–62.42	–51.13	3.01 x 10^{37}	7.28
6 + AcO^- → **6**/AcO^-	–57.36	–56.98	–43.29	5.40 x 10^{31}	1.54
6 + HSO_4^- → **6**/ HSO_4^-	–56.39	–55.90	–41.19	1.57 x 10^{30}	0.00
6 + $H_2PO_4^-$ → **6**/ $H_2PO_4^-$	–64.00	–63.79	–46.76	1.89 x 10^{34}	4.08

[a] Energy with ZPVE corrections scaled by the empirical factor 0.9857, in kcal/mol.

[b] In kcal/mol.

[c] Frequency calculation has been not achieved.

Table 2.

Hydrogen bond lengths between anions and donor atoms of receptors

Receptor/anion	F^-	Cl^-	Br^-	AcO^-	HSO_4^-	$H_2PO_4^-$
Receptor **1**				(O1, O2)	(O1, O2)	(O1, O2)
N1H···A	1.85012	2.47166	2.44423	1.88406 (O1)	1.96946 (O1)	1.87769 (O1)
N2H···A	1.85136	2.46904	2.38962	1.87717 (O2)	1.96425 (O2)	1.90499 (O2)
N3H···A	1.85122	2.34145	2.33575	1.86463 (O2)	1.97410 (O2)	1.90437 (O2)
N4H···A	1.85140	2.34523	2.39000	1.87240 (O1)	1.97798 (O1)	1.90398 (O1)
C1H···A	1.87909	2.83228	2.15180	3.03571 (O1), 3.00487 (O2)	–	–
C2H···A	2.10650	2.59052	2.10071	2.87587 (O1), 2.84836 (O2)	–	–
C3H···A	–	–	–	–	2.68537 (O1)	2.73732 (O1)
C4H···A	–	–	–	–	2.70068 (O2)	2.68531 (O2)
Receptor **2**				(O1,O2,O3)	(O1,O2)	(O1,O4)
N1H···A	1.93462	2.45276	2.09424	2.02719 (O1)	2.11092 (O1)	1.90362 (O1)
N2H···A	1.95733	2.44237	2.09192	2.02711 (O2) 1.97206 (O3)	2.89293 (O1)	2.77838 (O1)
N3H···A	1.93365	2.44757	2.09341	2.02718 (O2)	2.69272 (O1)	2.92110 (O1), 2.06033 (O4)
N4H···A	1.95805	2.44483	2.09310	2.02726 (O1)	1.95294 (O1)	1.92648 O1)
C1H···A	1.88711	2.62869	2.51496	2.25244 (O1)	2.29321 (O1)	–
C2H···A	1.88691	2.62774	2.51494	2.25263 (O2)	2.30446 (O1)	–
C3H···A	–	–	–	2.63068 (O1), 2.63200 (O2)	–	–
C4H···A	–	–	–	2.62398 (O1), 2.62528 (O2)	2.42978 (O2)	2.54753 (O2)
Receptor **3**					(O1,O2)	(O1,O2)
N1H···A	1.92270	2.36081	2.58060	2.06752 (O1)	2.13694 (O1)	2.06037 (O1)
N2H···A	1.89974	2.47481	2.46676	2.06859 (O1)	2.17150 (O1)	2.22519 (O1)
N3H···A	1.92427	2.35959	2.57922	2.06665 (O2)	2.17496 (O2)	2.06201 (O2)
N4H···A	1.89924	2.47677	2.46807	2.06897 (O2)	2.14123 (O2)	2.21657 (O2)
C1H···A	1.86566	2.58137	2.68641	2.31116 (O1)	2.33762 (O1)	2.23528 (O1)
C2H···A	1.86422	2.57799	2.69043	2.31112 (O2)	2.34619 (O2)	2.23403 (O2)
Receptor **4**					(O1,O2)	(O1,O2)
N1H···A	1.88679	2.31226	2.38962	1.99313 (O1)	2.09860 (O1)	2.03674 (O1)
N2H···A	1.84264	2.36048	2.49580	2.12819 (O1)	2.23095 (O1)	2.04714 (O1)
N3H···A	1.88727	2.31119	2.38812	2.07134 (O2)	2.11090 (O2)	1.99010 (O2)
N4H···A	1.84259	2.36150	2.49599	2.04153 (O2)	2.19990 (O2)	1.98311 (O2)
C1H···A	1.88077	2.62024	2.76440	2.23124 (O1)	2.25697 (O1)	2.13530 (O1)
C2H···A	1.88036	2.61592	2.76631	2.22351 (O2)	2.24508 (O2)	2.17760 (O2)
Receptor **5**					(O1,O2)	(O1,O2)
N1H···A	1.70077	2.25449	2.37152	1.93803 (O1)	2.03003 (O1)	1.94126 (O1)
N2H···A	1.72998	2.33735	2.49437	1.98515 (O1)	2.09297 (O1)	1.91416 (O1)
N3H···A	1.70077	2.25512	2.37209	2.00954 (O2)	2.02908 (O2)	1.87036 (O2)
N4H···A	1.72998	2.33625	2.49362	1.95026 (O2)	2.08262 (O2)	1.91124 (O2)
Receptor **6**					(O1,O2)	(O1,O2)
N1H···A	1.72568	2.45118	2.59853	2.09489 (O1)	2.34874 (O1)	2.16966 (O1)
N2H···A	1.72567	2.45991	2.59937	2.01713 (O1)	2.39500 (O1)	2.20023 (O1)
N3H···A	1.66535	2.37273	2.50406	2.05535 (O2)	2.37822 (O2)	2.16985 (O2)
N4H···A	1.66523	2.36497	2.50455	2.22820 (O2)	2.33703 (O2)	2.19970 (O2)

Table 3.

Reaction energies of complexes of receptors and monovalent anions, computed at the B3LYP/6–31+G(d,p)//B3LYP/6–31G(d) level

Reaction					ΔE [a]
Receptor **1**/anions:					
1	+	F^-	→	**1**/F^-	-95.63
1	+	Cl^-	→	**1**/Cl^-	-65.71
1	+	Br^-	→	**1**/Br^-	-72.54
1	+	AcO^-	→	**1**/AcO^-	-71.04
1	+	HSO_4^-	→	**1**/ HSO_4^-	-56.14
1	+	$H_2PO_4^-$	→	**1**/ $H_2PO_4^-$	-66.20
Receptor **2**/anions:					
2	+	F^-	→	**2**/F^-	-85.61
2	+	Cl^-	→	**2**/Cl^-	-60.31
2	+	Br^-	→	**2**/Br^-	-67.52
2	+	AcO^-	→	**2**/AcO^-	-58.05
2	+	HSO_4^-	→	**2**/ HSO_4^-	-50.91
2	+	$H_2PO_4^-$	→	**2**/ $H_2PO_4^-$	-57.04
Receptor **3**/anions:					
3	+	F^-	→	**3**/F^-	-87.61
3	+	Cl^-	→	**3**/Cl^-	-60.12
3	+	Br^-	→	**3**/Br^-	-68.20
3	+	AcO^-	→	**3**/AcO^-	-63.58
3	+	HSO_4^-	→	**3**/ HSO_4^-	-54.15
3	+	$H_2PO_4^-$	→	**3**/ $H_2PO_4^-$	-61.45
Receptor **4**/anions:					
4	+	F^-	→	**4**/F^-	-89.01
4	+	Cl^-	→	**4**/Cl^-	-58.18
4	+	Br^-	→	**4**/Br^-	-65.97
4	+	AcO^-	→	**4**/AcO^-	-61.20
4	+	HSO_4^-	→	**4**/ HSO_4^-	-51.25
4	+	$H_2PO_4^-$	→	**4**/ $H_2PO_4^-$	-63.64
Receptor **5**/anions:					
5	+	F^-	→	**5**/F^-	-74.47
5	+	Cl^-	→	**5**/Cl^-	-41.82
5	+	Br^-	→	**5**/Br^-	-48.91
5	+	AcO^-	→	**5**/AcO^-	-43.62
5	+	HSO_4^-	→	**5**/ HSO_4^-	-34.79
5	+	$H_2PO_4^-$	→	**5**/ $H_2PO_4^-$	-46.20
Receptor **6**/anions:					
6	+	F^-	→	**6**/F^-	-80.16
6	+	Cl^-	→	**6**/Cl^-	-50.74
6	+	Br^-	→	**6**/Br^-	-57.16
6	+	AcO^-	→	**6**/AcO^-	-48.45
6	+	HSO_4^-	→	**6**/ HSO_4^-	-50.41
6	+	$H_2PO_4^-$	→	**6**/ $H_2PO_4^-$	-54.60

[a] Energy without ZPVE corrections scaled by the empirical factor 1, in kcal/mol.

Captions for the illustrations

Fig. 1. Optimized structures of cyclic amide receptors, Top and bottom are side and top views, respectively.

Fig. 2. Optimized structures of complexes between **1** and anions.

Fig. 3. Optimized structures of complexes between **2** and anions.

Fig. 4. Optimized structures of complexes between **3** and anions.

Fig. 5. Optimized structures of complexes between **4** and anions.

Fig. 6. Optimized structures of complexes between **5** and anions.

Fig. 7. Optimized structures of complexes between **6** and anions.

Fig. 8. Gibbs free energy changes for association of receptors with alkaline ions.

Fig. 9. Gibbs free energy changes for association of receptors with oxygenated ions.

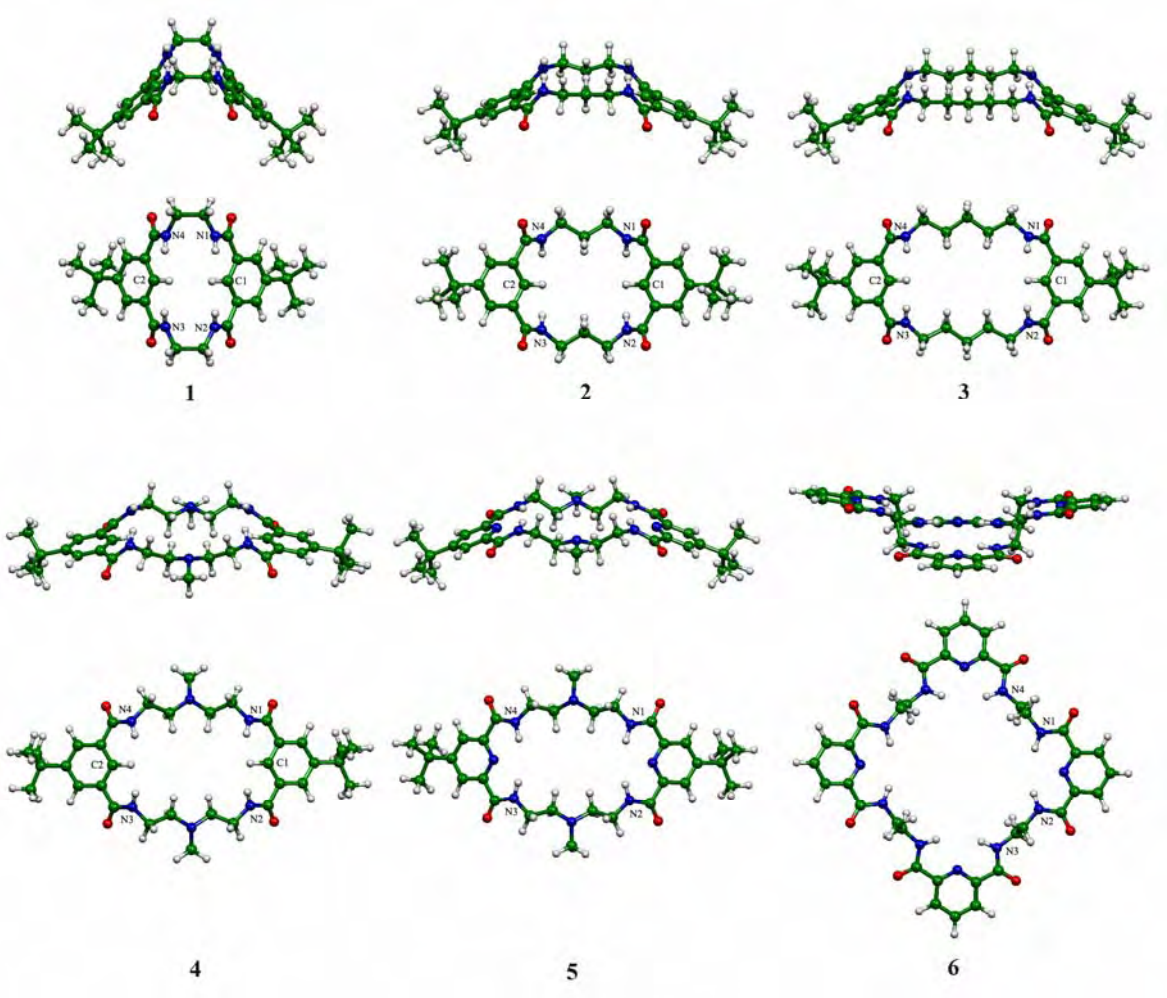

Fig. 1.

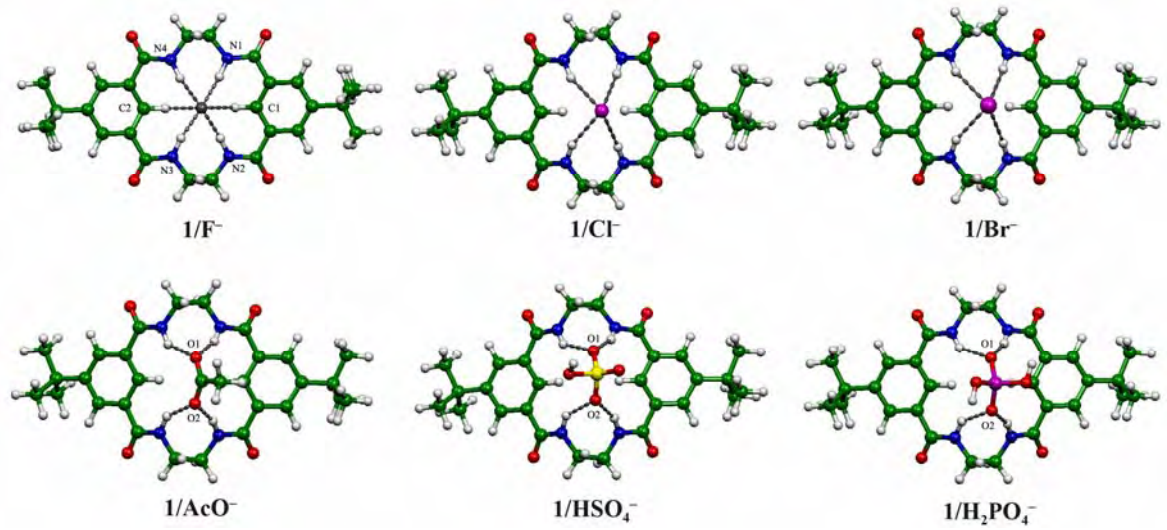

Fig. 2.

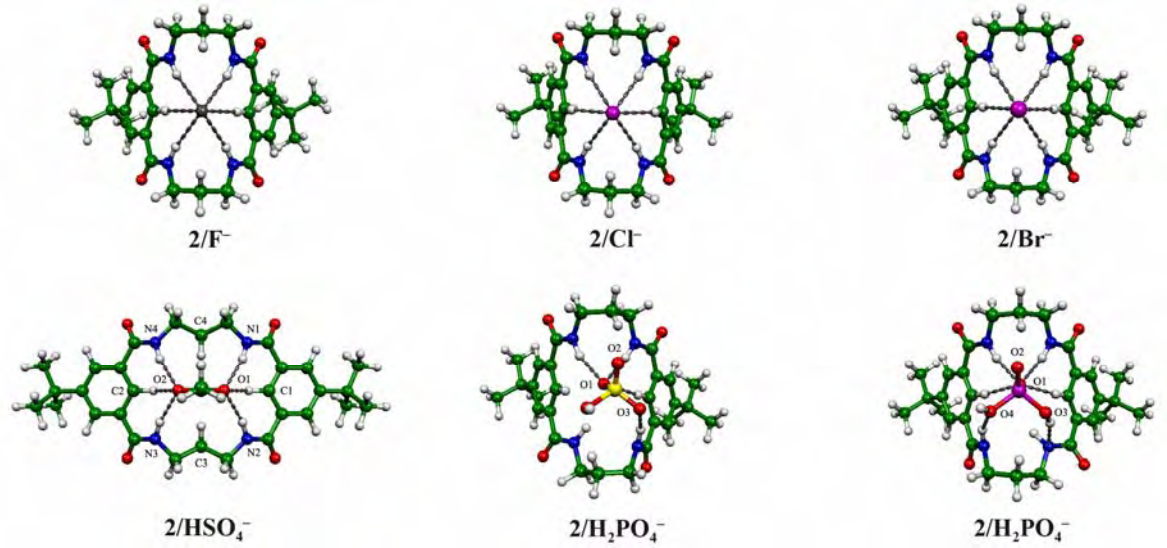
2/F⁻
2/Cl⁻
2/Br⁻
N4
C4
N1
O2
O1
C2
C1
N3
C3
N2
2/HSO4⁻
O2
O1
O3
2/H2PO4⁻
O2
O1
O4
O3
2/H2PO4⁻

Fig. 3.

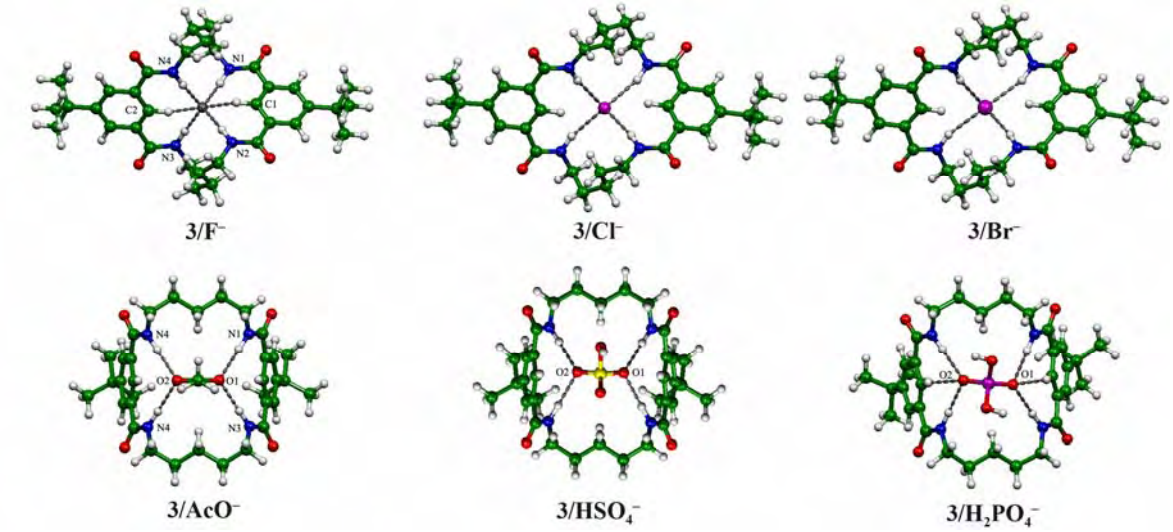

Fig. 4.

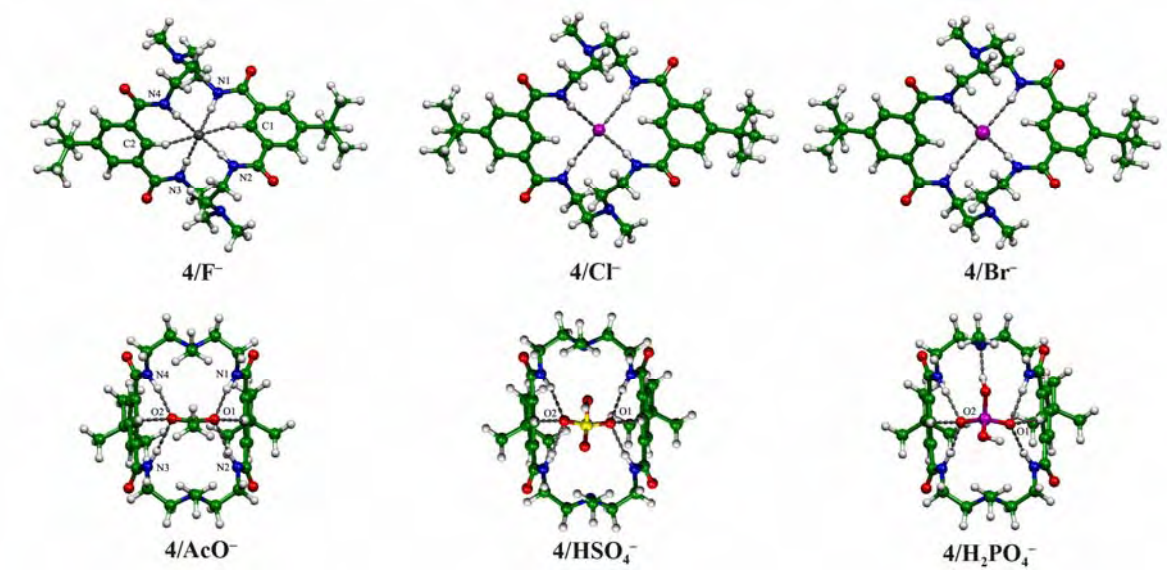

Fig. 5.

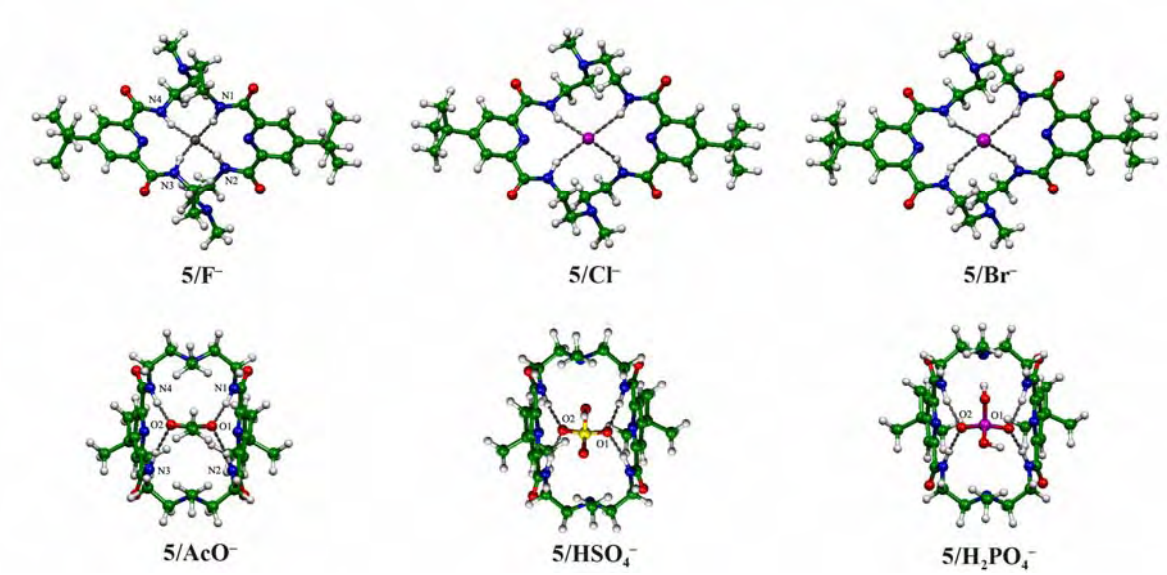

Fig. 6.

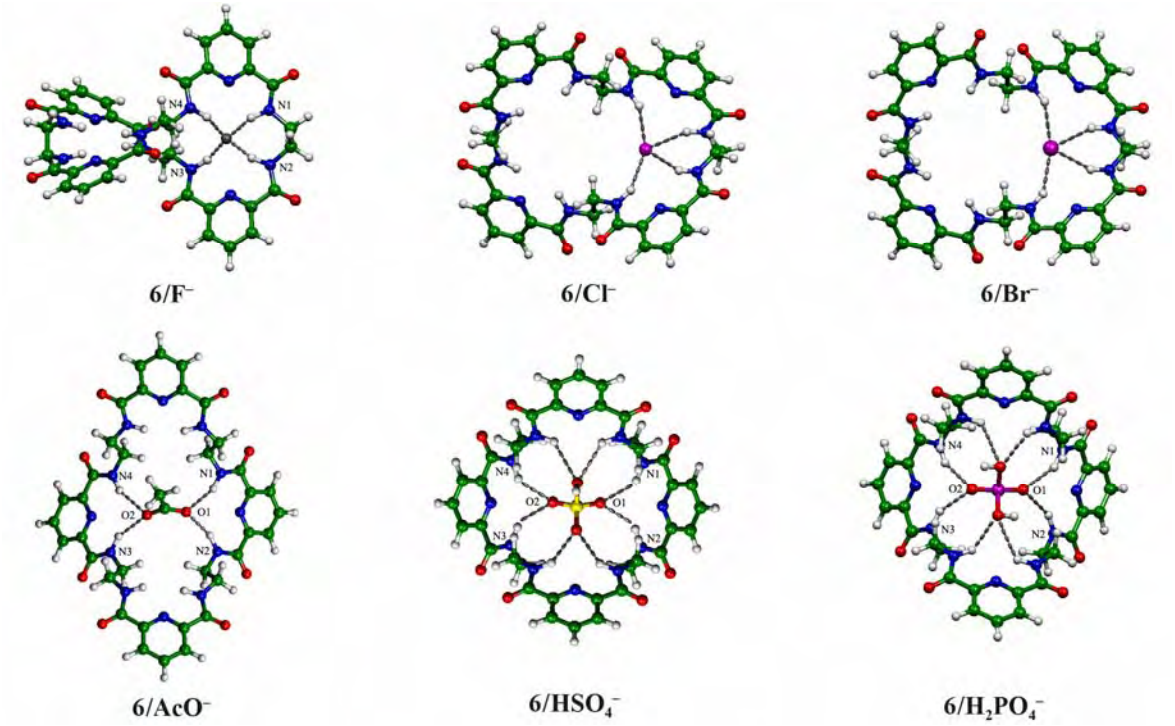

Fig. 7.

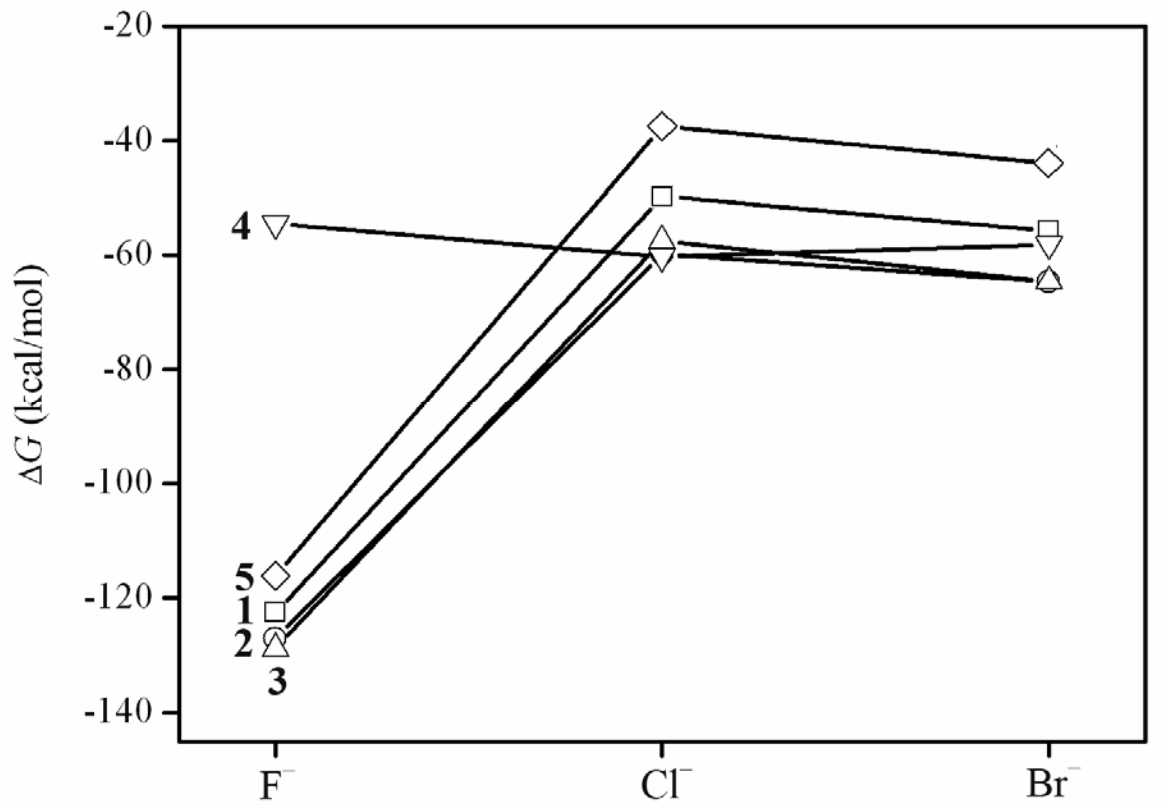

Fig. 8.

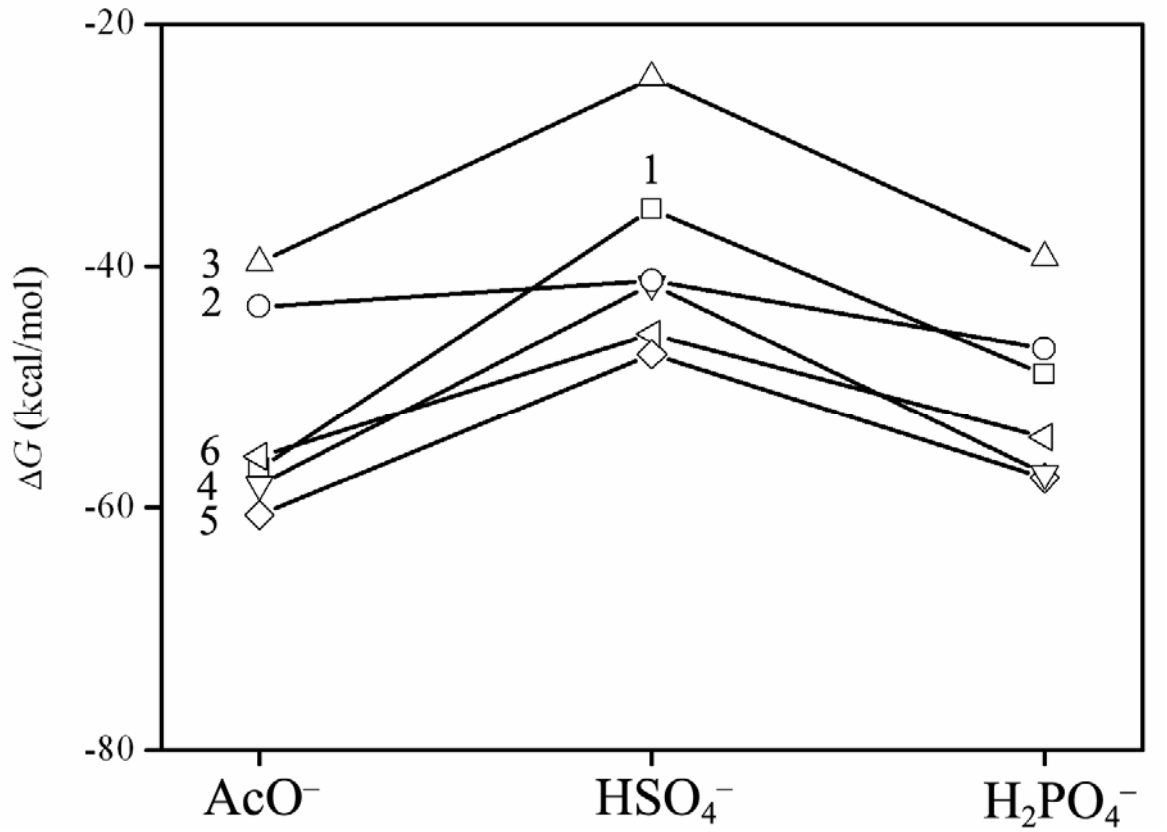

Fig. 9

ภาคผนวก E

Manuscript บทความเรื่อง “Anion recognition of alkaline–metal complexes of calix[4] arene receptors: An ONIOM investigation”

Anion recognition of alkaline–metal complexes of calix[4]arene receptors: An ONIOM investigation

Pornpan Chanapiwat, Viwat Vchirawongkwin, Vithaya Ruangpornvisuti *

Department of Chemistry, Faculty of Science, Chulalongkorn University, Bangkok 10330, Thailand

* Corresponding author. Tel.: +66–2218–7644; Fax: +66–2254–1309.
E–mail address: vithaya.r@chula.ac.th (V. Ruangpornvisuti).

Abstract

The ONIOM(B3LYP/6–31G(d):AM1) optimized structures of complexes of calix[4]arene receptor (**L**) with alkaline metals Li^+, Na^+ and K^+ and their complexes with halide ions $F^–$, $Cl^–$, $Br^–$, oxygen–containing anions $HCO_3^–$, $HSO_4^–$ and $CH_3COO^–$ ions were obtained. Binding energies and thermodynamic properties of complex receptors Li**L**$^+$, Na**L**$^+$ and K**L**$^+$ with these anions were determined. Binding energies of receptors Li**L**$^+$, Na**L**$^+$ and K**L**$^+$ are in decreasing orders: $F^–$ >> $CH_3COO^–$ > $HCO_3^–$ > $Br^–$ > $HSO_4^–$ > $Cl^–$, $F^–$ >> $CH_3COO^–$ > $HCO_3^–$ > $Br^–$ > $Cl^–$ > $HSO_4^–$ and $F^–$ >> $CH_3COO^–$ > $HCO_3^–$ > $Br^–$ > $Cl^–$ > $HSO_4^–$. All the alkaline–metal receptors Li**L**$^+$, Na**L**$^+$ and K**L**$^+$ exhibit their abilities to selectively fluoride ion.

Keywords: calix[4]arenes; alkaline metal; halide; oxygen–containing anion; binding energy; ONIOM

1. Introduction

Anions play an important role in several fields such as biology [1], the environment [2], catalysis [3] and potential medical application [4]. Thus the design of molecular sensors for anion recognition and sensing are interesting of chemists for many years, especially, in the research field of supramolecular chemistry [5]. The major need for designing is both sensitive and selective sensors for anions [6, 7]. Hosts containing a variety of donor (D) groups, D–H, such as ureas [8–11], amines [12], amides [13,14] and thioamides [15] have been widely investigated. Anion recognition of two binding–sites receptors lead to discovery of useful sensors not only for dicarboxylates but also monocarboxylates. Chromogenic azophenol–thiourea based anion sensors were developed for the selective colorimetric detection of acetate and other anions [16–18]. Furthermore chromogenic indoaniline–thiourea–based receptors were studied for fluoride detection sensors [19]. Anthracen urea and thiourea compounds were synthesized and investigated for their effective chromogenic anion sensors [20]. For fluorescent and luminescent chemosensors for detection of anions have been developed for dicarboxylate recognition [21]. Tripodal urea derivative such as aromatic carboxylate receptor was investigated for its association constant by NMR titration method [22]. The urea or thiourea groups incorporated receptors as anion recognition were studied in system of various solvents [23–25]. Previous theoretical work, the recognition of carboxylate and dicarboxylates by azophenol–thiourea derivatives were first investigated by the integrated MO:MO method and the oxalate is the most favorite ion to form complexes with both receptors of azophenol–thiourea derivatives [26]. Since determination of the binding and complexation energies of the complexes of the p–*tert*–butylsulfonylcalix[4]arene [27], p–*tert*–butylthiacalix[4]arene [28] and tetraamino–*tert* –butylthiacalix[4]arene [29] derivatives with zinc(II) cation were theoretically carried out, the complexes of these receptors with organic anions should be therefore investigated, particularly the calix[4]arene derivative functionalized by amino group.

As amino nitrogen atoms of the tetraamino–*tert*–butylthiacalix[4]arene derivatives have ability to bind to the zinc (II) cation [29, 30], their amino protons have to be able to bind with anion. As the complex formation of tetraamino–*tert*–butylthiacalix[4]arene derivatives with anions is expected and their anion recognition leads to development of anion sensors, binding

interactions between detected anions and their receptors are therefore very important information for discovering colorimetric and other detecting sensors.

In this work, binding interaction complexes of calix[4]arene receptor (**L**) with alkaline metals Li^+, Na^+ and K^+ and their complexes with halide ions F^-, Cl^-, Br^-, oxygen–containing anions HCO_3^-, HSO_4^- and CH_3COO^- ions have been investigated.

2. Computational method

Geometries of the tested host–guest complexes and its host, guest components were optimized using the hybrid density functional B3LYP [31, 32] methods and the two–layered ONIOM(MO:MO) approach (ONIOM) [33, 34] using B3LYP/6–31G(d) as high model and semiempirical AM1 [35], PM3 [36] and MNDO [37] as low models. The reliability of the ONIOM calculations at the integrated level [38], ONIOM(B3LYP/6–31G(d):AM1), ONIOM(B3LYP/6–31G(d):PM3) and ONIOM(B3LYP/6–31G(d):MNDO) approaches were examined by being employed in the geometrical optimizations of the tetraamino–*tert*–butylthiacalix[4]arene receptor and its complex with oxalate. Their geometrical data were compared to the data of the target geometry optimized at B3LYP/6–31G(d) level of theory [39]. Energies and geometries of oxalate/tatctb4a system as the examined host–guest complex carried out using the ONIOM(B3LYP/6–31G(d):AM1), ONIOM(B3LYP/6–31G(d):PM3) and ONIOM(B3LYP/6–31G(d):MNDO) methods were also compared with the target B3LYP/6–31G(d) geometry. The ONIOM(B3LYP/6–31G(d):AM1) calculation of the examined system provides reasonable result with relatively lower cost for the present host–guest interaction. The two–layered ONIOM(B3LYP/6–31G(d):AM1) for geometry optimization of the present host–guest investigation was therefore employed through out this work. The reliability of the ONIOM(B3LYP/6–31G(d):AM1) of the similar system was discussed in references [40,41]. The real and model systems used in the two–layer ONIOM(MO:MO) calculations for the hosts and host–guest interaction models are shown in Fig. 1. The geometrical structures of carboxylate guests and their total energies were optimized and computed at the B3LYP/6–31G(d) level of theory. All calculations were performed using the GAUSSIAN 03 program [42] and their structures were visualized using the MOLEKEL 4.3 program [43].

Energies of binding ($\Delta E_{\text{binding}}$) of guest on host of the ONIOM calculations of the present system are evaluated using the following equation:

$$\begin{aligned}\Delta E_{\text{binding}}\,[(\text{B3LYP/6–31G(d):AM1})](\text{host/guest}) = \\ \text{E}\,[(\text{B3LYP/6–31G(d):AM1})]\,(\text{host/guest}) \\ -\ \text{E}\,[(\text{B3LYP/6–31G(d):AM1})]\,(\text{host}) \\ -\ \text{E}\,[(\text{B3LYP/6–31G(d))}]\,(\text{guest})\end{aligned} \qquad (1)$$

To estimate the basis set superposition error (BSSE) for the energies of host/guest complex formation at the B3LYP/6–31G(d)//ONIOM(B3LYP/6–31G(d):AM1) level, counterpoise (CP) calculations were performed using the Boys–Bernardi's CP scheme [44–49]. The BSSE energies of the host/guest complex formation were used to compute the energies of BSSE corrected binding ($\Delta E^{\text{BSSE}}_{\text{binding.}}$).

The enthalpy ΔH^{298} and Gibbs free energy changes ΔG^{298} of all complexation reactions have been derived from the frequency computations at ONIOM(B3LYP/6–31G(d):AM1) level of theory. The equilibrium constant, K of binding process at 298.15 and 1 atmosphere was computed using thermodynamic relation of $\Delta G^{298} = -RT\,ln\,\text{K}$.

The binding selectivity of calix[4]arene receptor to guest B with respect to guest A has been derived from the selectivity coefficient (K^{A}_{B}) [50] which is defined as an equilibrium constant of ion exchange between ions A and B. Since exchange is a chemical reaction as eq. (2), it can be treated like any other mass action expression.

$$\text{AX} + \text{B} \rightleftharpoons \text{BX} + \text{A} \qquad (2)$$

Therefore, the selectivity coefficient can be defined as $K^{\text{A}}_{\text{B}} = \dfrac{[\text{BX}][\text{A}]}{[\text{AX}][\text{B}]}$. If the complexations of BX and AX are observed, their stability constants due to eqs. (3) and (4) can be expressed as $K_{\text{A}} = \dfrac{[\text{AX}]}{[\text{X}][\text{A}]}$ and $K_{\text{B}} = \dfrac{[\text{BX}]}{[\text{X}][\text{B}]}$.

$$\text{X} + \text{B} \rightleftharpoons \text{BX} \qquad (3)$$

$$\text{X} + \text{A} \rightleftharpoons \text{AX} \qquad (4)$$

The selectivity coefficient can be therefore written as $K_B^A = \frac{K_B}{K_A}$. If the value of the selectivity coefficient K_B^A is larger than one, this implies that B is preferred over A and if K_B^A is smaller than one then A is preferred over B.

3. Results and discussion

3.1 Complexes of receptor L with alkaline metals

The ONIOM(B3LYP/6–31G(d):AM1) optimized structures of complexes of calix[4]arene receptor (**L**) with alkaline metals Li^+, Na^+ and K^+ are shown in Fig. 2. Their binding energies are listed in Table 1.

3.2 Formation of alkaline–metal receptors with anions

The ONIOM(B3LYP/6–31G(d):AM1) optimized structures of alkaline–metal receptors Li**L**$^+$, Na**L**$^+$ and K**L**$^+$ with halide ions F^-, Cl^-, Br^-, oxygen–containing anions HCO_3^-, HSO_4^- and CH_3COO^- ions are sown in Figs. 3, 4 and 5. Their binding energies and thermodynamic properties of their formation are shown in Table 2. All formations between anions and alkaline–metal receptors Li**L**$^+$, Na**L**$^+$ and K**L**$^+$ are exothermic and spontaneous reactions. Bindings of these anions on the receptor Na**L**$^+$ are thermodynamically more stable than the receptors Li**L**$^+$ and K**L**$^+$, except the HSO_4^- ion. Binding energies of receptors Li**L**$^+$, Na**L**$^+$ and K**L**$^+$ are in decreasing orders: F^- >> CH_3COO^- > HCO_3^- > Br^- > HSO_4^- > Cl^-, F^- >> CH_3COO^- > HCO_3^- > Br^- > Cl^- > HSO_4^- and F^- >> CH_3COO^- > HCO_3^- > Br^- > Cl^- > HSO_4^-. Selectivity coefficients for these anions of the receptors are in orders: F^- >> CH_3COO^- > HCO_3^- > Br^-> Cl^-> HSO_4^- for Li**L**$^+$, F^- >> CH_3COO^- ≈ Br^- > HCO_3^- > Cl^- >> HSO_4^- for Na**L**$^+$ and F^- >> CH_3COO^- > HCO_3^- > Br^- > Cl^- > HSO_4^- for K**L**$^+$.

Plots of the binding free energy of the receptors with (a) halide anions and (b) oxygen–containing anions against the radius of alkaline metals of the receptors are shown in Fig. 6. It shows that the alkaline metals Li^+, Na^+ and K^+ hardly ever affect the stability of the halide

complexes of calix[4]arene receptor (**L**) with alkaline metals but affect the stability of CH_3COO^-, HCO_3^- and HSO_4^- as shown in Fig. 6(b).

It can be concluded that all alkaline–metal receptors Li**L**$^+$, Na**L**$^+$ and K**L**$^+$ exhibit their abilities to selectively fluoride ion. These alkaline metals Li^+, Na^+ and K^+ hardly ever have an influence on the fluoride recognition of the alkaline–metal receptors Li**L**$^+$, Na**L**$^+$ and K**L**$^+$.

4. Conclusions

Binding energies and thermodynamic properties of formation between complexes of calix[4]arene (**L**) with alkaline metals Li^+, Na^+ and K^+ formed as Li**L**$^+$, Na**L**$^+$ and K**L**$^+$ and halide ions F^-, Cl^-, Br^-, oxygen–containing anions HCO_3^-, HSO_4^- and CH_3COO^- ions these anions were determined. Binding energies of receptors Li**L**$^+$, Na**L**$^+$ and K**L**$^+$ are in decreasing orders: $F^- >> CH_3COO^- > HCO_3^- > Br^- > HSO_4^- > Cl^-$, $F^- >> CH_3COO^- > HCO_3^- > Br^- > Cl^- > HSO_4^-$ and $F^- >> CH_3COO^- > HCO_3^- > Br^- > Cl^- > HSO_4^-$. All formations between anions and alkaline–metal receptors Li**L**$^+$, Na**L**$^+$ and K**L**$^+$ are exothermic and spontaneous reactions. All alkaline–metal receptors Li**L**$^+$, Na**L**$^+$ and K**L**$^+$ exhibit their abilities to selectively fluoride ion. These alkaline metals Li^+, Na^+ and K^+ hardly ever have an influence on the fluoride recognition of the alkaline–metal receptors Li**L**$^+$, Na**L**$^+$ and K**L**$^+$.

Acknowledgements

The authors gratefully acknowledge the Thailand Research Fund for financial support (grant no. BRG5180016).

References

[1] S. Mangani and M. Ferraroni: In A. Bianchi, K. Bowman–James and E. Garcia–España (eds.), Supramolecular Chemistry of Anions, Wiley–VCH, New York (1997).

[2] J.M. Holloway, R.A. Dahlgren, B. Hansen, W.H. Casey, Nature 395 (1998) 785.

[3] J. Scheele, P. Timmerman, D.N. Reinhoudt, Chem. Commun. (1998) 2613.

[4] J.L. Sessler, P.I. Sansom, A. Andrievski, and V. Král: In A. Bianchi, K. Bowman–James and E. Garcia–España (eds.), Supramolecular Chemistry of Anions, Wiley–VCH, New York (1997).

[5] J.M. Lehn, Supramolecular Chemistry, Concepts and Perspectives; VCH: Weinheim, Germany, (1995).

[6] A. Bianchi, K. Bowman–James, E. García–España, Editors, Supramolecular Chemistry of Anions; Wiley–VCH: New York, (1997).

[7] P.A. Gale, Coord. Chem. Rev. 240 (2003) 191.

[8] S.K. Kim, J. Yoon, Chem. Commun. (2002) 770.

[9] E.J. Cho, B.J. Ryu, Y.J. Lee, K.C. Nam, Org. Lett. 7 (2005) 2607.

[10] S.J. Brooks, P.A. Gale, M.E. Light, Chem. Commun. (2006) 4344.

[11] V. Amendola, D. Esteban–goämez, L. Fabbrizzi, M. Licchelli, Acc. Chem. Res. 39 (2006) 343.

[12] M.A. Hossain, J.A. Liljegren, D. Powell, K. Bowman–James, Inorg. Chem. 43 (2004) 3751.

[13] C.R. Bondy, S.J. Loeb, Coord. Chem. Rev. 240 (2003) 77.

[14] C.R. Bondy, P.A. Gale, S.J. Loeb, Chem. Comm. 8 (2001) 729.

[15] T. Zielińskia, J. Jurczak, Tetrahedron 61(2005) 4081.

[16] D.H. Lee, K.H. Lee, J.–I. Hong, Org. Lett. 3 (2001) 5.

[17] D.H. Lee, H.Y. Lee, K.H. Lee, J.–I. Hong, Chem. Commun. (2001) 1188.

[18] D.H. Lee, H.Y. Lee, J.–I. Hong, Tetrahedron Lett. 43 (2002) 7273.

[19] D. Jiménez, R. Martínez–Máñez, F. Sancenón, J. Soto, Tetrahedron Lett. 43 (2002) 2823.

[20] P. Piatek, J. Jurczak, Chem. Commun. 20 (2002) 2450.

[21] T. Gunnlaugsson, A.P. Davis, J.E. O'Brien, M. Glynn, Org. Lett. 4 (2002) 2449.

[22] A. Fan, H.K. Hong, S. Valiyaveettil, J.J. Vittal, J. Supramol. Chem. 2 (2002) 247.

[23] H. Baerrigter, L. Grave, W.M. Nissink, L.A.J. Chrisstoffels, J.H. Vander Maas, W. Verboom, F. de Jong, D.N. Reindoudt, Org. Chem. 63 (1998) 4174.

[24] E. Fan, S.A. Van Arman, D. Kincaid, A.D. Hamilton, J. Am. Chem. Soc. 115 (1993) 369.

[25] K.H. Lee, J.–I. Hong, Tetrahedron Lett. 41 (2000) 6083.

[26] V. Ruangpornvisuti, J. Mol. Struct. (Theochem) 686 (2004) 47.

[27] B. Wanno, W. Sang–aroon, T. Tuntulani, B. Pulpoka, V. Ruangpornvisuti, J. Mol. Struct. (Theochem) 629 (2003) 137.
[28] V. Ruangpornvisuti, J. Mol. Struct. (Theochem) 683 (2004) 103.
[29] B. Wanno, V. Ruangpornvisuti, J. Mol. Struct. (Theochem) 685 (2004) 57.
[30] B. Wanno, V. Ruangpornvisuti, J. Mol. Struct. 787 (2006) 76.
[31] A.D. Becke, Phys. Rev. A38 (1988) 3098.
[32] C. Lee, W. Yang, R.G. Parr, Phys. Rev. B37 (1988) 385.
[33] F. Maseras, K. Morokuma, J. Comp. Chem. 16 (1995) 1170.
[34] S. Humbel, S. Sieber, K. Morokuma, J. Chem. Phys. 105 (1996) 1959.
[35] M.J.S. Dewar, C.H. Reynolds, J. Comp. Chem. 2 (1986) 140.
[36] J.J.P. Stewart, Comp. Chem. 10 (1989) 209.
[37] M.J.S. Dewar, W. Thiel, J. Am. Chem. Soc. 99 (1977) 4899.
[38] S. Dapprich, I. Komaromi, K.S. Byun, K. Morokuma, M.J. Frisch, J. Mol. Struct. (Theochem) 461 (1999) 1.
[39] V. Ruangpornvisuti, B. Wanno, J. Mol. Model. 13 (2007) 65.
[40] M. Remko, O.A. Walsh, W.G. Richards, J. Phys. Chem. A 105 (2001) 6926.
[41] M. Remko, J. Phys. Chem. A 106 (2002) 5005.
[42] M.J. Frisch et al., Gaussian 03, Revision D02, Gaussian Inc., Wallingford, CT, 2006.
[43] P. Flükiger, H.P. Lüthi, S. Portmann, J. Weber, Molekel 4.3, Swiss Center for Scientific Computing, Manno (Switzerland), 2000.
[44] S.F. Boys, F. Bernadi, Mol. Phys. 19 (1970) 553.
[45] I. Mayer, P.R. Surjan, Chem. Phys. Lett. 191 (1992) 497.
[46] L. Turi, J.J. Dannenberg, J. Phys. Chem. 97 (1993) 2488.
[47] S. Simon, M. Duran, J.J. Dannenberg, J Phys. Chem. A 103 (1999) 1640.
[48] A. Hamza, A. Vibok, G.J. Halasz, I. Mayer, J. Mol. Struct. (Theochem) 427 (2000) 501.
[49] M. Makowski, E.D. Raczyska, L. Chmurzyski, J. Phys. Chem. A 105 (2001) 869.
[50] Y. Long, Y. Liu, L. Lei, L. Nie, S. Yao, Analyst 126 (2001) 1090.

Table 1

Energetics and thermodynamic properties of formations between calix[4]arene and alkaline metals, computed at the ONIOM (B3LYP/6–31G(d):AM1) level

Host/guest formation	ΔE [a]	ΔH^{o}_{298} [a]	ΔG^{o}_{298} [a]	K	Log K	K^{A}_{B} [b]
L + Li^+ → $Li\mathbf{L}^+$						
L + Na^+ → $Na\mathbf{L}^+$						
L + K^+ → $K\mathbf{L}^+$						

[a] In kcal/mol.

[b] Selectivity coefficient of guests with respect to A complex.

Table 2

Energetics and thermodynamic properties of formations between alkaline–metal receptors and anions, computed at the ONIOM(B3LYP/6–31G(d):AM1) level

Host/guest complexes	ΔE [a]	ΔH^{o}_{298} [a]	ΔG^{o}_{298} [a]	K	Log K	K_B^A [b]
Receptor Li**L**$^+$:						
Li**L**$^+$/F^-	–152.81	–154.52	–141.69	2.44 x 10^{10}	10.39	1.53 x 10^5
Li**L**$^+$/Cl^-	–82.95	–84.07	–72.66	2.12 x 10^5	5.33	1.33 x 10^0
Li**L**$^+$/Br^-	–86.40	–87.43	–76.56	4.10 x 10^5	5.61	2.57 x 10^0
Li**L**$^+$/HCO_3^-	–96.75	–97.30	–82.84	1.18 x 10^6	6.07	7.41 x 10^0
Li**L**$^+$/HSO_4^-	–84.68	–84.50	–70.98	1.60 x 10^5	5.20	1.00 x 10^0
Li**L**$^+$/CH_3COO^-	–99.15	–99.96	–84.99	1.70 x 10^6	6.23	1.07 x 10^1
Receptor Na**L**$^+$:						
Na**L**$^+$/F^-	–153.03	–154.40	–142.89	2.98 x 10^{10}	10.47	1.20 x 10^6
Na**L**$^+$/Cl^-	–82.86	–83.65	–73.07	2.27 x 10^5	5.36	9.13 x 10^0
Na**L**$^+$/Br^-	–86.29	–87.03	–76.65	4.16 x 10^5	5.62	1.67 x 10^1
Na**L**$^+$/HCO_3^-	–89.63	–90.13	–75.17	3.24 x 10^5	5.51	1.30 x 10^1
Na**L**$^+$/HSO_4^-	–74.38	–74.51	–59.97	2.49 x 10^4	4.40	1.00 x 10^0
Na**L**$^+$/CH_3COO^-	–91.00	–91.44	–76.82	4.28 x 10^5	5.63	1.72 x 10^1
Receptor K**L**$^+$:						
K**L**$^+$/F^-	–153.02	–154.71	–140.01	1.84 x 10^{10}	10.26	5.33 x 10^5
K**L**$^+$/Cl^-	–82.78	–83.78	–71.27	1.68 x 10^5	5.22	4.86 x 10^0
K**L**$^+$/Br^-	–86.22	–87.73	–72.64	2.12 x 10^5	5.33	6.14 x 10^0
K**L**$^+$/HCO_3^-	–89.74	–90.49	–73.17	2.31 x 10^5	5.36	6.71 x 10^0
K**L**$^+$/HSO_4^-	–76.00	–75.76	–61.90	3.45 x 10^4	4.54	1.00 x 10^0
K**L**$^+$/CH_3COO^-	–91.03	–91.65	–75.25	3.28 x 10^5	5.52	9.52 x 10^0

[a] In kcal/mol.

[b] Selectivity coefficient of guests with respect to HSO_4^- complex.

Captions for the illustrations

Fig. 1 Molecule of guest (ball) and ball atoms of receptor are treated as high level of theory and other rest part is treated as low level in which have been used in the ONIOM(MO:MO) calculation.

Fig. 2 The ONIOM(B3LYP/6–31G(d):AM1) level optimized structures of the receptors Li**L**$^+$, Na**L**$^+$ and K**L**$^+$.

Fig. 3 The ONIOM(B3LYP/6–31G(d):AM1) level optimized structures of the complexes of Li**L**$^+$ with anionic guests. The hydrogen–bond distances and binding free energies (ΔG^{o}_{298}) are in angstrom and kcal/mol, respectively.

Fig. 4 The ONIOM(B3LYP/6–31G(d):AM1) level optimized structures of the complexes of Na**L**$^+$ with anionic guests. The hydrogen–bond distances and binding free energies (ΔG^{o}_{298}) are in angstrom and kcal/mol, respectively.

Fig. 5 The ONIOM(B3LYP/6–31G(d):AM1) level optimized structures of the complexes of K**L**$^+$ with anionic guests. The hydrogen–bond distances and binding free energies (ΔG^{o}_{298}) are in angstrom and kcal/mol, respectively.

Fig. 6 Plots of the binding free energy of the receptors with (a) halide anions and (b) oxygen–containing anions against the radius of alkaline metals of the receptors.

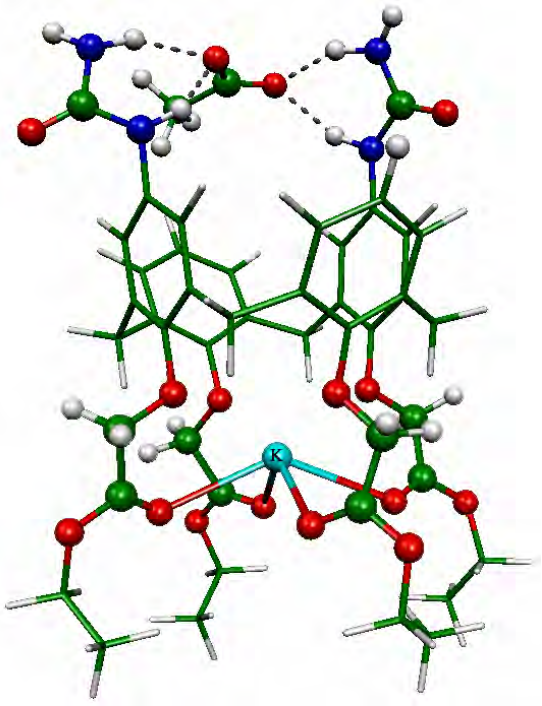

Fig. 1

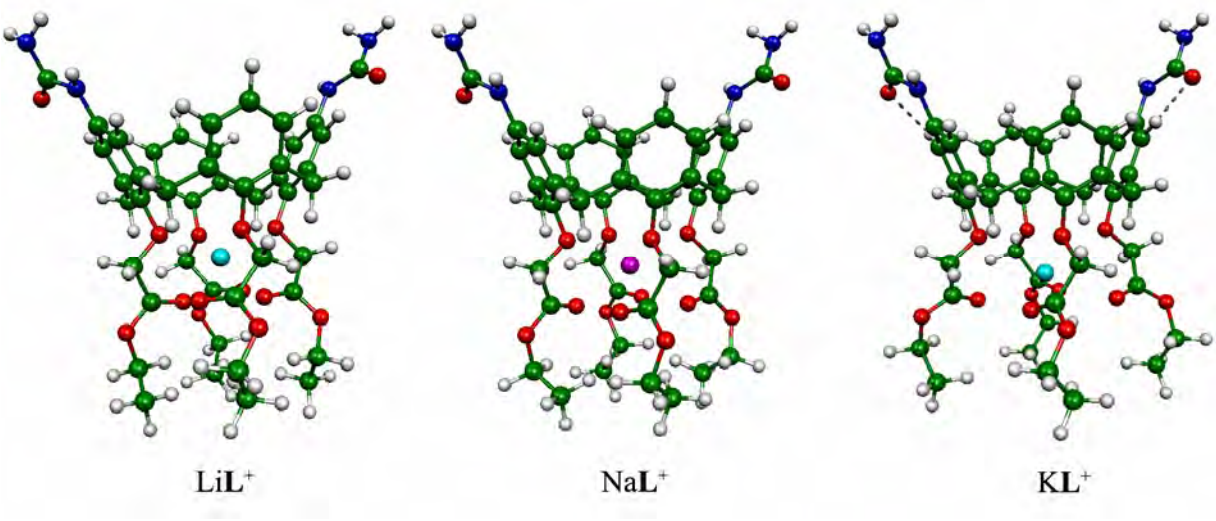

Fig. 2

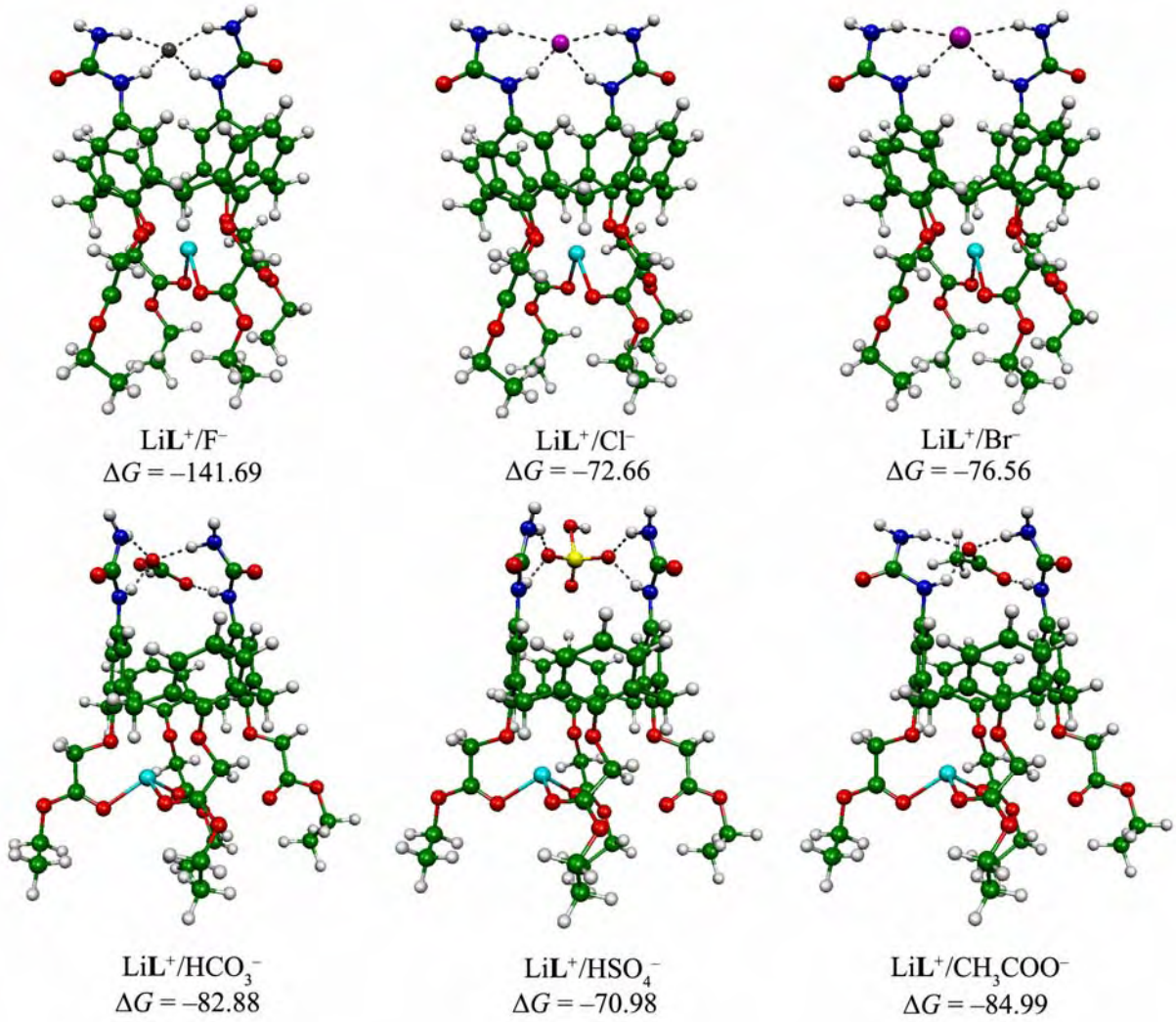
LiL+/F−
ΔG = –141.69
LiL+/Cl−
ΔG = –72.66
LiL+/Br−
ΔG = –76.56
LiL+/HCO3−
ΔG = –82.88
LiL+/HSO4−
ΔG = –70.98
LiL+/CH3COO−
ΔG = –84.99

Fig. 3

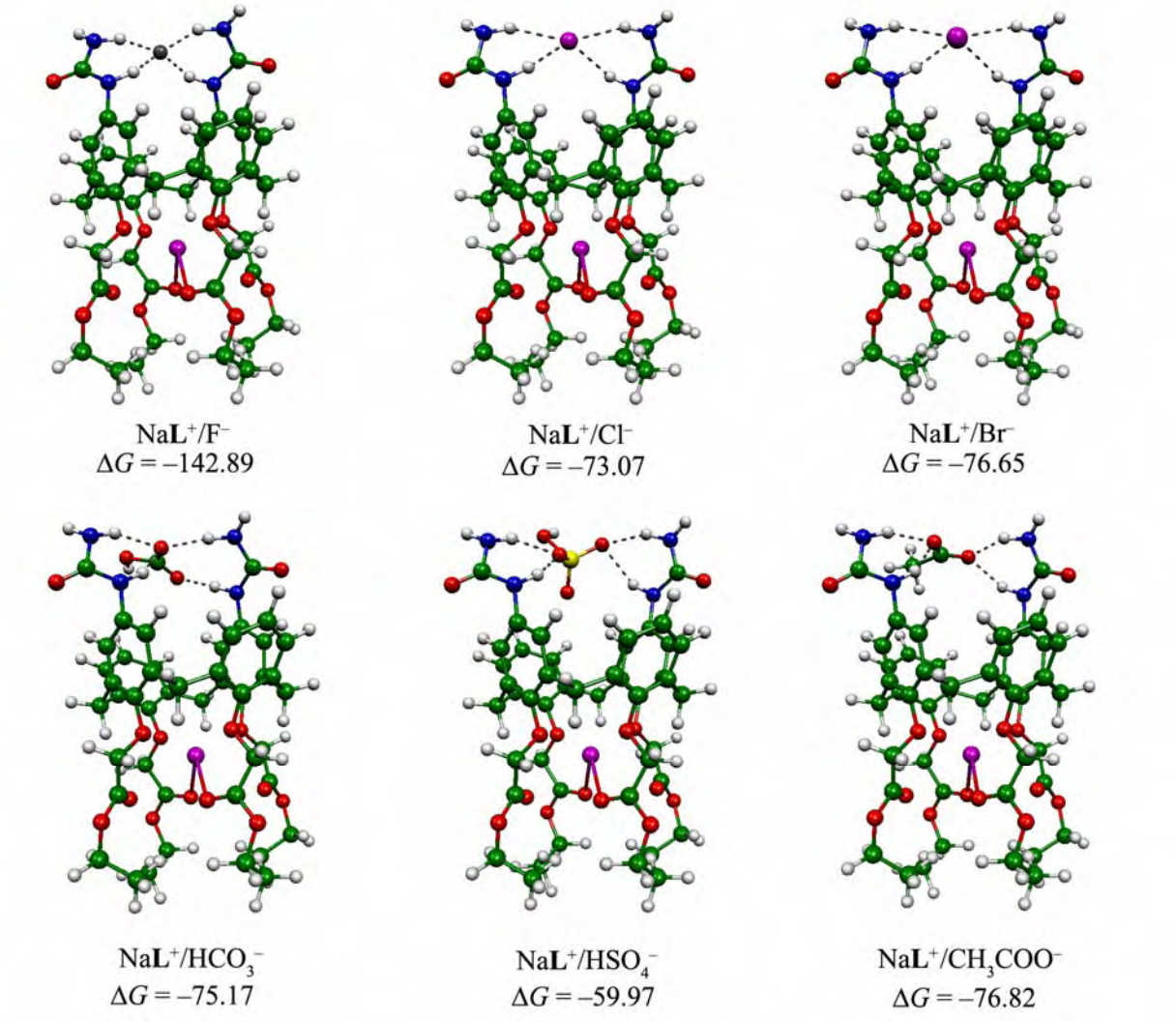
NaL+/F−
ΔG = –142.89
NaL+/Cl−
ΔG = –73.07
NaL+/Br−
ΔG = –76.65
NaL+/HCO3−
ΔG = –75.17
NaL+/HSO4−
ΔG = –59.97
NaL+/CH3COO−
ΔG = –76.82

Fig. 4

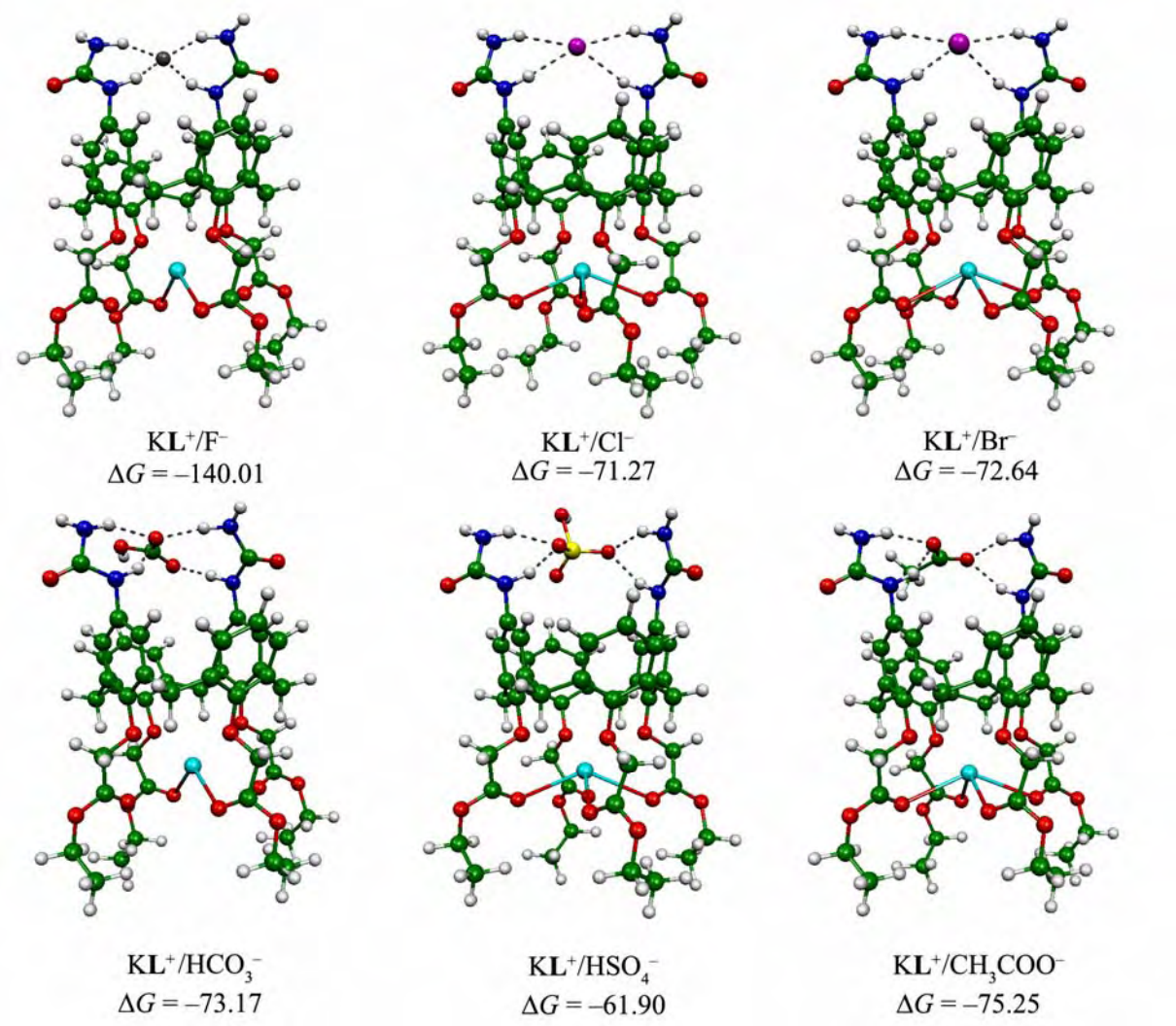
KL+/F−
ΔG = –140.01
KL+/Cl−
ΔG = –71.27
KL+/Br−
ΔG = –72.64
KL+/HCO3−
ΔG = –73.17
KL+/HSO4−
ΔG = –61.90
KL+/CH3COO−
ΔG = –75.25

Fig. 5

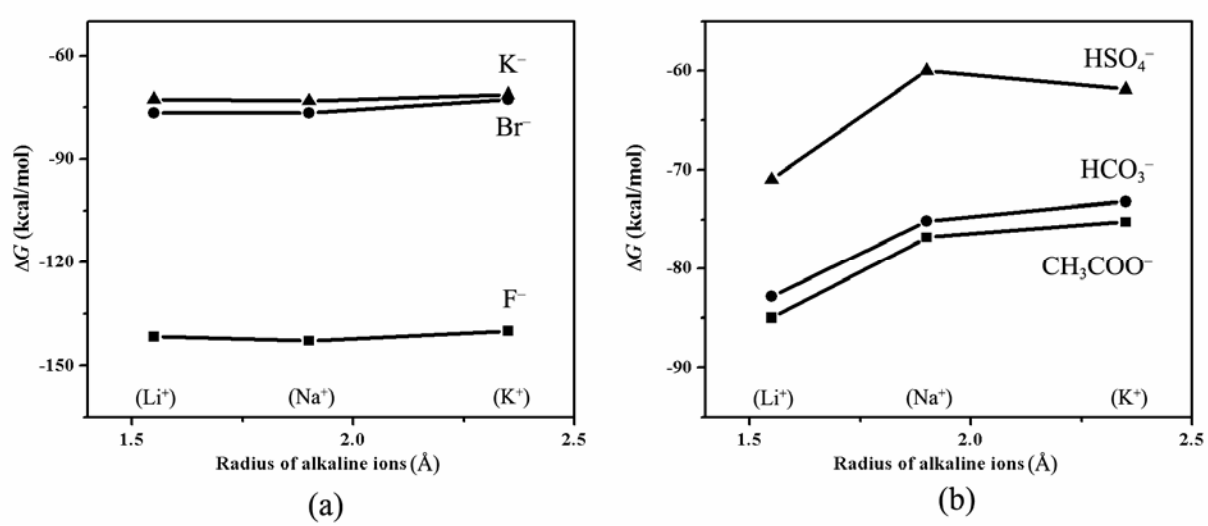
-60
-90
-120
-150
ΔG (kcal/mol)
K⁻
Br⁻
F⁻
(Li⁺)
(Na⁺)
(K⁺)
1.5
2.0
2.5
Radius of alkaline ions (Å)
(a)
-60
-70
-80
-90
ΔG (kcal/mol)
HSO4⁻
HCO3⁻
CH3COO⁻
(Li⁺)
(Na⁺)
(K⁺)
1.5
2.0
2.5
Radius of alkaline ions (Å)
(b)

Fig. 6